LITHIUM EXTRACTION FROM ZIMBABWEAN PETALITE WITH AMMONIUM BIFLUORIDE DIGESTION

Kalenga Tite Mwepu

A dissertation submitted in partial fulfillment of the requirements for the degree Master of Science in Applied Science (Chemical Technology) in the Department of Chemical Engineering, Faculty of Engineering, Built Environment and Information Technology.

Supervisor: Prof. Philip Crouse

Co-supervisor: Dr Salmon Lubbe

February 2020

Declaration

I, Kalenga Tite Mwepu, student No. 15261043, do hereby declare that this research is my original work and that it has not previously, in its entirety or in part, been submitted and is not currently being submitted, either in whole or in part, at any other university for a degree or diploma, and that all references are acknowledged.

SIGNED on this _____ day of_____12/02_____ 2020.

_____

Kalenga Tite Mwepu

Synopsis

Lithium carbonate is the precursor for most other lithium compounds. The market demand for lithium is increasing because it is used for many applications such as the preparation of electrode material and electrolyte for lithium-ion batteries, for treatment of manic depression, production of electronic grade crystals of lithium niobate and tantalite, and preparation of battery-grade lithium metal.

Previously reported methods of lithium extraction require high temperature calcination for phase transformation from α-spodumene into β-spodumene, that is energy consuming and costly. This step is required because of the higher chemical reactivity of β-spodumene.

The objectives of this research were to investigate the viability of ammonium bifluoride digestion of the petalite concentrate from the Bikita deposits without the initial thermal conversion to β-spodumene, in order to produce a high purity lithium carbonate in a cost efficient way, and optimising the remaining process parameters of the full process. Ammonium bifluoride is simpler and safer to use than conventional fluorination substances such as HF and F_2. The full process starts with petalite digestion using ammonium bifluoride, followed by acid roasting, water-leaching, purification of the solution, and precipitation of Li_2CO_3.

Petalite digestion was achieved at 100 ºC using a petalite/NH_4HF_2 molar ratio of 1:3 and at 500 ºC using a petalite/NH_4HF_2 molar ratio of 1:1, followed by acid roasting using an excess of H_2SO_4 at 100 °C and/or 200 °C. The product was then water leached at 80 °C with an agitation of 300 rpm using a solid-liquid ratio of 1:10, and filtered to remove the insoluble silicates. The aqueous Li_2SO_4 was purified by selective precipitation of the contaminants as hydroxides. To achieve this the pH was raised using calcium carbonate and calcium hydroxide. Finally, the lithium carbonate was precipitated by the addition of sodium carbonate.

After digestion of petalite at both 100 °C and 500 °C, XRD confirms that petalite was reacted and the major phases present in the insoluble were lithium fluoride (LiF), aluminium trifluoride (AlF_3) and cryolithionite ($Na_3Li_3Al_2F_{12}$) at the two digesting temperatures respectively. A 97 % lithium extraction was achieved after the leaching step when working at the conditions mentioned above. After precipitation of Li_2CO_3, the resulting product was washed with hot water and had a purity of 99 % (metal basis).

Research recommendations include: Treatment of the aqueous Li_2SO_4 when petalite is digested at 100 °C should be continued up to the precipitation of Li_2CO_3 to determine if digestion of petalite at 500 °C is necessary; the NH_4HF_2 and H_2SO_4 excesses used here should also be studied to determine whether the amounts may be reduced.

Keywords: Petalite; lithium; lithium extraction; digestion, leaching; lithium carbonate; Bikita Minerals.

Acknowledgements

I am greatly thankful to my supervisor Professor Philip Crouse and my co-supervisor Doctor Salmon Lubbe for their guidance, advice, support and encouragement throughout the research and the writing of this dissertation. They were able to help me to overcome the difficulties during my MSc experiments in the laboratory and have contributed significantly to make this dissertation possible.

In addition, I would like to thank Bikita Minerals (Pvt) Ltd for providing the petalite samples which were used in this research work, and the University of Pretoria for the facilities.

I also want to thank the Fluorochemical Expansion Initiative (FEI) for financial assistance.

I thank to my colleagues in the research group and friends at the University of Pretoria for their technical assistance during the ICP training and Clem Kadima, John Kabangu and Christian Bondo for valuable discussions.

Finally, my heart-felt appreciation goes to my loving family: my parents Vincent-Kalala Mwepu and Gertrude-Kabeya Kalenga, my brothers, and above all God.

This dissertation is dedicated with love to my younger brother Josue-Mwepu Ngoie who passed away while I was working on this project.

List of figures

List of tables

Contents

Abbreviations

S-L	Solid-liquid ratio
UV	Ultraviolet
ICP-OES	Inductively coupled plasma optical emission
XRF	X-ray fluorescence
XRD	X-ray diffraction
LCE	Lithium carbonate equivalent
SEM	Scanning electron microscope
TGA	Thermogravimetric analysis
ABF	Ammonium bifluoride
AHFS	Ammonium hexafluorosilicate

1 Introduction

1.1 Background

Since the end of World War II lithium production has increased due to a number of its uses, including the production of batteries, ceramics and glass. An annual increase of 9.7% in lithium demand is projected for the foreseeable future (Hien-Dinh et al., 2015, Hien-Dinh, 2015).

Recent years have shown an increase in the exploration of sources such as geothermal brines and clays, pegmatite in the United States, and oil brines in Canada and Australia (Jandova et al., 2012, Virolainen et al., 2016, Bradley and Jaskula, 2014).

The most common sources of lithium are salts in surface and subsurface brines as well as pegmatite minerals. These are considered as the most economically viable Li-containing minerals in the world (Vu et al., 2013, Garrett, 2004, Linnen et al., 2012). Lithium deposits are also found in minrals such as:

- Spodumene ($LiAlSi_2O$) at Bernic Lake (Manitoba, Canada) for (Heinrich et al., 1978);
- Zinnwaldite, $KLiFeAl(AlSi_3O_{10})(F,OH)_2$, in Russia in the Omchikandja mine and Yakutija and Krušnéhory, Cinovec area in the Czech Republic;
- Lepidolite, $K(Li,Al)_3(Si,Al)_4O_{10}(F,OH)_2$, in Zimbabwe at Bikita;
- Amblygonite, $LiAlPO_4F$, at several deposits in the world such as, South Africa, Rwanda, Brazil, Canada, Surinam, Zimbabwe, Mozambique, Namibia, California (Garrett, 2004);
- Petalite ($LiAlSi_4O_{10}$) found in Minas Gerais, in Western Australia, Aracuai in Brazil, Karibib in Namibia, Manitoba, Canada, Bikita, Zimbabwe.

Several mining activities based on the treatment of these minerals are found around the world:

- Greenbushes (Australia);
- Kings Mountain (North Carolina);
- Etta mine (Black Hills, South Dakota);
- Harding mine (Dixson, New Mexico);
- Strickland Quarry (Portland, Oregon);

- Pala (California);
- Bernic Lake mine in the central part of Canada in Manitoba;
- Karibib in Namibia;
- Minas Gerais in Brazil;
- Gonçalo in Portugal.

Petalite is one of the most important commercial Li-containing minerals and sources of lithium. Zimbabwe has a major deposit of petalite, $LiAlSi_4O_{10}$, at the Bikita mine. Zimbabwe is also known as one of the major producers of lithium concentrates among other countries in the world and its lithium reserve is estimated at 23000 Mt lithium. Other minor deposits in Zimbabwe are Matobo, Mazoe, Mutoko, Kamativi, Insiza, Mutare and Hwange districts (Sitando, 2012).

Petalite is also found in Kenora Ontario Canada, Karibib in Namibia, Aracuai in Brazil; Londonderry in Australia, Zavitinskoye in East Transbaikalia in Russia, and Utö in Sweden. (Sitando and Crouse, 2012, Garrett, 2004).

Petalite can be used to produce lithium and lithium compound like lithium carbonate (Li_2CO_3), lithium chloride (LiCl) and lithium fluoride (LiF).

Lithium is used in many industries with the highest contribution to glass, ceramics and the production of lithium ion batteries. The reasons for using lithium carbonate or other lithium compounds in the glass and ceramic manufacturing are to:

- lower the melting point to reduce the consumption of energy;
- to improve the strength of the glass product;
- to reduce the viscosity during manufacturing.

In battery production, lithium is mostly used in electrode materials and as electrolyte in rechargeable lithium ion batteries (Sitando, 2012).

Lithium is sold as mineral concentrates, brines, lithium compounds or lithium metal depending on the application. Consumption of lithium related products have increased significantly with suppliers predicting an up to 31 % increase of sales from 2011 to 2025 (Virolainen et al., 2016).

Lithium carbonate is considered as the precursor of other lithium compounds and as a feed chemical for lithium metal production (Jandová et al., 2010). Lithium fluoride finds applications in specialised UV optics, ceramic and the aluminium smelting process. Lithium chloride has applications as a source of lithium metal by electrolysis of LiCl/KCl at 450 °C or as a flux for aluminium in automobile parts and a desiccant for drying air streams. Lithium hexafluorophosphate ($LiPF_6$) is highly soluble in nonpolar solvents and is widely used as an electrolyte in lithium batteries.

Many studies on treatment of lithium minerals such as petalite, zinnwaldite lepidolite have been developed in recent years (Hien-Dinh, 2015, Hien-Dinh et al., 2015). The growing market demand for high purity lithium carbonate is attributed to its use in lithium ion batteries as well as electrodes in common batteries as well as many other applications (Hien-Dinh et al., 2015).

The global market has been estimated to increase by more than 20 % per year in the past few years because of the use of lithium-ion batteries: batteries (46 %), ceramics and glass manufacturing (27 %), lubricating greases (7 %), primary aluminum production (7 %), air treatment (2 %), continuous casting (4 %), rubber and thermoplastics (5 %) and other uses (9 %) (Daitch, 2018) .

The growing demand for pure lithium is also attributed to the fact that recent developments in telecommunication, where rechargeable lithium batteries power the majority of cellular phones and laptop computers, excel the need of minerals containing lithium (Hien-Dinh et al., 2015).

Traditionally lithium extraction is based on high temperature chemical roasting using sulfuric acid, dissolution in hydrochloric acid and purification with calcium sulfate and calcium hydroxide (limestone). The lithium is precipitated with sodium salt to lithium minerals (Wietelmann and Bauer, 2003, Kondás et al., 2006, Sitando, 2012, Sitando and Crouse, 2012). All these processes are used to transform lithium minerals or concentrate into a soluble form to produce lithium chemicals with a high-purity such as 99.9 % lithium carbonate. (Jaskula, 2015, Choubey et al., 2016).

The traditional acid roasting process requires a phase transformation of α-spodumene into β-spodumene at high temperature (1 100 °C). β-spodumene is soluble in sulfuric acid at 250 °C. This is followed by water leaching at 90 °C (Choubey et al., 2016, Sitando and Crouse,

2012, Hien-Dinh et al., 2015, Rosales et al., 2016). The use of sulfuric acid is preferred because of its availability in the market and is cheaper and easier to handle compare to HCl. The disadvantage of using HCl is that many other impurities also dissolve during the roasting, therefore the purification process becomes more complex (Sitando, 2012, Sitando and Crouse, 2012).

The lime-based extraction of lithium also requires roasting of the lithium minerals and lime at 1 030 to 1 040 °C, followed by water leaching of the clinker (Hien-Dinh et al., 2015). This process has been applied commercially by Foote Mineral Company in order to produce lithium hydroxide. All these lithium extraction methods adopt high temperature calcination for phase transformation from α-spodumene into β-spodumene and are energy-consuming and costly (Kuang et al., 2012, Guo et al., 2019).

Petalite extraction is energy intensive, requires various chemicals and is time consuming. These problems often render the extraction of lithium from petalite, at a large scale, not economically viable.

1.2 Aim of the study

The overall aim of the study was to develop a refined process, continuing previous work done in the Department, for the extraction of lithium from Bikita petalite. The specific objectives were:

- To investigate the possibility of using of ammonium bifluoride digestion at different temperatures without thermal pretreatment;
- To optimize the acid leaching process;
- To optimize the purification process after the leaching;
- To determine the optimum precipitation conditions of lithium carbonate after purification, with respect to its yield and purity.

1.3 Scope of research

The scope of this research project included:

- Chemical characterisation of the petalite using ICP-OES and XRF;

- Mineralogical characterisation using XRD;
- Determine of optimum digestion conditions using ammonium bifluoride;
- Optimise the acid roasting and leaching conditions;
- Optimisation of the solution purification conditions;
- Precipitation of Li_2CO_3 to ensure a high yield of product;
- Comparing commercial and synthesised Li_2CO_3.

All work was done at bench scale, using petalite sample sizes of less than 100 g.

2 Literature review

2.1 Lithium, its history, properties and sources

2.1.1 Discovery

Lithium, from the Greek *lithos* meaning ‘stone’, was discovered by Johan August Arfwedson in 1817. Arfwedson discovered a new salt by analysing petalite, spodumene and lepidolite from the island of Utö, a township of Haninge in Sweden (Wietelmann and Bauer, 2003, Hien-Dinh et al., 2015).

In 1818, Christian Gmelin (1792-1860) was the first to observe that lithium salts give a bright red flame when burning. However, the two men were unsuccessful in isolating the element as a salt. The element was later isolated by electrolysis of lithium oxide by William Thomas Brande and Sir Humphry Davy. Jons Jacob Berzelius gave it the name lithio. Lithium commercial production started in 1923 by the German company Metallgesellschaft AG via the electrolysis of a rotten mixture of lithium chloride and potassium chloride (Wietelmann and Bauer, 2003).

2.1.2 Properties of lithium

Lithium is the metal with the lowest molecular weight and has a density half that of water. As the other alkali metals, lithium readily reacts with water or air, although not as violent as sodium. It does not exist in the native state in nature. The physical properties of lithium are summarised in Table 1. Being a strong reducing agent, lithium cannot be isolated by reduction of its oxide extracted by aqueous electrolysis (Evans, 2014). Due to these difficulties above, lithium is recovered as lithium carbonate which is used to produce other lithium compounds.

Lithium metal can be produced by electrolysis mixture of potassium chloride and lithium chloride (Garrett, 2004).

Table 1: Properties of lithium (Wietelmann and Bauer, 2003, Bale and May, 1989)

Properties	Values
Symbol	Li
Atomic number	3
Atomic mass	6.941 $g \cdot mol^{-1}$
Melting point	180.54 °C
Boiling point	1 342 °C
Heat of fusion	431.4 $J \cdot g^{-1}$
Hardness	0. 6
Density (at 20 °C)	0.534 $g \cdot cm^{-3}$

2.1.3 Lithium sources

Lithium is considered as the 27th most abundant element in minerals, lake brines, sea water, hard rock, ores and oil residues. The commercial sources of lithium are minerals and brines (Wietelmann and Bauer, 2003, Grady, 1980).

Table 2: Typical analysis of Li_2O content in some minerals (Wietelmann and Bauer, 2003, Sitando, 2012)

Minerals	Li_2O %
Amblygonite ($Li,Al[F,OH]PO_4$)	≥7
Spodumene concentrate ($LiAlSi_2O_6$)	≥7
Spodumene, glass-grade ($LiAlSi_2O_6$)	≥4.8
Petalite ($LiAlSi_4O_{10}$)	≥4
Lepidolite ($K[Li,Al]_3[Al,Si]_4O_{10}F_2$)	≥3.5
Zinnwaldite ($K[Li,Al,Fe]_3[Al,Si]_4O_{10}F_2$)	2.0-5.0
Eucryptite ($LiAlSiO_4$)	4.5-6.5

2.1.3.1 Minerals

Lithium is found in 150 different lithium minerals; however, only few of these are commercially important. Spodumene, petalite, lepidolite, zinnwaldite, amblygonite and eucryptite are used as mineral ore concentrates (Wietelmann and Bauer, 2003, Garrett, 2004). One of the biggest producers of lithium is Australia. Mineral concentrates are used directly in glass and ceramic industries (Bale and May, 1989).Table 2 shows the main lithium containing minerals and their lithium content (Bale and May, 1989).

2.1.3.2 Lithium aluminum silicates

The following minerals belong to the group of lithium aluminum silicates (Brandt and Haus, 2010):

- Spodumene ($LiAlSi_2O_6$);
- Petalite ($LiAlSi_4O_{10}$);
- Eucryptite ($LiAlSiO_4$).

These minerals are discussed in the sections below.

Spodumene ($LiAlSi_2O_6$) is combined with quartz, having a monoclinic pyroxene structure containing SiO_2 chains that are linked together with aluminum ions. The color can vary from white to gray-green. Theoretically the Li_2O content in spodumene is 8.03 %, but due to the presence of Na^+ and K^+ that partially replace Li^+, the lithium concentration is normally between 6 –7.5 %. At different mining sites, analysis revealed that the Li_2O content in spodumene ores is estimated to vary in the range from less than 1% to more than 5 %.

When heated at 1 000 °C, spodumene undergoes an irreversible phase change from α-spodumene to β-spodumene with an increase in volume and decrease in density from 3.2 to 2.4 $g \cdot cm^{-3}$. The transformation renders β-spodumene soluble in acid, thus lithium can be extracted from the ore concentrate. Note that most lithium minerals currently extracted are lithium pegmatites. Pegmatites are known as coarse grained igneous rocks, formed by crystallisation of magmatic fluids in which spodumene (8. 0 % Li_2O) is considered as the most commercial lithium mineral. 50 % of the world's extraction of spodumene is converted through metallurgical processes into Li_2CO_3 (Brandt and Haus, 2010).

Large deposits of spodumene are found in Bikita (Zimbabwe), Greenbushes (Australia), Ontario and Manitoba (Canada) and North Carolina (USA) (Wietelmann and Bauer, 2003, Garrett, 2004).

Petalite ($LiAlSi_4O_{10}$), a member of the feldspathoid group, is also known as castorite, crystallizing as a monoclinic crystal system as white, gray or reddish in color. The theoretical Li_2O content is 4.9 %, but differs at mining areas between 3.5 and 4.5 %.

As mentioned, at 1 100 °C petalite transforms (or decomposes) into β-spodumene and become chemically reactive in an acid or base. In its natural state, petalite is resistant to chemical attack. Lithium extraction via acid leaching can only occurs after the phase transformation.

Large deposits of petalite are found in Bikita (Zimbabwe), Kenora and Ontario (Canada), Karibib (Namibia), Aracuai (Brazil), Londonderry (Australia), Utö (Sweden) and at the Transbalkin area in Russia (Wietelmann and Bauer, 2003, Sitando, 2012, Garrett, 2004).

Eucryptite ($LiAlSiO_4$) has the highest theoretical content of Li_2O at 11. 1 %. In the lithium aluminum silicate group, eucryptite is the rarest and mainly occurs in combination with petalite such as in Zimbabwe at the Bikita mine.

Spodumene and petalite can be distinguished by SiO_2 content (Meshram et al., 2014).

- Spodumene: $LiAlSi_2O_6$ or $Li_2O.Al_2O_3.4SiO_2$;
- Petalite: $LiAlSi_4O_{10}$ or $Li_2O.Al_2O_3.8SiO_2$;

The thermal transformation of petalite into β-spodumene and quartz can be considered as a decomposition reaction (Wietelmann and Bauer, 2003, Garrett, 2004).

2.1.3.3 Micas

The mica minerals are known to be a subgroup of the aluminosilicates, formed by direct crystallization from molten magma. They should be acknowledged to be the results of the pneumatolytic deposits such as lepidolite and zinnwaldite. These minerals are discussed below.

Lepidolite ($K\ [Li,Al]_3[Al,Si]_4O_{10}[F,OH]_2$)

Depending of its origin and weathering conditions, Li_2O content in lepidolite is theoretically between 3.3 and 7.74 %. Some deposits frequently contain 3 – 4 % Li_2O and 3 – 5 % of rubidium and cesium oxides with a color varying from pink to grayish violet.

Large deposits of lepidolite are found in Bikita (Zimbabwe), Bernic lake, (Manitoba, Canada), Karibib (Namibia), Mina Gerais (Brazil) and Sociedad Mineria de Pegmatite (Portugal) (Wietelmann and Bauer, 2003, Garrett, 2004).

Zinnwaldite ($K[Li,Al,Fe]_3[Al,Si]_4O_{10}[F,OH]_2$)

Based on the chemical formula, zinnwaldite can be considered as a variety of lepidolite with a high iron content. The Li_2O content varies at the different mining areas. The emerald known as cryophyllite contains up to 5 % Li_2O (Wietelmann and Bauer, 2003).

2.1.3.4 Lithium phosphates

Amblygonite is a complex phosphate with the general formula $(Li,Na)Al(FOH)PO_4$. Pure amblygonite ($LiAlFPO_4$) has a theoretical Li_2O content of 10.1 %, montebrasite ($LiAl(OH)PO_4$) 10.3 %, with triphyline ($LiFePO_4$) and lithiophilite ($LiMnPO_4$) 9.5 % Li_2O.

They are the principal constituents of amblygonite, which is milky white to gray in color. Amblygonite deposits have a Li_2O content varying between 7 – 9 %. However, amblygonite does not occur in large accumulation. Most of the time the mineral is associated with other lithium minerals.

With the discovery of new minerals, amblygonite is no longer considered as a suitable source for lithium production. Due to the small deposits, triphyline and lithiophilite have not been exploited for industrial production.

Deposits of amblygonite are found in Rwanda, Zimbabwe, Canada, Namibia, South Africa, and the United States of America (Wietelmann and Bauer, 2003, Garrett, 2004).

2.1.3.5 Lithium in natural brines

In the last decade, lithium-containing brines have been considered as one of the most important sources of lithium chemicals production. Sources such as lakes, seawater, oil-field waters and geothermal waters are considered as the biggest sources of lithium and lithium chemicals. In brines, lithium chloride can be concentrated naturally by evaporation using solar energy as shown in Figure 1 (Wietelmann and Bauer, 2003, Garrett, 2004, Brown and Beckerman, 1990).

Figure 1: Aerial photograph of a lithium brine operation in the Salar de Atacama, Chile extracted from (Brown et al., 2016)

According to Jaskula (2011), brines are the biggest source for lithium carbonate production with a lower production cost compared to ore extraction. Lithium brines are processed and found in Salar de Atacama (Chile), Argentina in South America, USA and China (Wietelmann and Bauer, 2003, Brandt and Haus, 2010). The disadvantage of brines is that it contains low lithium concentrations as shown in Table 3.

Table 3: Brine reserves and deposits (Dinh, 2015)

Country	Deposit	Li,wt%,	Predicted resources (Mt)
	Cauchari	0.062	0.9
	Diablillos	unstated	0.9
Argentina	Olaroz	0.09	0.2 – 0.3
	Rincon	0.04	0.5 – 2.8
	Salar del Hombre Muerto	0.062	0.8 – 0.9
	Sal de Vida	unstated	0.3
Bolivia	Salar de Uyuni	0.096	5. 5-10. 2
Canada	Beaver hill Lake	unstated	0.52 – 0.59
	Fox Creek	0.01	0.5
Chile	Maricunga	0.092	0.2 – 0.4
	Salar de Atacama	0.14	3 – 35.7
	Dangxioncuo / DXC	0.045	0.1 – 0.2
China	Lake Zabuye	0.097	1.3 – 1.5
	Qaidam / Qinghai /	0.03	1 – 3.3
India	Sua Pan	0.002	unstated
Israel	Dead Sea	0.002	2
	Bonneville Salt Flats	0.004	unstated
	Brawley	unstated	1
	Great Salt Lake	0.006	0.5
USA	Salton Sea	0.022	1 - 2
	Searles Lake	0.0083	0.03
	Clayton Valley / Silver	0.03	0.3
	Smackover	0.038	0.75 - 1

2.1.3.6 Clay deposits

Lithium bearing clays are considered as one of the most important sources of lithium and are generally found near the surface. In such cases, open-pit mining can be used for lithium

extraction. No blasting is normally necessary due to the relatively soft nature of the clays. (Brown et al., 2016)

Hectorite [$Na_{0,33}(Mg,Li)_3Si_4O_{10}(F.OH)_2$] is an example of one of these clays, containing a high-magnesium-lithium content. The lithium concentration varies between 0.24 and 0.53 % (Garrett, 2004).

Commercial hectorite processing is both expensive and difficult, compared to mineral and brine processing (Garrett, 2004).

2.1.3.7 Lithium reserves

Lithium reserves in the world (Brine and pegmatite deposits) are found in Australia, Canada, Portugal and Brazil, see Table 4. Zimbabwe has the largest pegmatite deposit containing a significant amount of lithium in Bikita pegmatite. Pegmatite is defined as an igneous rock composed of interlocking mineral grains (Brandt and Haus, 2010).

Table 4: The reserve estimations of lithium in the world (Martin et al., 2017)

Country	Reserves (1000 Mt Li)
Chile	7500
China	540
Argentina	800
Australia	580
Brazil	190
USA	38
Zimbabwe	23
Portugal	10

Other countries not mentioned above have lithium deposits but in much lower quantities and their deposits are not currently exploited or mined.

Petalite from the Bikita mine, situated in Masvingo Province, Zimbabwe, was used during this project. The mining area (pegmatite area) is located 75 km east of Victoria and 64 km North-East of Masvingo as shown in Figure 2 and Figure 3 below (Garrett, 2004).

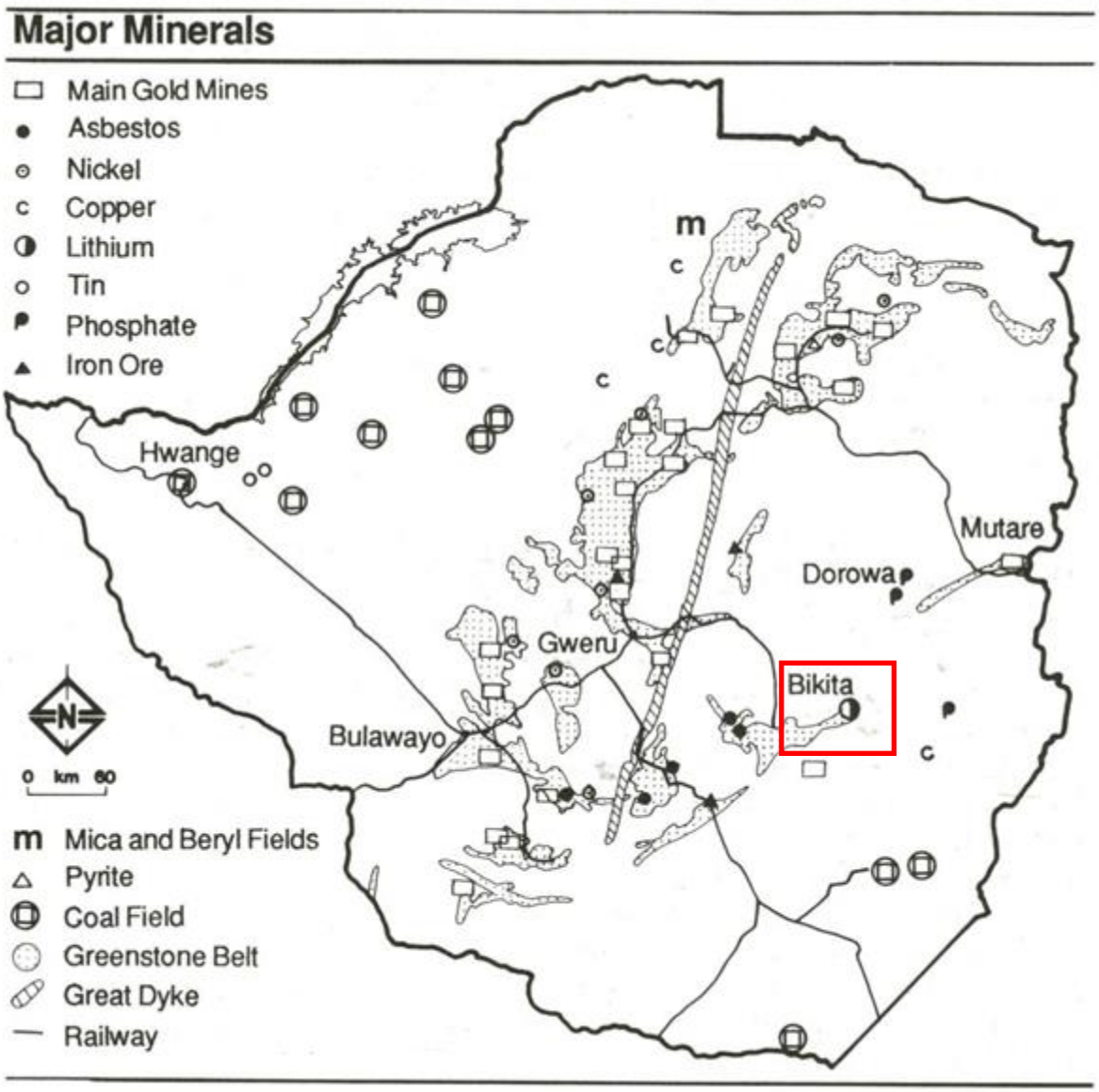

Figure 2: Major minerals and their mining areas in Zimbabwe

ZIMBABWE

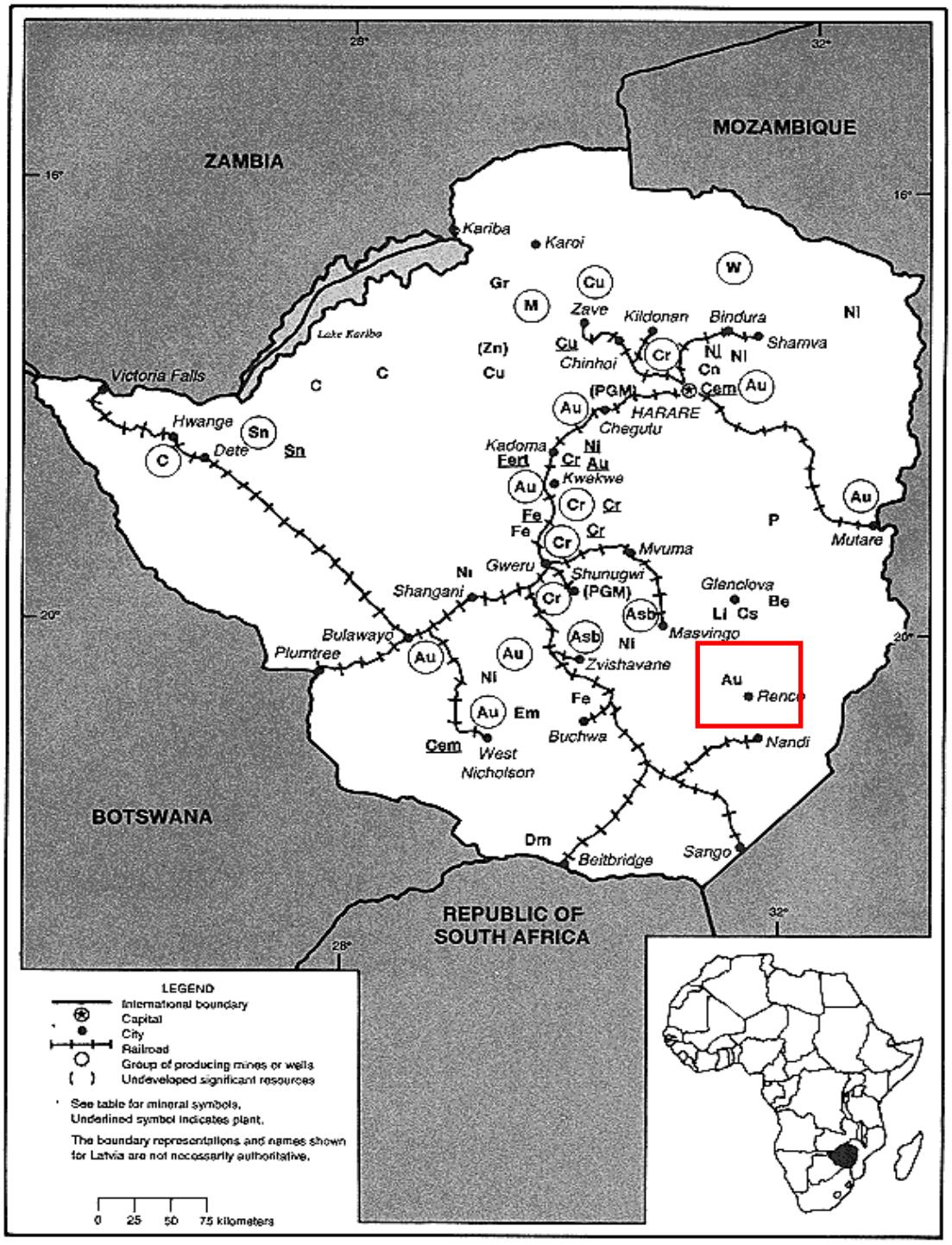

Figure 3: Mineral deposits in Zimbabwe

This pegmatite area is divided into four sectors, represented as: Al Hayat, Bikita, Southern, and Nigel and are distinctly zoned (Garrett, 2004, Cooper, 1964). It has been proved that this deposit is a commercial viable lithium deposit. In 1961 the estimated reserves were 6 million tons at 3.5 % Li, in 1979 it was estimated at 12 million Mt with an average grade of 1.4 % Li. In 2002 the estimated reserves were 23 million Mt (Garrett, 2004, Cooper, 1964).

Lithium and cesium minerals are distinctly zoned according the order of abundance in the pegmatite area. The lithium minerals are petalite, lepidolite and spodumene. Other minerals are pollucite ($H_2O,2Cs_2O,2Al_2O_3,9SiO_2$), beryl ($Be_3Al_2(SiO_3)_8$), eucryptite ($LiAlSiO_4$), amblygonite and bikitaite ($H_2LiAlSi_2O_7$) (Garrett, 2004).

The Al Hayat sector contains the largest petalite deposit with up to 20 to 100 % of the lithium-bearing part of the pegmatite (Cooper, 1964).

The Bikita sector is similar to the Al Hayat sector with lepidolite, spodumene, petalite and amblygonite as the dominant lithium minerals (Garrett, 2004).

The structure of pegmatite in the south-eastern sector is revealed to be more complex than the other sectors due to the fact that the intermediate zones are covered by rubble on the surface and some lepidolite intergrown with albite occurs. This sector also contains fine-grained minerals such as albite, lepidolite, and quartz and occasionally muscovite (Cooper, 1964).

From the above description, the Al Hayat sector is the most prolific source of petalite with lesser amount of spodumene and lepidolite, while Bikita sector and south-eastern sectors are considered as a potential source of lepidolite and beryl, with lesser volumes of spodumene, amblygonite and some petalite (Cooper, 1964).

2.2 Lithium applications and market detail

The most common lithium chemical used is lithium carbonate. It is mostly used in glass and ceramic manufacturing, as well as the production of lithium ion batteries. The reasons of using lithium carbonate or lithium compounds in glass and ceramic manufacturing are (Bale and May, 1989) :

- to lower the melting point;

- to reduce the energy consumption;
- to improve the strength of the glass; and
- to reduce the viscosity during manufacturing.

In battery production, lithium is used as energy storage devices such as rechargeable lithium ion batteries because of its high electrode potential, low atomic mass, high charge- and power-to-weight ratio. Lithium-ion batteries can generate approximately 3 volts per cell, compared with 2.1 volts for lead-acid or 1.5 volts for zinc-carbon cells.

Other lithium applications are (Garrett, 2004):

- Steel castings to provide thermal insulation and ensures the lubrication of the surface of the steel in the continuous casting process;
- Iron castings where lithium reduces the effect of veining, thereby reducing the number of defective casts in applications, such as engine blocks.

The estimated lithium global market in 2015 is given in Table 5 below.

Table 5: Estimation of the global lithium market in 2015 (Martin et al., 2017)

Application	Percentage (%)
Glass and ceramics	32
Batteries	35
Lubricating greases	9
Continuous casting	5
Air treatment	5
Primary aluminium production	1
Other uses	13

2.2.1 Lithium applications

A wide variety of lithium compounds are sold commercially. It is subdivided into the most known compounds, namely 33 inorganic lithium chemicals and 36 organic lithium compounds. Other are available upon request (Garrett, 2004). The compound used most is lithium

carbonate, with many applications in industry, with the highest contribution to glass and ceramic manufacturing, and the production of lithium ion batteries (Lee, 2015).

According to Garrett (2004), since 1993, 50 % of the lithium used was as lithium carbonate and only 20 % as lithium hydroxide. Other lithium chemicals with industrial importance are butyl-lithium (C_4H_9Li), lithium metal, and lithium chloride (Brown et al., 2016, Ober, 2007). It should be noted that the majority of these compounds are produced by processing lithium carbonate. Lithium metal is produced by electrolysis of a molten lithium chloride/potassium chloride mixture. Potassium chloride acts as a solvent and supports the electrolyte. The electrolytic cell is constructed with a cathode made of steel where the molten lithium is produced, and the carbon anode where the chlorine evolves (Garrett, 2004).

Lithium carbonate (Li_2CO_3) has a white colour, widely used to produce other metal oxides, has a density of 2110 $kg \cdot m^{-3}$ and a melting point of 723 °C (Brown et al., 2016). Lithium carbonate can be produced from lithium sulphate or lithium chloride after extraction of the concentrate material. The resulting solution is treated with sodium carbonate to precipitate Li_2CO_3. The powder is washed with hot water to remove contaminants like sodium chloride or sodium sulphate (Evans, 2014).

Lithium chloride (LiCl) is produced in the same manner as lithium carbonate, dissolving the concentrate with hydrochloric acid. The insolubles are filtered and lithium chloride precipitated (Brown et al., 2016). It is reported that LiCl is used in applications as a component of fluxes for transition-metal alloys, chemical fluxes pre-deposited on the path of gas tungsten electric arcs in order to increase weld penetration, arc temperature and arc voltage (Ebensperger et al., 2005, Marya and Edwards, 2002). LiCl is a white solid with a density of 2.068 $g \cdot cm^{-3}$ and a melting point of 605 °C (Kipouros and Sadoway, 1998).

Lithium bromide (LiBr) is a hygroscopic chemical compound, attracts and retains water molecules and therefore useful as a desiccant in air conditioning system (Brown et al., 2016). LiBr is made in the same way as lithium chloride. It is used in organic chemical reactions where Li_2CO_3 is dissolved in hydrobromic acid and the pH of the solution adjusted to more than 7. LiBr can also be produced by reacting Li_2CO_3 or lithium hydroxide with bromine (Garrett, 2004).

Lithium hydroxide is an inorganic compound with the chemical formula LiOH. This compound is available as anhydrous or monohydrate with the formula as $LiOH.H_2O$. LiOH is produced in metathesis reactions between Lithium carbonate and calcium hydroxide according to Reaction 1:

$$Li_2CO_3 + Ca(OH)_2 \rightarrow 2LiOH + CaCO_3 \quad (1)$$

According to Garrett (2004), LiOH is used in the grease industry. It provides good lubricating properties for bearing surfaces due to fact that it is water insoluble, stable over a wide shear range and temperatures between -55 and 200 °C. These greases are used for military, industrial, automobile, marine and aircraft applications. In addition, LiOH is used as an additive in dyestuffs and fluxing agent in inorganic pigments by increasing the brilliance of specific pigments.

LiOH has a melting point of 462 °C, with density of 1.46 $g \cdot cm^{-3}$ for the anhydrous form and 1.51 $g \cdot cm^{-3}$ for the monohydrate respectively (Brown et al., 2016).

Lithium fluoride has the chemical formula LiF. It is used as a flux for glass but mainly as a component of molten salts in the form of potassium bifluoride (Garrett, 2004),

Fluorine electrolysis is more efficient when the electrolyte contains a few percent of LiF. The importance of using LiF in this case is possibly because it facilitates the formation of lithium-carbon-fluorine on the electrodes (Garrett, 2004).

LiF is also used in UV optics because it has the highest UV transmission of all material. LiF is known to be more transparent to short UV wavelength than any other material. LiF is used in the battery industry as a precursor to prepare lithium hexafluorophosphate which is an electrolyte in lithium ion batteries (Sitando, 2012).

In organic compounds, lithium is used as a catalyst in the production of synthetic rubbers, plastics and pharmaceuticals. Lithium alkyls such as N-butyl lithium can be prepared via the reaction of the desired alkyl halide (usually the chloride) with finely lithium metal dispersed in a hydrocarbon solvent (Garrett, 2004).

As a catalyst, N-butyl lithium is used to initiate or to facilitate the reactions between two compounds as in the case of styrene and butadiene in order to form abrasion-resistant synthetic rubbers that require no vulcanization (Ober, 2007).

Ober (2007) reported that lithium metal and lithium compounds are used in the medical field as catalysts in the production of analgesic, anticholesterol agents, antihistamines, contraceptives, sleep inducers, steroids, tranquilizers and Vitamin A. Lithium carbonate is used in pharmaceutical-grade treatment of manic-depressive psychosis (Mohandas and Rajmohan, 2007).

In metallurgy, during the electrolytic reduction of aluminum dissolved in a cryolite bath, lithium carbonate has the advantage for reducing the melting point of the cryolite bath, lowers the temperature of the cells and increases the electrical conductivity of the cell (lowering the require overvoltage). It reduces the fluorine emissions from the electrolytic cells by 25 - 50 % and saving energy and lowers cost (Ober, 2007, Ebensperger et al., 2005, Garrett, 2004, Jandová et al., 2009).

Li_2CO_3 reacts with the cryolite (Na_3AlF_6) solvent present in the electrolytic cell to form lithium fluoride to present a very high fluxing ability, electrical conductivity and low volatility (Garrett, 2004, Jandová et al., 2009).

During the manufacture of specialized aircraft parts, lithium is alloyed with metals like aluminum, cadmium and copper to reduce weigh, allowing fuel saving during the lifetime of the aircraft (Brown et al., 2016, Srivatsan and Sudarshan, 1991). The aluminum–lithium alloy shows remarkable properties. For example lithium addition to aluminum can decrease the density and improve the stiffness compared to conventional aluminum alloys of comparable strength in the aircraft industry (Srivatsan and Sudarshan, 1991).

The Figure 4 below gives schematics of the products derived from Li_2CO_3 and Figure 5 gives a picture cost of the applications of lithium, for each industry sector.

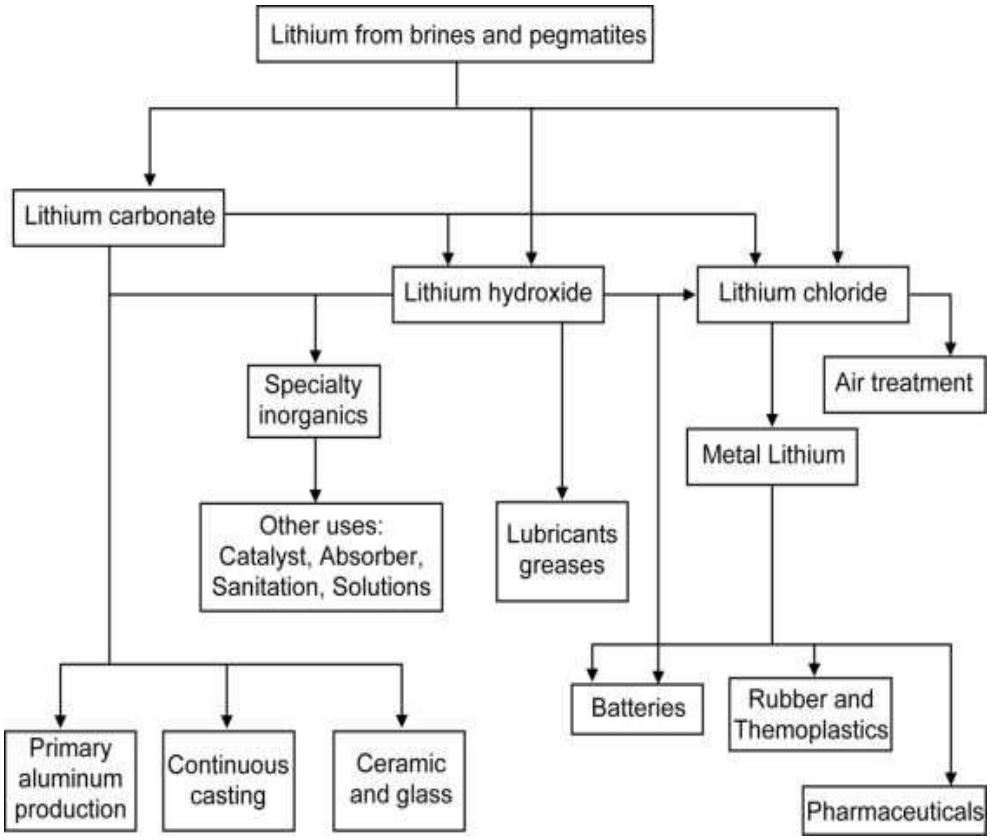

Figure 4: Industrial application of lithium and lithium compounds (Dinh, 2015)

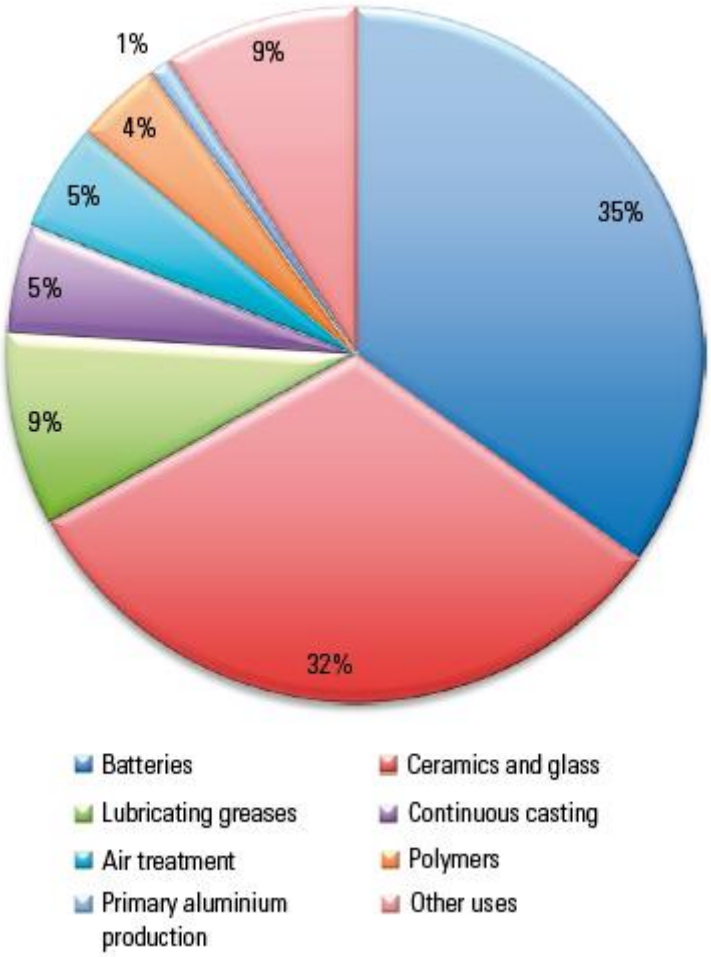

Figure 5: The estimation of global market of lithium in 2016 (Brown et al., 2016)

For all the lithium compound mentioned above, lithium carbonate is considered as the starting industrial material for the production of all lithium chemicals, including lithium metal (Jandová et al., 2009)

2.2.2 Lithium market

According to Vikström et al. (2013), the USA was the main producer of lithium between the 1950s and the midst of 1980s. In 1997, there was a 50 % decline in the Li_2CO_3 price because of the high volume of lithium produced from brine (Ebensperger et al., 2005).

Since 2001, the lithium market has shown a remarkable increase due to the use of lithium in rechargeable batteries for electronic devices and electric vehicles, with China as a big consumer. Rechargeable lithium ion and lithium polymer batteries are now used in mobile

telephones, laptop batteries and digital cameras, replacing nickel cadmium and nickel metal hydride batteries (Ebensperger et al., 2005, Peiró et al., 2013, Lee, 2015).

According to Ebensperger et al. (2005), factors influencing the demand of lithium are society based uses over a period which is the reflection of the demand of compounds that contain lithium as an input. The increased demand of lithium compounds has been done mainly to the battery industry and lithium alloy production, especially in aluminum used in the aerospace industry.

Staiger and Rödel (2016) reported that the production of lithium, measured as lithium carbonate equivalent (LCE), which is considered a universal conversion factor for all above mentioned lithium compounds, is around 175 000 tones LCE. According to projections, this number will increase to 300 000 tones LCE by 2020 and over 400 000 tones LCE by 2025 as shown in the Figure 6 below.

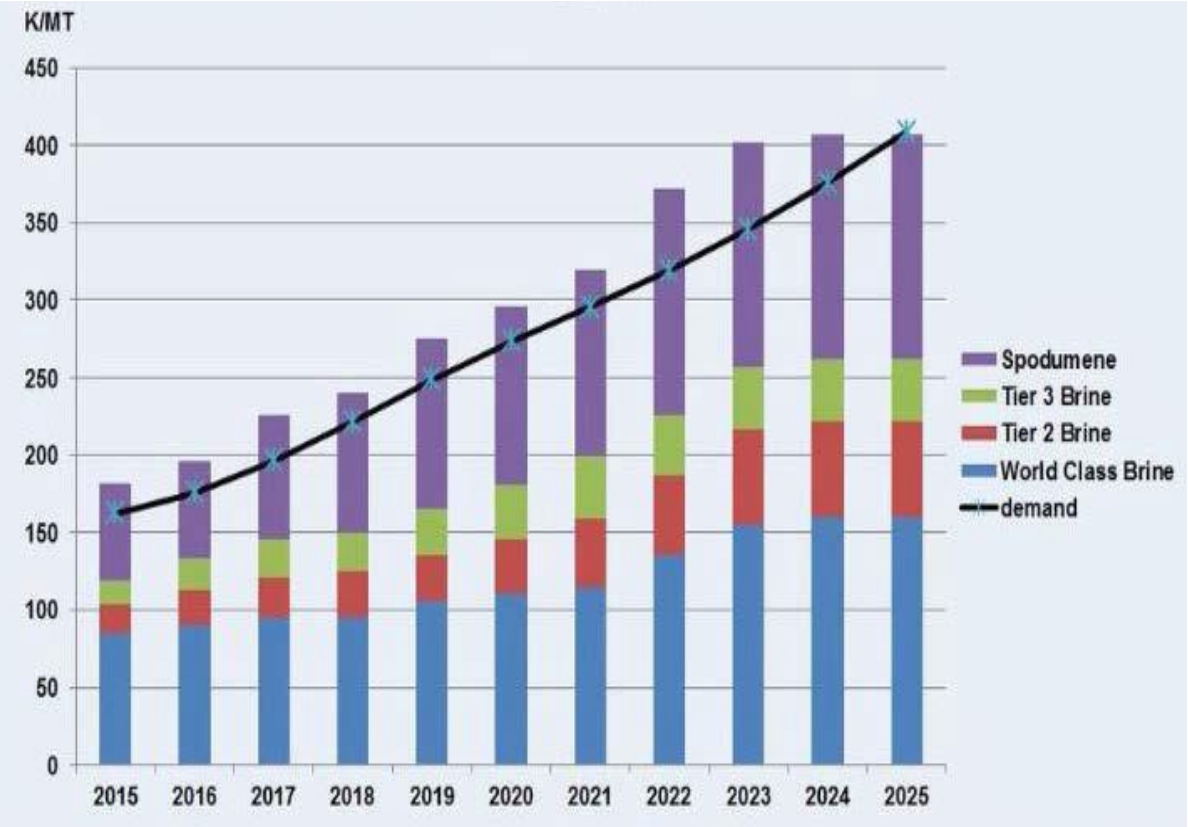

Figure 6: Global LCE supply and demand

Consumption of lithium increased from less than 100 tons of LCE per annum in the early 1900s to more than 70 000 tons per annum one hundred years later (Ebensperger et al., 2005). In addition, this consumption is justified by the fact that lithium metal, lithium carbonate, lithium bromide, lithium chloride, lithium hydroxide and other compounds are used in many industrial applications as shown in the Figure 7 below.

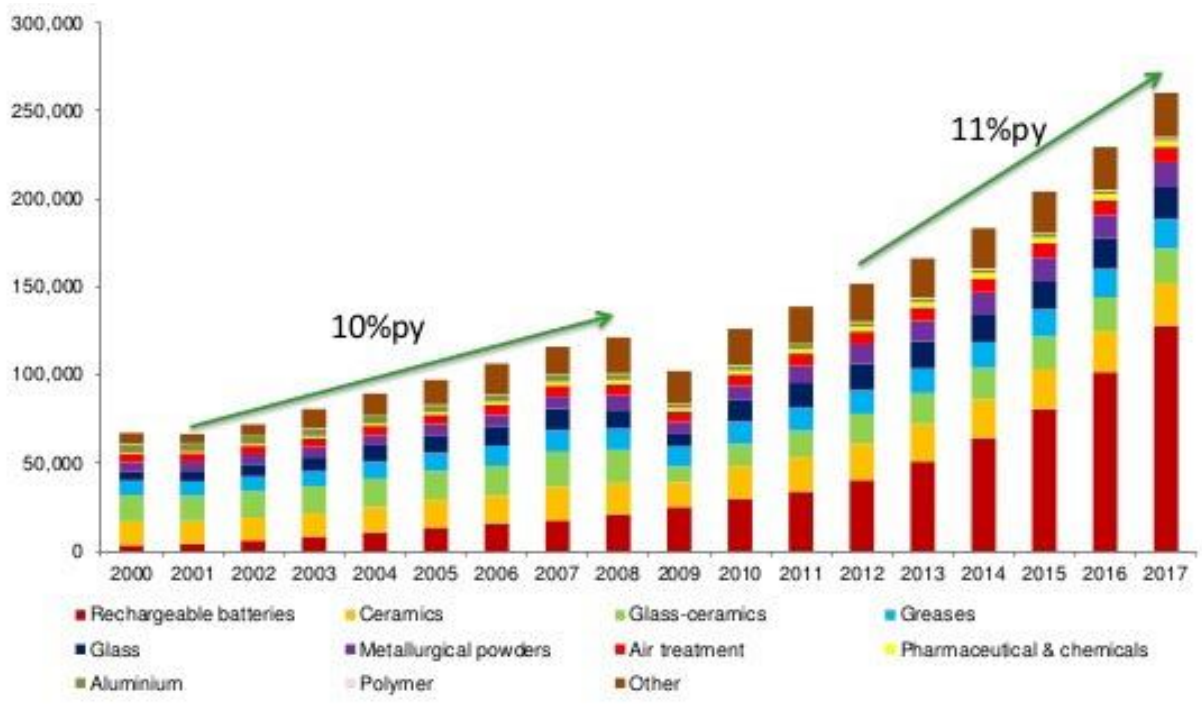

Figure 7: World consumption of lithium by end use

2.3 Lithium ore concentrate processing

2.3.1 Lithium processing technologies

Lithium from pegmatite minerals can be recovered through processes such as acid roasting, purification and precipitation.

However, the minerals amblygonite and triphyline can be treated directly with an appropriate digestion agent, but others like spodumene,lepidolite and petalite require pretreatment in order to change the phase from α-spodumene into β-spodumene at high temperature in the range 1000 – 1100 ^{o}C (Wietelmann and Bauer, 2003).

2.3.2 Lithium extraction

The extraction process of lithium starts with crushing and grinding of the ore to reduce the particles size to between 20 to 80 mm. A flotation process is used to increase the concentration of lithium ore. The concentrated lithium (60 % – 80 %) ore is then leached with sulfuric acid.

2.3.3 Acid digestion process

The fundamental of all processes based on lithium extraction is to convert lithium into soluble form. Depending on the digestion process, the end product will be either lithium carbonate, lithium chloride or lithium hydroxide (Wietelmann and Bauer, 2003). Different methods are used to process lithium after pre-treatment at high temperature. The ore concentrate is usually processed by using acid leaching in order to dissolve lithium.

The sulfuric acid digestion can be applied on a lithium ore before further processing. The sulfuric acid process is based on the decomposition of the material at temperatures varying between 250 - 400 ^{o}C as shown in the reaction below (Wietelmann and Bauer, 2003, Sitando, 2012, Kondás et al., 2006):

$$Li_2OAl_2O_34SiO_2\,(s)+H_2SO_4 \rightarrow Li_2SO_4\,(s) + Al_2O_34SiO_2\,(s) + H_2O\,(g) \qquad (2)$$

Acid digestion is followed by hot water leaching to produce a solution of lithium sulfate containing an insoluble residue. In most cases, the resulting solution is contaminated with some soluble metals such as aluminum, calcium, iron, magnesium and other impurities which can be removed by pH control (Garrett, 2004, Wietelmann and Bauer, 2003). The purified solution is then evaporated near the boiling point to take advantage of the decreasing solubility of lithium carbonate at higher temperature varying between 90 – 100 ^{o}C (Wietelmann and Bauer, 2003).

According to Wietelmann and Bauer (2003), the sulfuric acid extraction process gives a high extraction yield and has a relatively favorable energy balance compared with other processes. This is because HCl is a highly aggressive leaching agent compared to H_2SO_4 and can also be used. The disadvantage of using HCl is that more impurities will be dissolved and the purification will be more complex (Garrett, 2004).

Jandová *et al* reported a high lithium extraction of 96 % in 2009 and 90 % in 2010 after roasting zinnwaldite waste with $CaSO_4$ and $Ca(OH)_2$ at 950 °C or $CaCO_3$ at 825 °C.

Lithium extraction yield of 95 % using HCl gas during lepidolite roasting at 910 °C (Löf and Lewis, 1942). The resulting product was characterized as a mixture of LiCl and other impurities. LiCl was purified by distillation, fractional crystallization and solvent extraction to obtaining LiCl as a final product.

However, the two processes mentioned above require high temperatures and have little significance compare to the sulfuric acid process. The Table 6 below shows the lithium extraction yields from different processes.

Table 6: Lithium recovery for different processes

Reference	Mineral	Roasting		Leaching		Li recovery %	Final product
		Additive	Temp ^oC	Solvent	Temp ^oC		
Jandová *et al*., 2009	Zinnwaldite	$CaSO_4$ and $Ca(OH)_2$	950	H_2O	90	96	Li_2CO_3
Jandová *et al*., 2010	Zinnwaldite	$CaCO_3$	825	H_2O	90–95	90	Li_2CO_3
Löf & Lewis, 1942	Lepidolite	HCl gas	910	Li was extracted as gas		95	LiCl

The motivation of using sulfuric acid as a roasting agent is dictated by the availability of the acid and is commercially most common (Garrett, 2004). According to Jandová et al. (2010), lithium recovery from spodumene, petalite and lepidolite, sulfuric acid is considered a better process, providing a high lithium extraction yield between 70 and 97 % depending on the lithium starting mineral.

2.3.4 Alkali digestion

Calcination with limestone and digestion of the mineral are done in a single operation. The mixture is dried and heated with excess lime to produce a clinker, calcium orthosilicate and lithium aluminate. The clinker is grounded and leached with water. The process is highly temperature dependent at 1 040 °C (Wietelmann and Bauer, 2003, Yan et al., 2012). When the temperature is too high, it results in a glassy clinker which hinders subsequent leaching of lithium hydroxide. When it is too low, the process will result to incomplete reaction. Lithium hydroxide is leached with water followed by filtration. The resulting solution is evaporated to crystallise lithium monohydrate or lithium hydroxide (Kondás et al., 2006). This process has a high energy requirement and gives a lithium yield appreciably lower than sulfuric acid process (Wietelmann and Bauer, 2003).

2.3.5 Ion exchange

Ion exchange processes are based on heating the lithium ore with sodium or potassium salts. In advanced hydrothermal decomposition processes, solutions containing Na_2CO_3, NaOH, Na_2SO_4 at elevated temperatures and high pressures are used (Wietelmann and Bauer, 2003, Kondás et al., 2006). The heating process will lead to replacement of Li^+ ions with Na^+ or K^+ with formation of a water soluble lithium salt. Due to the elevated temperature and high pressure, the process is no longer attractive compared to the acid digestion process.

2.3.6 Gypsum process

The gypsum process is used for the decomposition of lepidolite and zinnwaldite with a mixture of calcium sulfate and calcium oxide and/or with calcium hydroxide. The resulting product is water-soluble lithium carbonate (Kondás et al., 2006).

2.3.7 Sulfate process

This method is used for processing of lepidolite and clays (Dinh, 2015, Kondás et al., 2006). It is a high temperature decomposition of lithium minerals with potassium and/or sodium sulfate. The resulting product is lithium carbonate (Kondás et al., 2006).

2.3.8 Leaching process

In hydrometallurgy processes, leaching is known as a primary extractive operation by which a metal of interest is transferred from concentrate minerals into an aqueous solution. The process involves the selective dissolution of valuable minerals, in which the ore concentrate is brought into contact with an active chemical solution known as a leach solution (Muzenda et al., 2011, Smit, 2001).

For a lithium extraction process to be successful, parameters such as particle size, nature of the solvent, temperature and agitation speed are very important (Coulson and Richardson, 1996).

Particle size plays a major role to facilitate the chemical reaction. The valuable metals must have small enough particles in order to be physically exposed to the leach solution. The most important is the degree of exposure of the mineral to ensure complete leaching of a mineral grain in an ore. The degree of exposure influences the rate at which leaching proceeds. In addition, when the particles have a smaller size, the interfacial area between the solid and liquid will also be greater, and therefore will lead to a high rate of material transfer because the solute have a small distance to diffuse within the solid. Generally, the rate of leaching increases with decreasing particle size (Smit, 2001, Coulson and Richardson, 1996).

The solvent used for the leaching process should be selective to lithium and its viscosity should be sufficiently low in order to facilitate its flow during the contact with the solid. HCl is known as an aggressive leaching agent that also dissolves impurities and renders the purification process more complex (Garrett, 2004, Coulson and Richardson, 1996). H_2SO_4 and water are less aggressive and hence more selective than HCl.

Temperature has a big effect on the lithium dissolution rate by increasing the leaching rate. In most cases, the solubility of the metal extracted will increase with increased temperature and this will result in higher extraction rates (Coulson and Richardson, 1996).

Agitation of the solvent is important because it increases the diffusion rate and allows the diffusion of species into the solution and from the mineral surface, especially when the diffusion is slow. Additionally, stirring the pulp prevents sedimentation with more effective use of the interfacial surface (Smit, 2001, Coulson and Richardson, 1996).

2.3.9 Precipitation process

In hydrometallurgy processes, precipitation plays an important role to separate and recover metals from solution. During the leaching process, apart from the element of interest, other, other elements may also be dissolved into solution.

It is essential that these contaminants be removed from the solution to recover the element of interest.

Roasting and leaching processes of lithium concentrates are not always selective since some impurities can be co-dissolved with lithium. In order to produce pure lithium, the purification process must be effective in removing these impurities. In case of metal sulphides and hydroxides, impurities can be precipitated selectively from solution by pH control (Jackson, 1986).

For any dissolution reaction, the thermodynamic tendency is governed by the solubility product K_S. Solubility of a substance is defined as the mathematical product of ions concentrations of the devolved substance raised to the power of their stoichiometric coefficients as shown in equation (4) below. When the solubility product is small, the lower is its solubility (Jackson, 1986).

For metal hydroxides, when in equilibrium with water, dissociates into ions as follows (Jackson, 1986):

$$M(OH)_n \rightleftharpoons M^{z+} + nOH^- \quad (3)$$

The solubility product is expressed as follows:

$$K_s = [M^{z+}][OH^-]^n \quad (4)$$

The square brackets indicate activity, M is the metal and n being the stoichiometric coefficient.

2.3.9.1 Conditions for an electrolyte to precipitate

According to the following reaction:

$$A_xB_y \rightleftharpoons xA^{n-} + yB^{m+} \quad (5)$$

Three different conditions exist for precipitation to proceed, related to the solubility product:

$K_s < [A^{n-}]^x [B^{m+}]^y$: The solution is unsaturated.

$K_s = [A^{n-}]^x [B^{m+}]^y$: The solution is saturated.

$K_s > [A^{n-}]^x [B^{m+}]^y$: The solution is supersaturated.

According to Jackson (1986) and Sitando (2012), the solubility product (K_s) must exceed a certain point before observing the supersaturation precipitation phenomenon as shown by equation below.

$$\sigma = \frac{C - C^*}{C^*} \quad (6)$$

σ is the relative supersaturation, C is the concentration of the substance to precipitate and C^* is the equilibrium solubility.

Supersaturation can be used to manipulate the particle size of a salt when the latter is precipitated. When the solubility of a salt is exceeded through the addition of another chemical to result in high supersaturation, it will lead to rapid nucleation and formation of a fine and poor filterable precipitate. To get a crystalline precipitate with a coarse particle size, the relative supersaturation must be maintained as long as possible during nucleation (Sitando, 2012). Factors to manipulate are heating and dilution.

One of the most important parameters during pH-controlled precipitation reactions is the filtration process. To increase yield, the precipitate should be washed with demineralised water, or a suitable dilute electrolyte solution to avoid losses of the major element.

In the case of hydroxide precipitation, the technology is simple, inexpensive and well established, compared to other processes in hydrometallurgy.

In the Figure 8 below (Jackson, 1986) shows the pH range over which different metals precipitate as hydroxides. On the figure, each metal is soluble in solution for pH value on the left and insoluble for pH value on the right. This can be used for selective precipitation of several metal hydroxides by pH control.

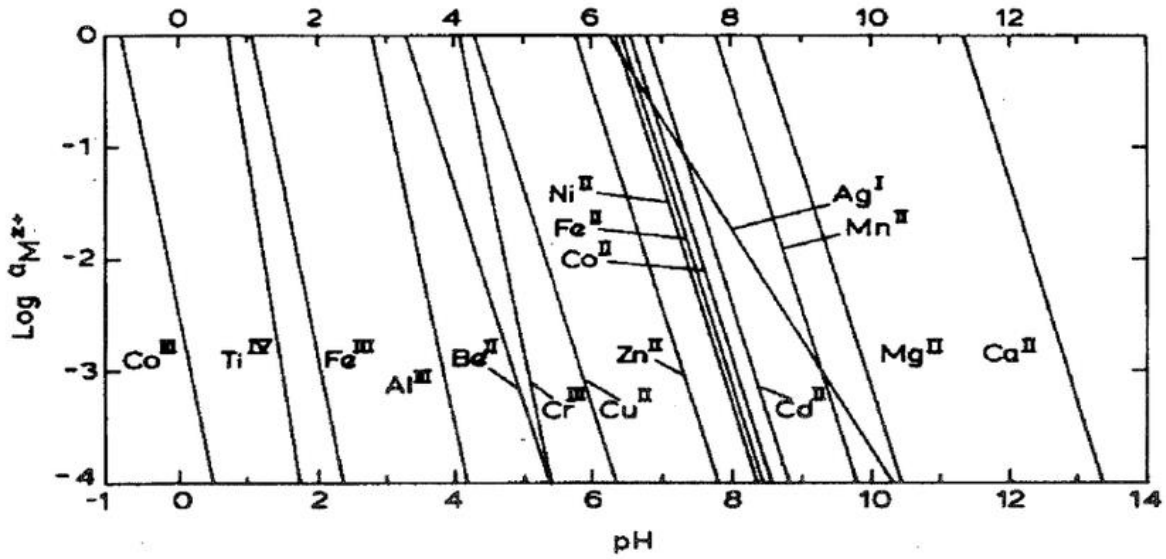

Figure 8: Metal hydroxide precipitation diagram (based on data at 25 °C)

2.3.9.2 Phenomena during precipitation reactions

The following sections discuss some definitions and phenomenons encountered during a precipitation reaction (Bruno and Sandino, 1987).

Co-precipitation is the deposition of the main substance with foreign substances which do not precipitate with the reagent employed under specific experimental conditions.

Adsorption is the adhesion of atoms, ion or molecules from a gas, solution or solid dissolved to the surface of a precipitate. The adsorbed ions or molecules are removed from the surface by washing the precipitate.

Occlusion is the imprisonment of the co-precipitated particles between the particles of the main precipitate. To remove the occluded particles, the precipitate must be dissolved in an appropriate solvent.

The removal of iron can be carried out either as Fe^{2+} or Fe^{3+} in a basic medium by pH control. From a theoretical point of view, iron precipitate from pH 2 to 8, according to Figure 8.

Jackson (1986) reported that at pH 3, precipitation could decrease the activity of iron (III) to less than 10^{-4} mol.dm^{-3} (10^{-4} M). At a pH 8 the precipitation can achieve the same concentration level of the metal in the form of iron (II) as shown on the Figure 8.

2.3.10 Recovery of lithium from leach solution

The recovery of lithium has been studied by many researchers and industrial producers. Sitando (2012), Jandová et al. (2010), Margarido et al. (2014), Lagos and Becerra (2005), Garrett (2004) recover lithium as lithium carbonate (Li_2CO_3) through precipitation from the leach solution. However, Li_2CO_3 is the main product and used by producer as feed material in the production of other lithium compounds.

Various carbonating agents have been tested by Lagos and Becerra (2005) to precipitate lithium from lithium chloride liquors. The best result was achieved by precipitating with an aqueous solution of sodium carbonate. The sodium chloride or sodium sulfate and can be washed during filtration with hot water. Ammonium carbonate was tested and this resulted in a co-precipitation of ammonium chloride which is not eliminated by washing with hot water. Carbon dioxide is not effective due to the very slow reaction kinetics. Alvani et al. (2002) concluded that, after testing the three reagents mentioned above, the best Li_2CO_3 was obtained by reprocessing Li_2TiO_3 pebbles in order to recover Li as Li_2CO_3. Lithium carbonate precipitation was achieved by agitating and slow addition of sodium carbonate to ensure a homogeneous product with adequate morphology.

The recovery of lithium carbonate via precipitation from lithium sulphate or lithium chloride is performed according to the following reaction (Lagos and Becerra, 2005):

$$Li_2SO_4\,(aq) + Na_2CO_3\,(aq) \rightarrow Li_2CO_3\,(s) + Na_2SO_4\,(aq) \qquad (7)$$

$$2LiCl\ (s) + Na_2CO_3\ (aq) \rightarrow Li_2CO_3\ (s) + 2NaCl\ (aq) \quad (8)$$

The precipitation of lithium using sodium carbonate from lithium chloride solutions are more difficult even with good settling, filtering and washing characteristics than working with Li_2SO_4 solution. This is explained by the fact that NaCl increases the solubility of lithium carbonate from 7.5 $g \cdot L^{-1}$ to 9.3 $g \cdot L^{-1}$ as shown in Figure 9 (Burkert and Ellestad, 1970).

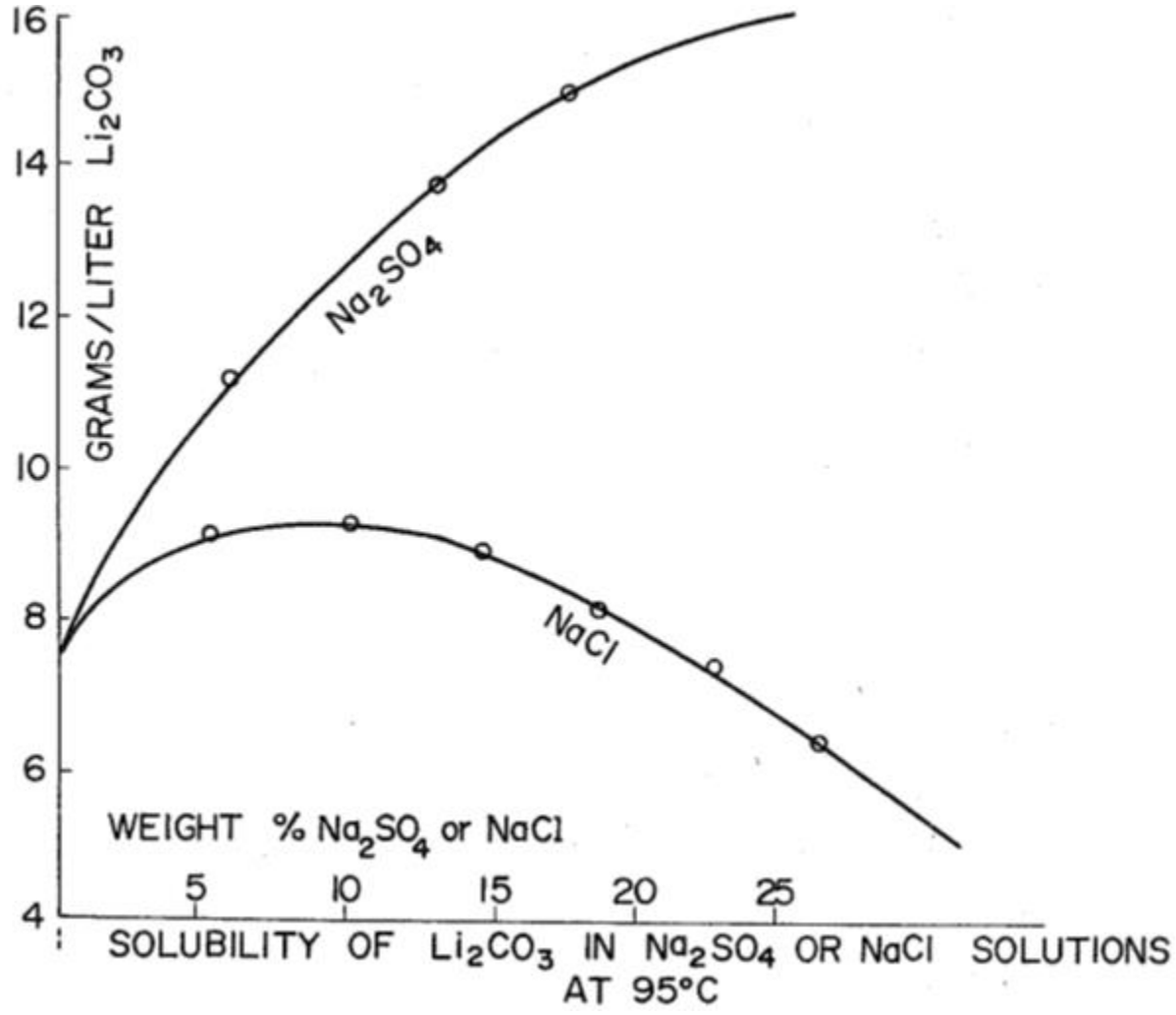

Figure 9: Precipitation of lithium carbonate from lithium chloride solution

This is the reason why lithium sulfate is the preferable route to obtain high lithium carbonate recovery.

2.3.11 Conditions for Li_2CO_3 precipitation

The precipitation of Li_2CO_3 from lithium sulfate solution with good settling, filtering and washing properties requires decreasing the solubility of Li_2CO_3 with increased solution temperature.

The following conditions need to be considered during the precipitation process:

- Temperature: Lithium carbonate precipitation is carried out between 80 – 100 °C. The solubility of lithium carbonate decreases with increased temperature (Garrett, 2004, Wietelmann and Bauer, 2003)

Table 7: Solubility of lithium carbonate at different temperatures

Li_2CO_3 (g) per 100 g water	
T (°C)	Wt%
20	1.33
25	1.29
30	1.25
40	1.17
50	1.08
60	1.01
80	0.85
100	0.72

- Concentration of reactants: Li_2CO_3 is known to have an appreciable solubility in the mother liquor as mentioned in Table 7. It is desirable to work with rather concentrated solutions to minimise the volume of the solution used. In many cases, the concentration of the lithium sulphate solution used varies between 200 $g \cdot L^{-1}$ and 300 $g \cdot L^{-1}$ depending on the amount of the impurities (Burkert and Ellestad, 1970). According to Jandová et al. (2009), at least 9 $g \cdot L^{-1}$ of lithium is necessary to get high recovery during the precipitation;

- Na_2CO_3 excess: The use of approximately 10 to 15 % excess Na_2CO_3 during the process over the stoichiometric amount of Li_2SO_4 is preferable. The use of Na_2CO_3 excess is desirable since, by increasing its concentration, the solubility of Li_2CO_3 is decreasing in the mother liquor (Burkert and Ellestad, 1970);
- pH: The precipitation of Li_2CO_3 occurs when the pH is adjusted to above 9 which is ideal for Li_2CO_3 precipitation by evaporating water present in solution (Lagos and Becerra, 2005);
- The precipitate obtained should be washed with hot water in order to eliminate co-precipitated impurities such as Na_2SO_4 and Na_2CO_3.

2.3.12 Toxicology of lithium carbonate

According to Wietelmann and Bauer (2003) lithium is more toxic than sodium; 5 g can cause fatal poisoning. Lithium salts have been used during treatment of manic–depressive illnesses with a therapeutic dose of 170 – 280 mg Li per day in the form of lithium carbonate. Lithium and some lithium compounds might be corrosive to the mucosa of the respiratory tract, eyes and skin due to alkalinity, this side effects is related to lithium hydride and lithium hydroxide.

Note that no industrial disease or health problems related to the ingestion of lithium compounds have been reported so far (Wietelmann and Bauer, 2003).

2.4 Lithium brine processing

Brines lake deposits are located in Chile, China, USA and Argentina with lithium concentration between 1000 – 3000 ppm with a high magnesium to lithium ratio. Currently, lithium is extracted from 13 pegmatite deposits. Greenbushes mine is considered the biggest source in the world. 65 % of lithium production is from brine lake deposits and over 80 % from minerals (Peiró et al., 2013).

Lithium from brine can be recovered by solar evaporation, precipitation, and adsorption processes.

In case of precipitation, lithium from brine is recovered using different precipitant agents such as $Ca(OH)_2$, Na_2CO_3, Na_2SO_4, NaOH, $CaCl_2$, but in some cases, impurities such as calcium and magnesium are first removed using lime and sodium oxalate. Recovery by adsorption process

is described using magnesium-doped lithium manganese oxide and H_2TiO_3 as adsorbents to remove Li and HCl effluent for desorption. By evaporation process, lithium from brine is recovered as lithium carbonate by evaporating salty water for 12-18 months from ponds using solar energy (Hien-Dinh, 2015).

2.5 Fluoride digestion process

2.5.1 Selection of digesting agent

Fluorine (F_2), hydrogen fluoride (HF) and ammonium fluorides (NH_4HF_2 and NH_4F) are known to be the main fluorinating agents in industry and all of them may be used for dissolving silica from ore concentrate (Andreev et al., 2007a).

According to Andreev et al. (2007b), fluorine and hydrogen fluoride gases have a number of disadvantages such as the formation and accumulation of solid waste that cannot be recycled. F_2 and HF are lethal compounds at higher concentrations. In addition, their application results in the generation of another toxic compound, namely SiF_4 gas. They also require special working conditions and utilisation. SiF_4 results from the attack of HF on topaz concentrate ($AI_2SiO_4(F,OH)_2$ in order to destroy silicon compound from topaz concentrate (Andreev et al., 2007b). Therefore, it is technologically beneficial to use ABF for the decomposition of minerals containing silicon.

2.5.2 Ammonium bifluoride

Ammonium bifluoride ($NH_4F{\cdot}HF$) is an inorganic compound produced by mixing ammonia and hydrogen fluoride (liquid) according to the reaction below (Solvay, 2013):

$$2HF\ (l) + NH_3\ (g) \rightarrow NH_4HF_2\ (s) \qquad (9)$$

Ammonium bifluoride contains two ions, namely ammonium cation (NH_4^+) and hydrogen bifluoride anion (HF_2^-). $NH_4F{\cdot}HF$ is characterised by a centrosymmetric triatomic bifluoride anion, known as the strongest hydrogen bond having a length of 114 pm between F–H and a bond energy greater than 155 $kJ{\cdot}mol^{-1}$.

Ammonium bifluoride (NH_4HF_2) can be found as a solid or aqueous solutions which are clear and colorless (Solvay, 2013). In solid form, the ammonium cation is surrounded by four fluoride centers in a tetrahedron, with hydrogen-fluoride bonds present between the hydrogen

atoms of the ammonium ion and the fluoride atoms. Industrial solution concentrations are between 28 % and 30 % (Solvay, 2013). The Table 8 gives the typical physical properties for ammonium bifluoride.

Table 8. Physical properties of ammonium bifluoride

	Solid NH_4HF_2	Aqueous NH_4HF_2 29%
Melting point	125.6 °C	Not available
Relative density	1.5	1.08
pH	2 (5.9 $g \cdot L^{-1}$)	< 1
Flash point	Non-flammable	
Decomposition temperature	230 °C	

Ammonium bifluoride is used in industrial textile processing or laundry applications for pH adjustment. Ammonium bifluoride products are primarily produced for etching of glass, brick, cleaners and ceramics.

2.5.3 Ammonium bifluoride applications

Ammonium bifluoride is known as a component with ability to dissolve silica. It contains fluorine which is the most reactive chemical elements and the lightest member of halogen group (Biswas et al., 2017). Ammonium acid fluoride can be used to decompose, dissolve or damaged oxide bonds to generated new compounds which can be easily handled (Andreev et al., 2007a, Andreev et al., 2007b, Du Plessis et al., 2016, Nel et al., 2011, Nhlabathi et al., 2012, Retief et al., 2014). These authors used ABF as source of anhydrous HF (AHF) for the dissolution of silica-containing minerals at varying decomposition temperatures and pressures. Retief et al. (2014) claimed separation of silicon from zirconia-based material using ABF in order to produce an ammonium heptafluozirconate ($(NH_4)_3ZrF_7$) and ammonium hexafluorosilicate $(NH_4)_2SiF_6$ compounds. Nel et al. (2011) and Du Plessis et al. (2016) respectively studied reaction kinetics between plasma-dissociated zircon and ABF by also forming ($(NH_4)_3ZrF_7$) and $(NH_4)_2SiF_6$. Nhlabathi et al. (2012) extended the work reported by Nel et al. (2011) in order to refine the kinetics.

Kuang et al. (2012) published a study on lithium extraction from α-spodumene using hydrogen fluoride (HF) as a digesting agent, without heat treatment. The results showed that HF reacts with α-spodumene, breaking the oxide bonds Li–O, Al–O, Si–O and Al–O–Si, forming Li_3AlF_6

and AlF_3, which can be dissolved in H_2SO_4. Gama et al. (2013) also observed a separation of silicon from molybdenum disilicide ($MoSi_2$) using anhydrous HF (AHF) by forming molybdenum metal (Mo). HF was used in these studies as the principal source of fluorine, at relatively low temperature.

$$MoSi_2(s) + 8HF(g) \rightarrow Mo(s) + 2SiF_4(g) + 4H_2(g) \quad (10)$$

$$MoSi_2(s) + 11HF(g) \rightarrow MoF_3(g) + 2SiF_4(g) + 5.5H_2\ (g) \quad (11)$$

In the case of Nel et al. (2011), ammonium acid fluoride was used to dissolve the amorphous silica at the temperature 240 °C and according to the below reaction:

$$3ZrSiO_4(s) + 16NH_4F \cdot 1.5HF(s) \rightarrow 3(NH_4)_3ZrF_7(s) + 3(NH_4)_2SiF_6(g) + 12H_2O(l) + NH_4F\ (g) \quad (12)$$

$(NH_4)_3ZrF_7$ is obtained after washing, filtering, and drying the reaction products since $(NH_4)_2SiF_6$ is soluble in water.

In general, ABF is used in its molten state, and used as facile source of AHF. According to Andreev et al. (2007a), this interaction occurs in two stages originally resulting in formation of ammonium heptafluorosilicate and ammonium hexafluorosilicate in case of topaz concentrate as shown in the reactions (13) and (14 below:

$$Al_2(SiO_4)F_2\ (s) + 8NH_4F.HF\ (s) \rightarrow (NH_4)_2SiF_6(g) + 4H_2O(l) + 2(NH_4)_3AlF_{6(}s) \quad (13)$$

$$(NH_4)_2SiF_6(g) \rightarrow SiF_4(g) + 2NH_3(g) + 2HF(g) \quad (14)$$

In the contest of this project, the reaction between petalite and ammonium bifluoride can be described as follows:

$$Li_2OAl_2O_38SiO_2(s) + 42NH_4HF_2(s) \rightarrow 2LiF(s) + 2AlF_3(s) + 8(NH_4)_2SiF_6(g) + 26NH_3(g) + 20H_2O(l) + 28HF\ (g) \quad (15)$$

$$1.5Li_2OAl_2O_38SiO_2(s) + 42NH_4HF_2(s) \rightarrow Li_3AlF_6(s) + 2AlF_3(s) + 12(NH_4)_2SiF_6(g) + 18NH_3(g) + 30H_2O\ (g) \quad (16)$$

The $(NH_4)_2SiF_6$ and NH_3, are soluble in water. Lithium fluoride, lithium cryolite and aluminium trifluoride are obtained by washing, filtering, and drying the lithium residue. The Table 9 and Table 10 show the solubility of lithium fluoride and lithium cryolite (Stubblefield and Bach, 1972).

Table 9: solubility of lithium fluoride in water

12 (g) LiF per 1500 mL of water	
T (°C)	Wt%
23.7	0.132
25.4	0.133
30.8	0.137
40.5	0.137
50.1	0.142
51.2	0.141
60.2	0.145
71.4	0.148
81.8	0.150

Table 10: Properties of some alkali aluminium hexafluoride in water

	Trisodium aluminium hexafluoride	Trilithium aluminium hexafluoride (Lithium cryolite)	Tripotassium aluminium hexafluoride
Melting point	1 027 °C	1 454 °C	1 025 °C
Bulk density (20 °C)	500 – 800 $kg \cdot m^{-3}$	400 – 500 $kg \cdot m^{-3}$	450 – 650 $kg \cdot m^{-3}$
Relative density (20 °C)	2.9	2.7	2.8
Solubility in water (25 °C)	0.41 $g \cdot L^{-1}$	0.41 $g \cdot L^{-1}$	1.4 $g \cdot L^{-1}$
pH (20 °C)	6 (0.41 $g \cdot L^{-1}$ at 20 °C)	6 (1.1 $g \cdot L^{-1}$ at 20 °C)	6 (1.4 $g \cdot L^{-1}$ at 25 °C)
Flash point	Non-flammable		

2.5.4 Toxicology of ammonium bifluoride

The following information on health and safety precautions was extracted from Segal (2000) on hydrogen fluoride and ABF Solvay (2013).

Skin contact: NH_4HF_2 and HF in contact with the skin can cause serious burns and can also lead to the destruction of cells in the area of soft tissue and bone tissue. This causes the disruption of calcium cells and the disruption of normal metabolism of magnesium resulting in excruciating pain.

Eye Contact: NH_4HF_2 and HF in contact with eyes can cause eye lesions which can lead to the destruction of the cornea. Severe exposure can even lead to blindness and total vision loss.

Inhalation: Inhalation of NH_4HF_2 and high concentration of hydrogen fluoride gas may cause severe burns of the mucous membranes and respiratory blockages. The signs of acute symptoms may include cough, chills, the stuffiness, fever and cyanosis (which is a blue skin color).

Ingestion: Ingestion of NH_4HF_2 and HF solution or solid can result to serious burns in the mouth and gastrointestinal tract in stomach. The ingestion of even a low concentration of HF can lead to systemic effects such as strictest hypocalcaemia by decreased calcium in the blood and heart dysthymia that can result in death.

2.5.5 Safety precautions

Before starting to handle ammonium bifluoride, the work place or laboratory should be prepared for any emergency. The environment must be ventilated to avoid any possibility of inhaling hydrogen fluoride that could escape of equipment.

In case of a laboratory, it must be ensured that the laboratory is equipped with a smoke hood for the evacuation of HF gas or HF is handled in a properly functioning fume hood.

The personal protective equipment below should be used in handling the NH_4HF_2 gas at all time:

- Face shield;
- Laboratory coat;
- Neoprene or polyvinyl chloride (PVC) gloves (double glove as necessary);
- Wrist guards to cover the gap between gloves and lab coat sleeves or gauntlet gloves;
- Long pants or equivalent.
- Shoes that cover the top and sides of the feet completely.

2.5.6 Recycling of ammonium hexafluorosilicate

During the dissolution of petalite using ammonium bifluoride, the fluorine is released with the gas stream in the form of $(NH_4)_2SiF_6$. During the formation of gaseous ammonium hexafluorosilicate (AHFS), it can crystallise at lower temperatures. In practice, the solid compounds will be deposited on the reactor walls, and cleaning may often be needed.

Andreev et al. (2007b), studied the process of sublimation and desublimation of $(NH_4)_2SiF_6$. Ammonium hexafluorosilicate was dissolved in ammonium hydroxide to obtain silicon dioxide and ammonium fluoride as shown in Figure 10.

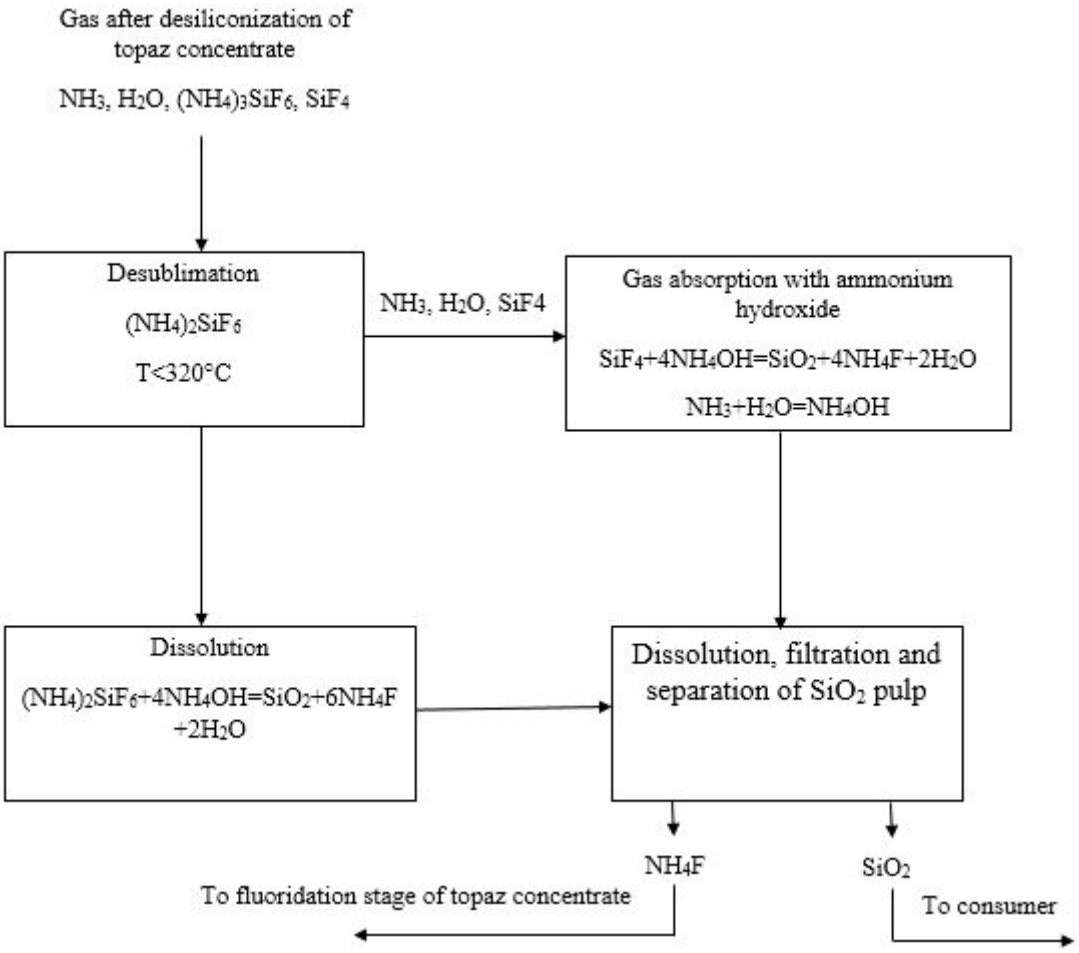

Figure 10: Basic diagram of utilisation of fluorine containing gases

Ammonium hexafluorosilicate can be also used for many other applications such as in photovoltaic applications, dealumination, selective removal of surface acidity in zeolite, as active agents in the formulation of mouthwashes and dentifrices as well as catalysis products in the frosted glass industry (El Guendouzi et al., 2016).

3 Experimental

3.1 Materials and reagents

The petalite concentrate used was sourced from Bikita Minerals (Pvt) Ltd in Zimbabwe. The following analytical grade chemicals were also used: NH_4HF_2 and H_2SO_4 from Merck Chemicals. Deionized water was used for all aqueous applications.

3.2 Apparatus

A Spectro Arcos inductively-coupled plasma optical-emission spectrometer (ICP-OES) was used for lithium analysis. A thermo ARL9400 XP X-ray fluorescence spectrometer (XRF) was used to determine the elemental composition of the petalite concentrate. A PANalytical X-ray diffractometry (XRD) was used to determine the mineral phases of the petalite concentrate. A Hitachi 7300 was used for the thermogravimetric analysis (TGA) of ABF. A Perkin-Elmer Fourier –transform infrared spectroscopy (FTIR) was used to obtain the infrared spectrums of the petalite. A Mettler PM2000MC balance was used for weighing. pH measurements were done with a pH meter model Adwa AD 111. Particle size analysis was performed using a Malvern Mastersizer 3000.

See Appendices 7.1 – 7.5 for a detailed description of the analytical instrumentation used during the project. The instrumentation includes ICP-OES, XRD, XRF, SEM, TGA and PSD.

3.3 Methods

3.3.1 Mineralogical composition and chemical composition of the petalite concentrate

The crystallographic analysis of the mineral was done by X-ray diffraction (XRD). XRD pattern of the concentrate confirmed that the Zimbabwean concentrate is mainly composed of petalite (79.9%) and also contains some associated minerals. The Zimbabwean concentrate phases and phase amounts (weight %) were identified using XRD X'Pert Highscore Plus software.

The Zimbabwean concentrate used contained an average of 2 % of Li as element. The chemical composition of main components present in the concentrate was determined using XRF and

ICP-OES. The samples were fluxed with sodium borate at 1 100ºC, then the resulting product was dissolved in sulfuric acid for analysis.

3.3.2 Effect of temperature on digestion (dissolution) of petalite with ABF

A series of articles on fluxing silicate compound using ammonium bifluoride as a fluxing agent are published (Andreev et al., 2007a, Andreev et al., 2007b, Nhlabathi et al., 2012, Gama et al., 2013, Du Plessis et al., 2016, Retief et al., 2014). They studied dissolution of silica compounds using ammonium bifluoride (ABF) by varying the temperature and observed different temperature ranges for the dissolution.

Using these studies as a basis, a number of experiments were performed between 25–600 ºC in order to investigate the impact of the temperature on dissolution of petalite and to determine the optimum working temperature. After mixing petalite and ABF, the sample was placed into an alumina crucible for digesting at a specific temperature.

The amount of ammonium bifluoride (ABF) was calculated based on the chemical reaction in Equation (15) and (16).

According to Equation (15) and (16), the petalite compound will interact with ammonium bifluoride forming ammonium hexafluorosilicate which is soluble in water and can be removed during the washing process (Andreev et al., 2007a).

Working at temperatures between 25 °C and 100 °C, digestion was done using 5 g of petalite ($LiAlSi_{14}O_{10}$) and 37.5 g of ABF (NH_4HF_2) in alumina crucible. A three-time molar excess ammonium bifluoride (ABF) was calculated based on the chemical reaction in Equation (15). The furnace was preheated to the desired temperature and the containers were inserted and left for the set period. To quench the reaction, water was added to the reaction product to dissolve the water-soluble products and filtered. The remaining solid was dried and weighed.

Working at temperatures between 200 °C and 600 °C using stoichiometric molar ABF based on the chemical reaction in Equation (16), digestion was done using 5 g of petalite ($LiAlSi_{14}O_{10}$) and 12.26 g of ABF in alumina crucible . The furnace was heated to the desired temperature with the containers inserted and kept for 2 hours. To quench the reaction, water

was added to the reaction product to dissolve the water-soluble products and filtered. The remaining solid was dried at 100 °C and weighed.

3.3.3 Roasting of the Zimbabwean petalite concentrate after digestion with ABF

A weighed amount of the resulting product after digestion was mixed with H_2SO_4 in 500 mL PTFE griffin beaker as a reactor. An excess H_2SO_4 was added to the mixture and placed in the laboratory furnace. The roasting temperature was studied between 100 to 200 ^oC for 60 minutes where after the samples were removed and cooled at room temperature.

Roasting reaction of the final product after digestion with ABF is shown in the following equation (Kuang et al., 2012):

$$2LiF_{(s)}+2AlF_{3(s)}+4H_2SO_{4(conc)}\rightarrow Li_2SO_{4(s)}+Al_2(SO_4)_{3(s)}+8HF_{(g)} \quad (17)$$

$$2Li_3AlF_{6\ (s)}+2AlF_{3(s)}+9H_2SO_{4(l)}\rightarrow 3Li_2SO_{4\ (s)}+2Al_2(SO_4)_{3\ (s)}+18HF_{(g)} \quad (18)$$

3.3.4 Leaching studies

The solvent after H_2SO_4 roasting was distilled water. Parameters tested included stirring speed, solid/liquid mass ratio, leaching at various temperatures and times to optimize the leaching conditions.

Leaching experiments were performed using 500 mL PTFE griffin beaker as a reactor. A measured volume of distilled water was added to the reactor, placed on a hot plate magnetic stirrer and then heated to the desired temperature using the thermometer to control the temperature. A magnetic stirrer was used to keep the reaction products in suspension during the reaction. The reaction time started when the solution reached the desired temperature. Samples were withdrawn at selected time interval, filtrated, washed and ICP analysis was done to calculate the extraction rate.

3.3.5 Solution purification

Acid roasting and water leaching of lithium concentrates are not always selective since some impurities can be dissolved with lithium. In order to produce pure lithium, the purification process must be effective in removing these impurities. In case of metal sulphides and hydroxides, impurities can be precipitated selectively from solution by pH control (Jackson, 1986).

The purification process involved the removal of the cationic contaminants, then the removal of sulfates and finally Li_2CO_3 product recovery by precipitation with Na_2CO_3. The possible cations in the leach liquor include the alkaline metals such as (K^+, Na^+, Rb^+, Li^+) and metals such as (Ca^{2+}, Fe^{3+}, Mg^{2+}, Al^{3+}) that are also dissolved. The solution purification experiments were conducted using beakers, stirring hotplates, and a pH meter to determine the optimum purification conditions as shown in Figure 11.

Figure 11: Equipment for purification by precipitation

After the precipitation of the metals, the precipitate was filtrated and the cake washed with water. Calcium hydroxide $Ca(OH)_2$ is used to precipitate magnesium at a pH of 10.4. The amount of sodium carbonate (Na_2CO_3) equivalent to the amount of calcium in solution (Ca) was used to precipitate the excess Ca in solution at the room temperature with a pH varying between 10 and 11.

At each stage of the purification process, a pH meter was used to determine the pH of solutions and ICP-OES was used to determine the concentration of lithium and impurities in the solution. The purification experiments were performed in triplicate and the average error for the three experiments was below 4 %. The purified leach liquor was adjusted to a pH of 7–8 and subjected to evaporation at 95–100 ºC in order to precipitate Li_2CO_3 (Wietelmann and Bauer, 2003).

3.3.6 Recovery and characterisation of lithium carbonate

The purified leach liquor was subjected to evaporation between 95–100 ºC to about 40 % of its original volume of the solution, filtrated in order to remove the Ca residues before the precipitation of Li_2CO_3.

The evaporation was stopped at a lithium concentration of more than 5 $g.L^{-1}$. The precipitation of Li_2CO_3 was carried out using a hot saturated solution of Na_2CO_3 which was added drop-wise to the filtrate at 95–100 ºC.

Precipitation was done at high temperature because the solubility of lithium carbonate decreases with increasing temperature (Wietelmann and Bauer, 2003). Na_2CO_3 is used to precipitate Li_2CO_3. The soluble contaminants (the residual Na_2SO_4 and excess of Na_2CO_3) are washed and removed from the precipitate with hot water during filtration (Lagos and Becerra, 2005). A white Li_2CO_3 powder was precipitated, removed from the solution by vacuum filtration and the filtrate returned to the reactor and evaporated to increase the product yield.

After performing all steps, Li_2CO_3 was dried at about 100 ºC. Analytical analysis was recorded by means of ICP-OES. The concentrations were done by taking into account the changes in volume and mass during each operation because of the precipitant agents added to the solution.

The chemical reaction below was used to precipitate lithium carbonate:

$$Li_2SO_4(aq) + Na_2CO_3\,(aq) \rightarrow Li_2CO_3(s) + Na_2SO_4(aq) \qquad (19)$$

The final dried product (Li_2CO_3) was characterised by ICP-OES.

The synthesised Li_2CO_3 was also characterised and compared to the commercial Li_2CO_3 using SEM and XRD.

3.3.7 Overall process

The flow sheet below summarises the methods described above.

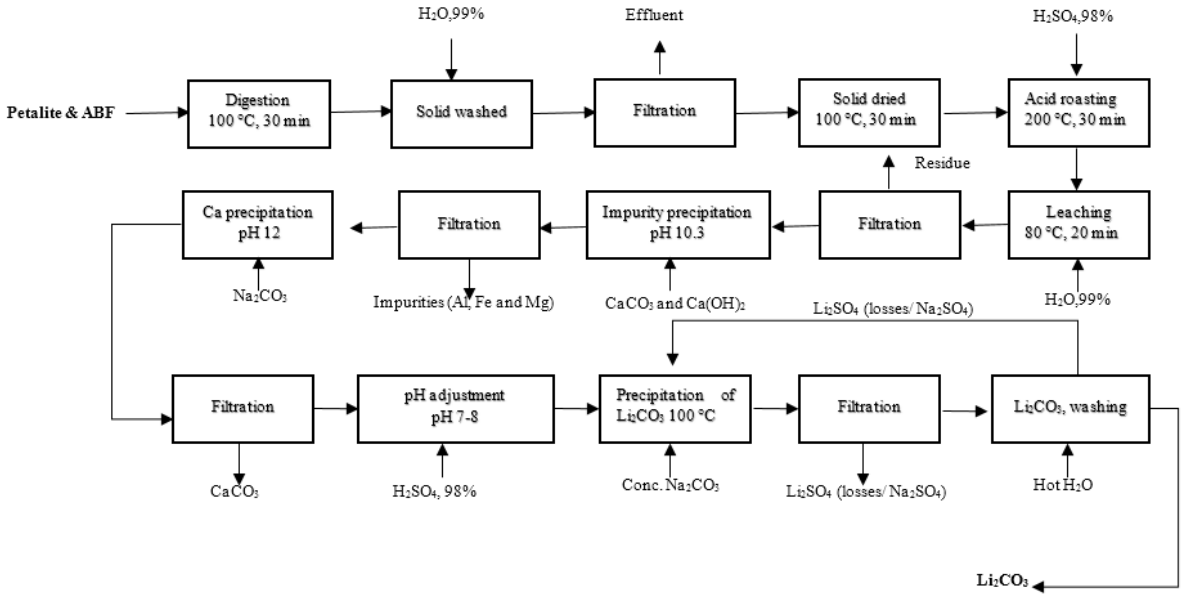

Figure 12: Proposed flow sheet

4 Results and Discussion

4.1 Feed material particle size distribution

Figure 13 presents the particle size distribution of the Zimbabwean petalite (concentrate) as received. As showed by the particle size analyzer, 90 % particle size is less than 73.6 μm, 50 % particle size is less than 26.9 μm and 10 % is less than 3.48 μm. The advantage of using a smaller particle size is that more surface area will be exposed during the chemical attack, therefore enhancing the leaching rate. In hydrometallurgy, the particle size is considered as one of the most important technical details for good production.

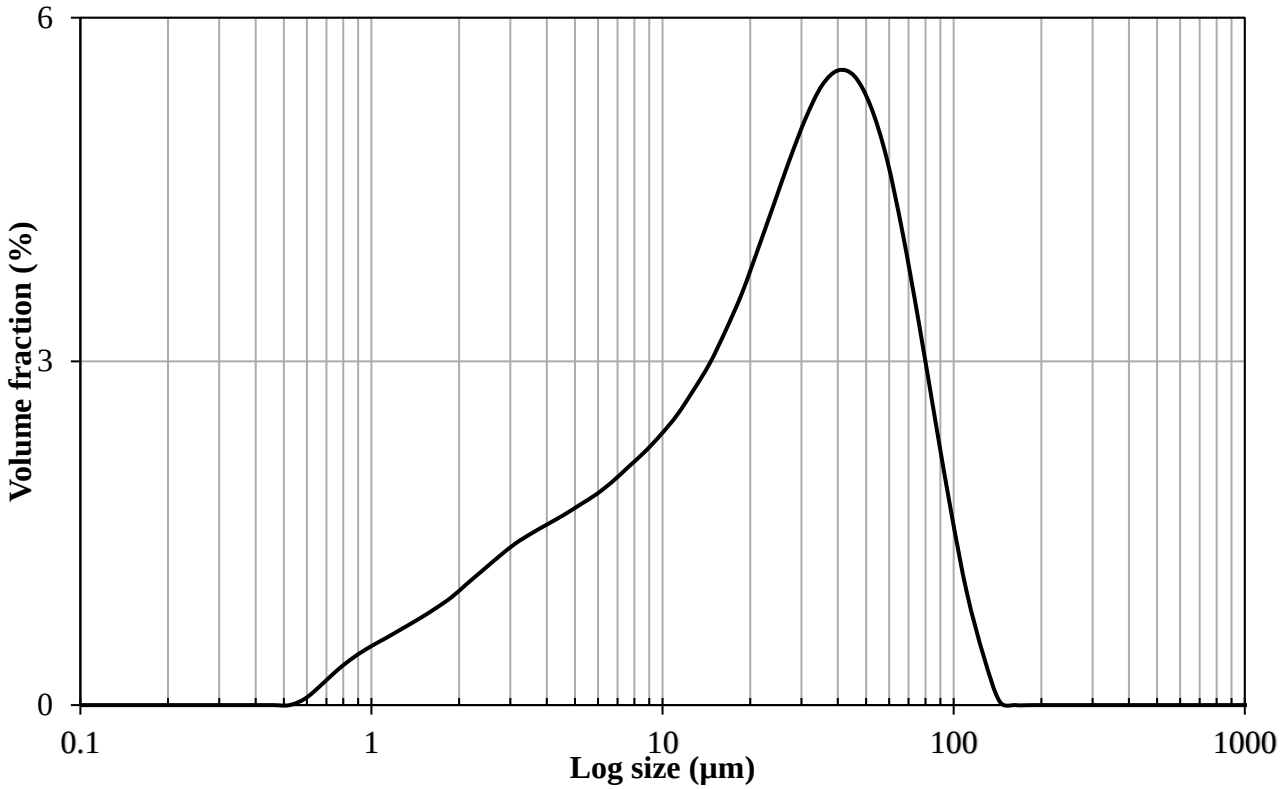

Figure 13: Particle distribution of Zimbabwean petalite

4.2 Mineralogical composition of the concentrate

The crystallographic analysis of the mineral was done by X-ray diffraction and can be found in Table 11 below. XRD results in Table 11 confirmed that the lithium pegmatite (Zimbabwean concentrate) is mainly composed of petalite. It also contains some associated minerals such as,

quartz, bikitaite, spodumene, lepidolite, and albite. The petalite concentrate will be used to extract lithium in order to produce Li_2CO_3.

Table 11: Semi-quantitative mineral content of the petalite (XRD analysis)

Mineral phase	(Wt. %)
Quartz (SiO_2)	6.1
Bikitaite ($LiAlSi_2O_6$ H_2O)	7.3
Petalite ($LiAlSi_4O_{10}$)	79.9
Spodumene ($LiAlSi_2O_6$)	2.1
Lepidolite($K(Al_{0.62}Li_{0.38})_2Li_{0.92}Si_4Al_{0.42}O_{10}(OH)_{0.485}F_{1.51}$)	1.1
Albite ($NaAlSi_3O_8$)	3.5

4.3 Mineral component of petalite concentrate

A petalite concentrate used contained 2.0 % of Li, as element. The chemical composition is shown in the Table 12. The analysis was performed on ICP-OES for lithium, and XRF for the remaining elements. XRF is not reliable for elements below sodium. The fluorescence from lighter elements has a lower energy to reach the detector, a higher concentration of these elements is required. Unfortunately, lithium is too light and could not be detected using XRF.

Table 12: Chemical composition of the Zimbabwean petalite using ICP-OES and XRF

Component	ICP-OES	XRF (%)
SiO_2	-	78.6
Al_2O_3	-	17.8
Li_2O	4.3	-
Fe_2O_3	-	0.08
Na_2O	-	0.20
MgO	-	0.15
K_2O	-	0.14
CaO	-	0.09
Rb_2O	-	0.03
MnO	-	0.01
P_2O_5	-	0.01
O_2	-	0.01
Cr_2O_3	-	0.01
SrO	-	<0.01
Co_3O_4	-	<0.01
SO_3	-	2.87
TOTAL		99.99

4.4 Digestion results

This study provides data on the digestion of petalite using ABF in the range between 25–600 °C. At lower temperatures (below 100 °C), a three-time molar excess ABF was used in order to investigate the impact of the temperature on the digestion of petalite. However, at higher temperatures (200–600 °C), stoichiometric ratios were used to minimize ABF consumption in

order to investigate the impact of the temperature on the dissolution of petalite. The resulting was acid roasted, water leached, solution was purified by pH control, and precipitation of lithium carbonate from the prepared lithium carbonate solution.

4.4.1 Reactions below 100 °C

Experiments were done by varying the digestion temperature of the reaction mixture to determine the minimum reaction temperature. The mixture was kept at temperature for 15, 30, 60, 120, 180 and 240 min at constant temperatures between 25 and 100 °C. The petalite conversion (m/m_o) is equal to the ratio of the lithium mass (m) at time t and the initial mass (m_o) of lithium in the sample.The digesting products were mixed with an excess acid and roasted. The resulting products were leached and disolved with water at 80°C,and ICP-OES was used to determine lithium mass (m). The experiments were performed in triplicate and the average error for the three experiments was calculated. The results are presented in Figure 14 below.

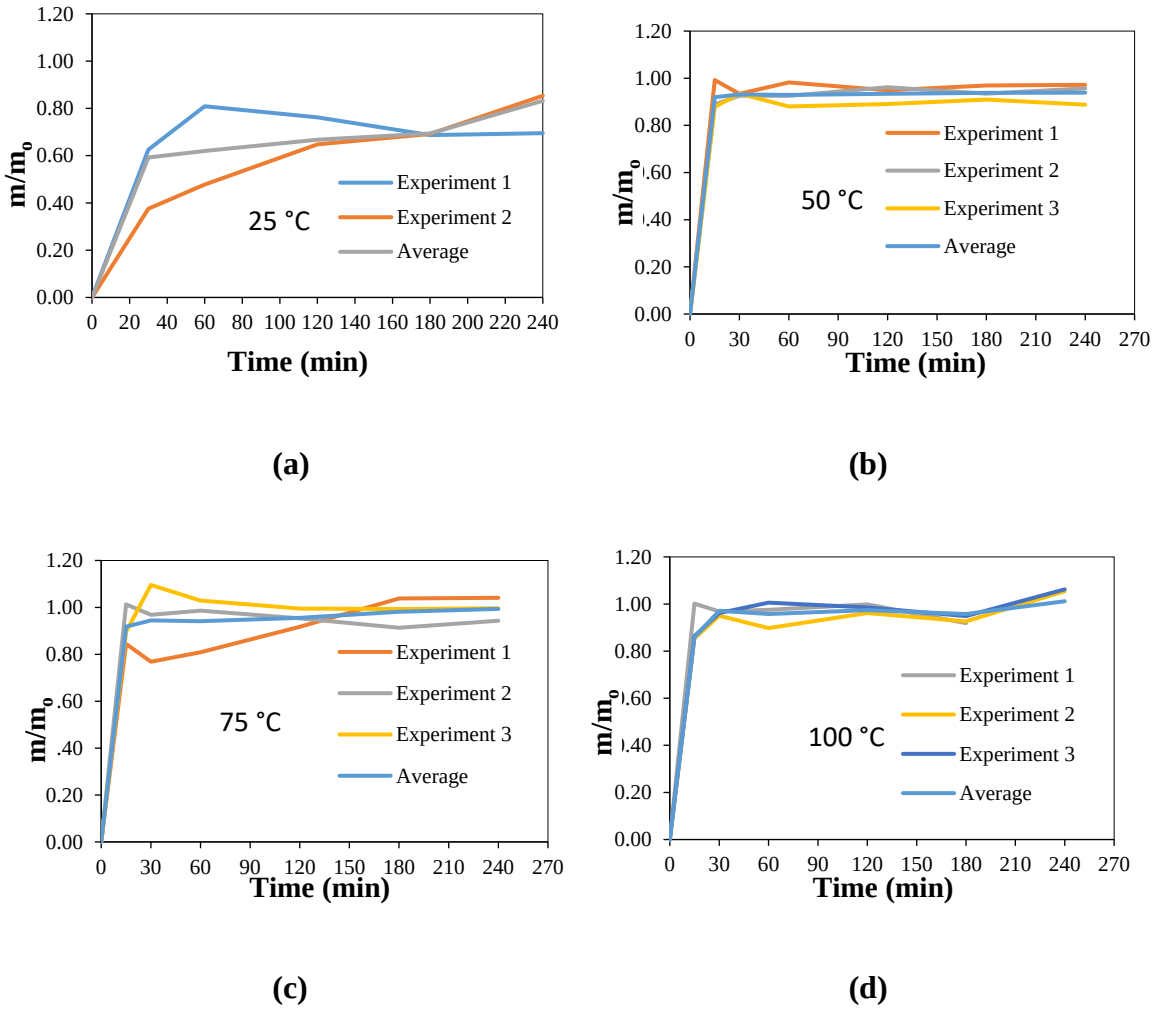

Figure 14: Petalite conversion vs time for the reaction of petalite with NH_4HF_2 at (a) 25°C, (b) 50 °C, (c) 75 °C and (d) 100 °C.

The reaction times reported include the heating period of the crucible and sample inside the furnace. The times are therefore indicative rather than exact. As seen in Figure 14 (a), the decomposition reaction already starts at 25 °C. After 60 min, petalite conversion remains constant at 75 %. Figure 14 (b) shows that the conversion rate increases at higher temperature. After 30 min at 50 °C, the petalite conversion remains constant at 93 %. Figure 14 (c) shows that an increase in temperature to 75 °C increases the conversion reaction of petalite to above 95 %. Figure 14 (d) shows that at 100 °C, the petalite approaches full conversion after 30 min of reaction At 100 °C, the decomposition α_{max} of 97 % is less than 30 min. The optimum is fixed at 100 °C for 30 min.

ABF melts at 125 °C. The reactions reported above thus commence in the solid state, for all temperatures. As soon as the two solids are mixed, slurry formation and evolution of ammonia are observed, as predicted by Reaction (15). Except at room temperature, the reaction reaches a maximum conversion in less than 30 min. As noted, the maximum yield improves as a function of temperature, with full conversion at 100 °C. Our conclusion is that the reaction is not diffusion limited, as might be expected. It appears to reach a thermodynamic limit, dictated by the equilibrium position in the semi-aqueous environment of the slurry.

Figure 15 shows how the reaction between Zimbabwean petalite and ABF is temperature dependent. The degree of conversion (α_{max}) increases when the temperature increases. At 100 °C, the decomposition time α_{max} of 97 % is less than 40 min. The optimum is fixed at 100 °C for 30 min of reaction.

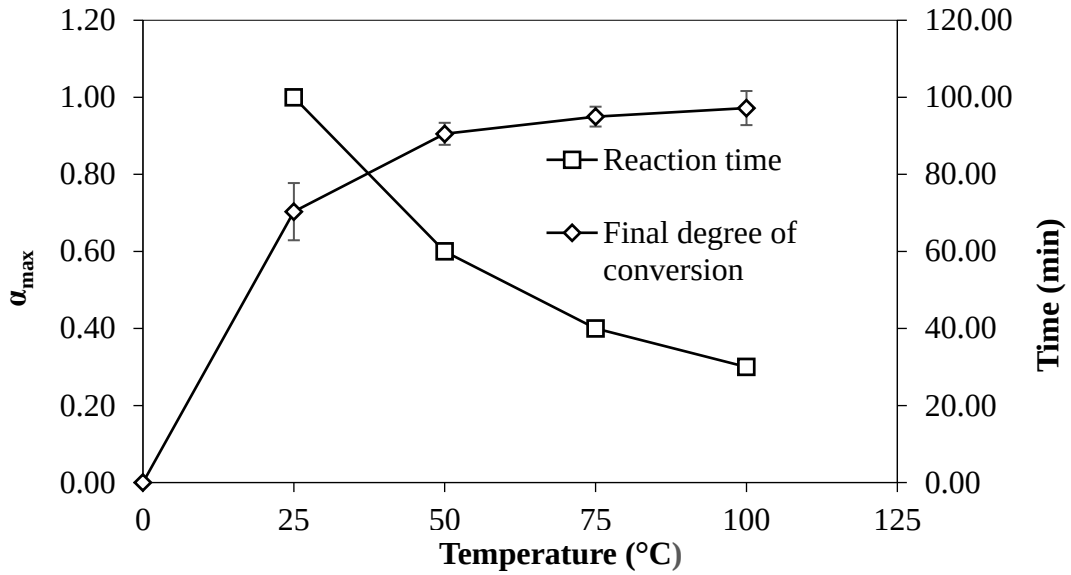

Figure 15: Final degree of conversion (α_{max}) of Zimbabwean petalite at different temperatures and time to reach α_{max}.

Figure 16 shows a dynamic thermogram of ABF. The melting point is confirmed to be at 125 °C, and mass loss is observable above that temperature. This confirms the literature reports that ABF melts in the range between 115 °C and 220 °C (House and Engel, 1993). Mass loss is complete at around 220 °C. The reaction takes place via decomposition of the compound into ammonia and hydrogen fluoride, as shown in Reaction (20):

$$NH_4HF_{2\,(s)} \rightarrow NH_{3\,(g)} + 2HF_{(g)} \quad (20)$$

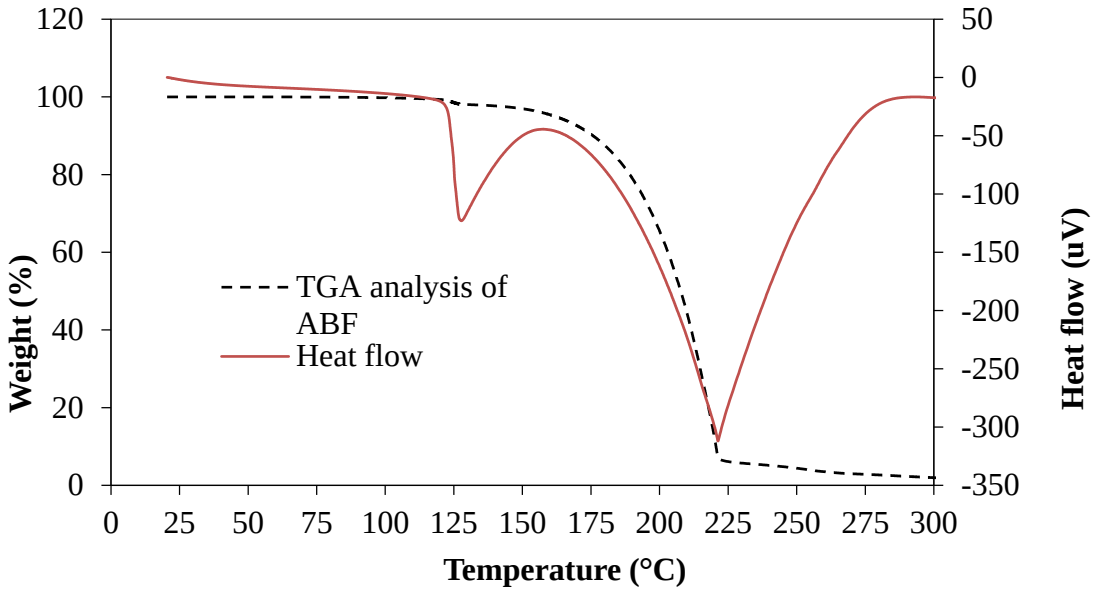

Figure 16: Dynamic thermogram of ABF decomposition

Figure 17 (a) and (b) show the XRD patterns of the petalite concentrate before and after reaction with ABF at 100 °C.

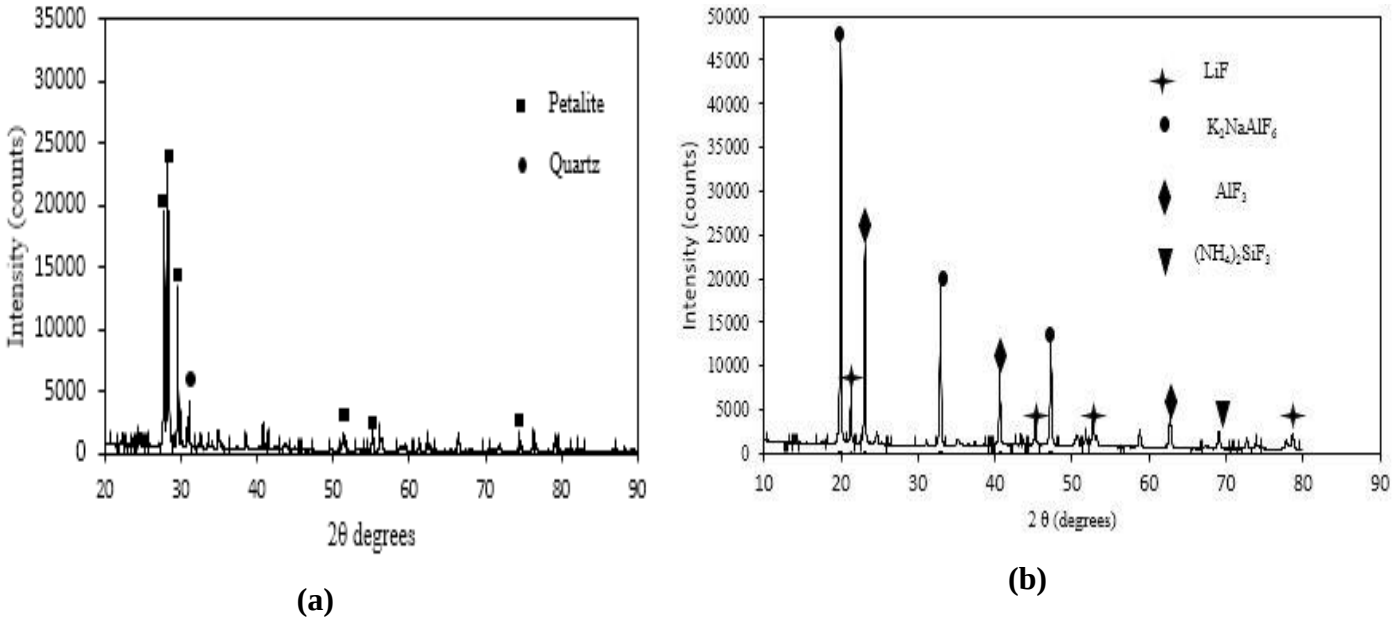

Figure 17: XRD pattern of Zimbabwean petalite (a) before and (b) after reaction with NH_4HF_2

4.4.2 Reactions above 100 °C

Working at higher temperature between 200 °C and 600 °C, different experiments were done by varying the digestion temperature in order to optimise the consumption of ABF and to investigate the effect on the petalite. After stoichiometric mixing of petalite and ammonium bifluoride, the mixture was placed into an alumina crucible, heated in a furnace for two hours to the set temperature and then cooled down. As seen in Figure 18 (b) and (c), when working at 200 and 300 °C, petalite was partially reacted resulting in formation of LiF. From 400, 500 and 600 °C in Figure 18 (d),(e) and (f), dissolution of petalite was almost completed. This leads to the formation of cryolithionite ($Li_3Na_3Al_2F_{12}$).

According to Rosales et al. (2013), cryolithionite formation is due to the opening of the ore during the reaction, releasing Li^+, Na^+ and Al^+ ions from petalite ($LiAlSi_4O_{10}$) and albite ($NaAlSi_3O_8$) to react with the digesting agent as shown the equations below.

$$NaAlSi_3O_{8(s)}+5NH_4HF_{2(s)}\rightarrow NaF_{(s)}+AlF_{3(s)}+(NH_4)_2SiF_{6(g)}+3NH_{3(g)}+4H_2O_{(l)}+2SiO_{2\ (s)} \quad (21)$$

$$Li_3AlF_{6(s)}+AlF_{3(s)}+3NaF_{(s)}\rightarrow Li_3Na_3Al_2F_{12(s)} \quad (22)$$

The increase in temperature favours the reaction of the petalite and albite, and enhances the intensity of the peaks corresponding to cryolithionite.

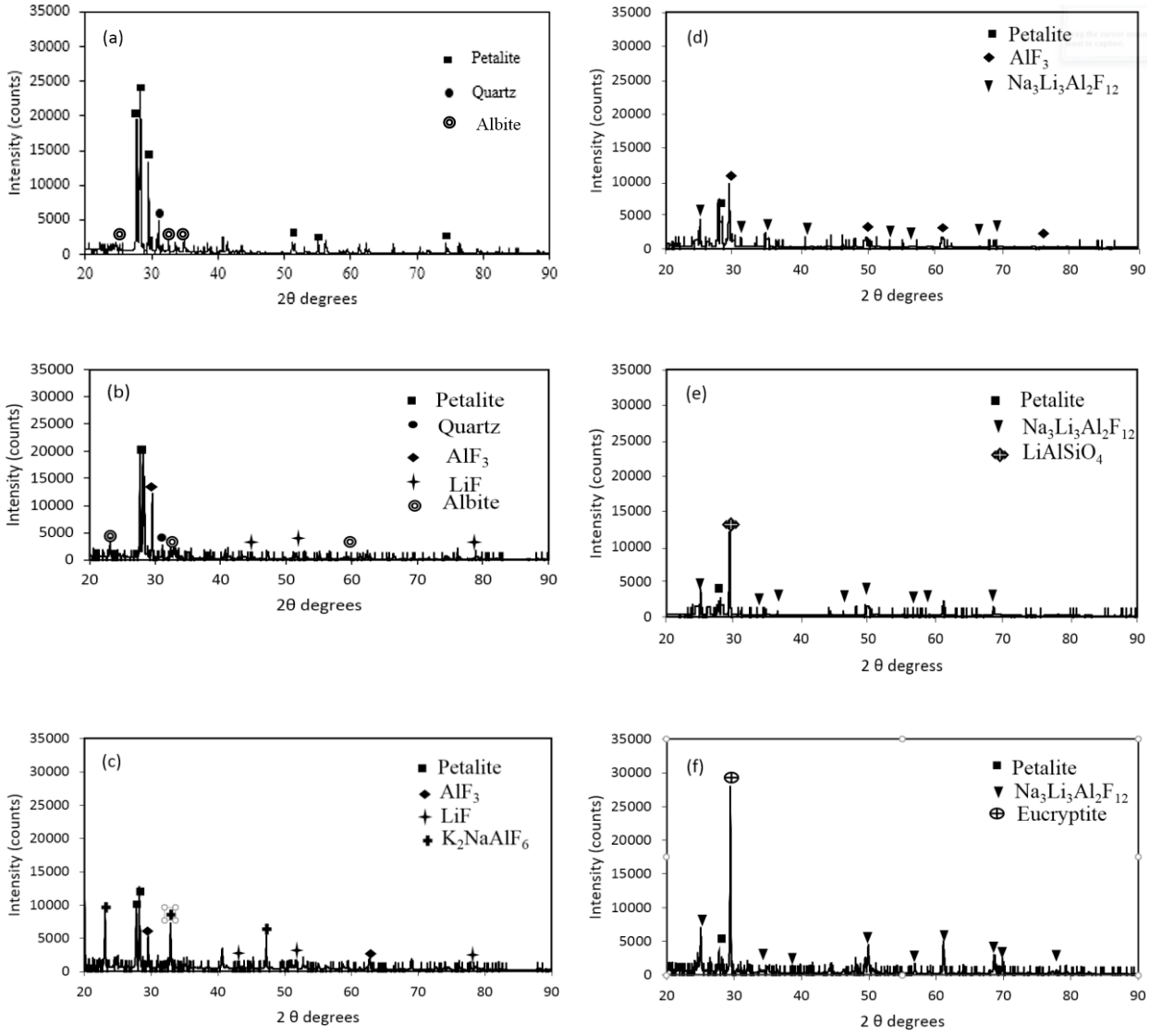

Figure 18: XRD pattern of petalite of residues obtained at the following conditions (Ore/ABF ratio 1/1: (a) Zimbabwean petalite before reaction, (b) 200 °C, (c) 300 °C, (d) 400 °C, (e) 500 °C, (f) 600 °C.

Digestion of petalite was studied by thermogravimetric analysis (TGA) at a heating rate of 10 ºC/min. Petalite interaction with ammonium bifluoride was studied at stoichiometric ratios based on Equation (16).

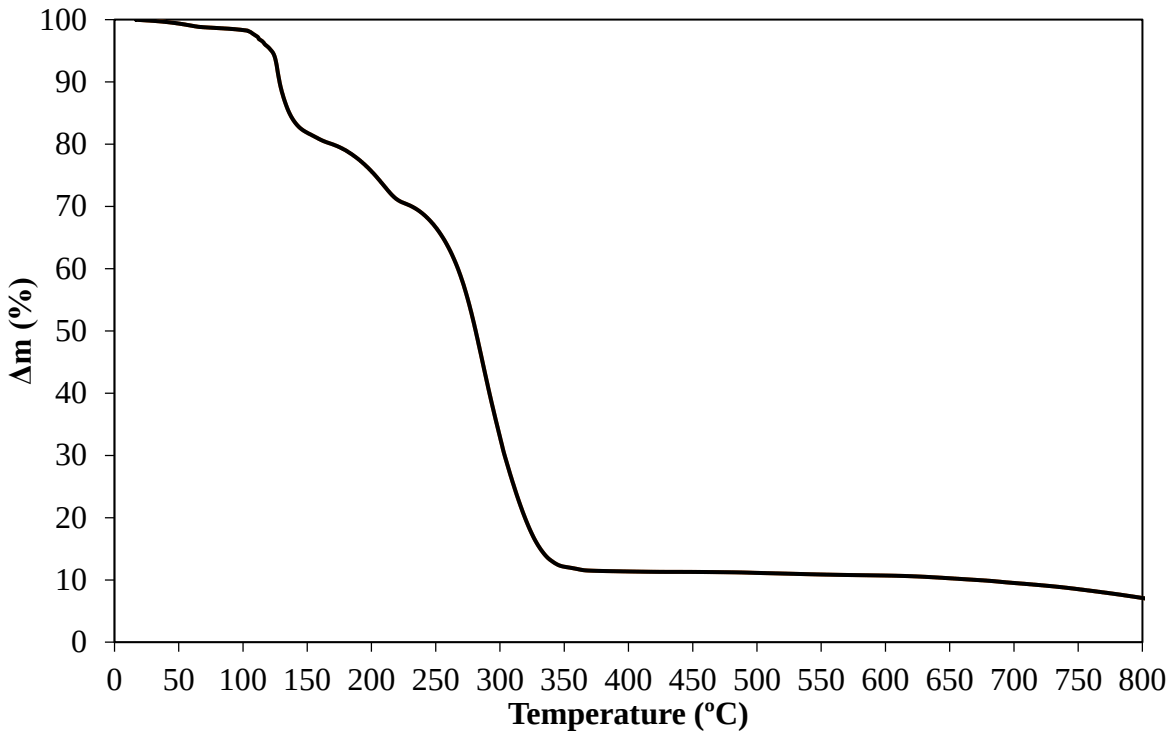

Figure 19: TGA of a roughly stoichiometric ratio of ABF and petalite

Without further work, only a tentative interpretation of the observations is possible. ABF melts and starts decomposing in the range 115 °C to 220 °C (House and Engel, 1993). Up to ~150°C mass loss is due to ABF losses, along with water released by the reaction. Ammonium hexafluorosilicate is formed and evaporates between 230 °C and 370 °C. Between 370 °C and 1 000 °C, only solid fluorides remain, viz. cryolithionite and aluminium fluoride and eucryptite.

This indicates that petalite has completely reacted with ammonium bifluoride to form cryolithionite and other compounds as shown in Figure 18 (d),(e) and (f).

FTIR analyses of the residues during the digestion of petalite was done

FTIR analyses of the residues after digestion were performed, as shown in Figure 20. In Figure 20 (a), the spectrum of unreacted ore, the peak at 625 cm^{-1} can be assigned to the absorption band of Si–Si, and the peaks at 1000 and 1100 cm^{-1} to the bulk Si–O–Si and Si–O modes, respectively (Hoshino and Adachi, 2007). They are still prominent at 200 °C, but decrease dramatically as the treatment temperature increases, Figure 20 (c) 300 °C, (d) 400 °C, (e) 500 °C, and (f) 600 °C.

The bands observed at 1443 cm^{-1} and 3290 cm^{-1} , observed up to 400 °C are attributed to N-H bending and stretching respectively (Kabacelik and Ulug, 2008), evidence for the presence of undecomposed ammonium fluorometallates. At 500 °C and above, IR activity is well below 900 cm^{-1}. The peaks around 580 cm^{-1} are attributed to the formation of AlF_6^{3-} in the form of AlF_3. (Duke et al., 1990).

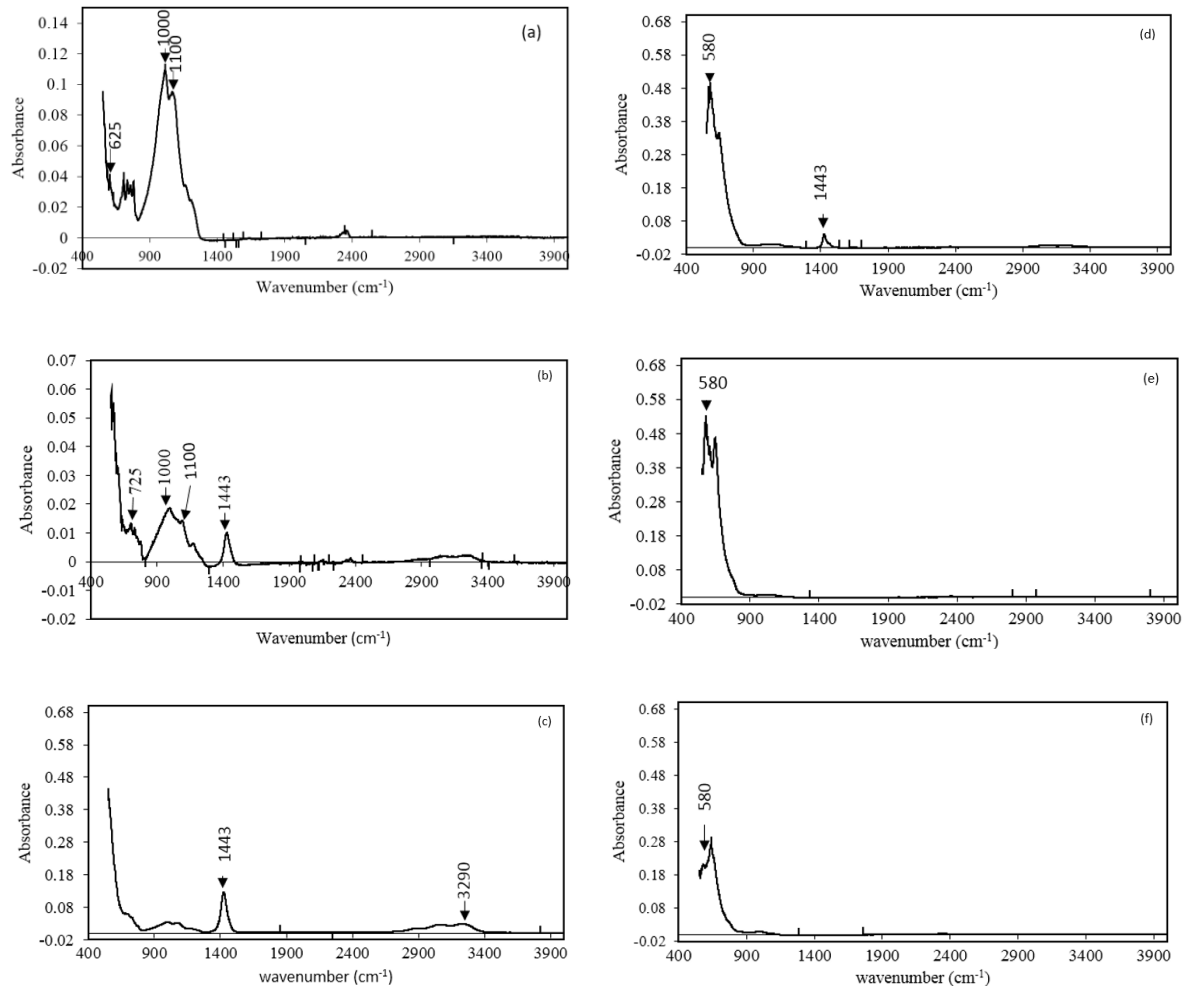

Figure 20: FTIR spectra of petalite sample and residues after digestion at different temperatures: (a) petalite sample, (b) 200, (c) 300, (d) 400, (e) 500 and (f) 600 °C

The resulting product was washed with water to remove all water soluble compounds, filtered and dried at 100 ºC. These insoluble products were mixed with an excess of sulfuric acid and roasted at 300 °C for 30 min. The resulting product was cooled to room temperature, water was added and dissolved at 90 °C for 60 min.

The increase in digestion temperature between 200 to 600 ºC increases the reaction efficiency as shown in Figure 21. This interaction results in the dissolution of the petalite with the ammonium bifluoride. The reaction efficiency using the stoichiometric amount to extract more than 95 % Li.

From Figure 20 (d),(e) and (f), respectively at 400, 500 and 600 ºC, all the ammonium fluorosilicate was decomposed and the remaining product consisted of cryolithionite ($Li_3Na_3Al_2F_{12}$) and aluminium fluoride. Based on the results in Figure 20 (d),(e) and (f) **,** the increase of the temperature favors the dissolution of the Zimbabwean petalite and enhances cryolithionite peaks, therefore increase lithium extraction. The results indicate that below 400 °C, lithium extraction was still below 95 % due to the presence of petalite peaks after digestion. From 400 °C up to 600 °C the extraction was above 95%. A digestion temperature of 500 ºC was considered the optimal for both economic and efficient reasons.

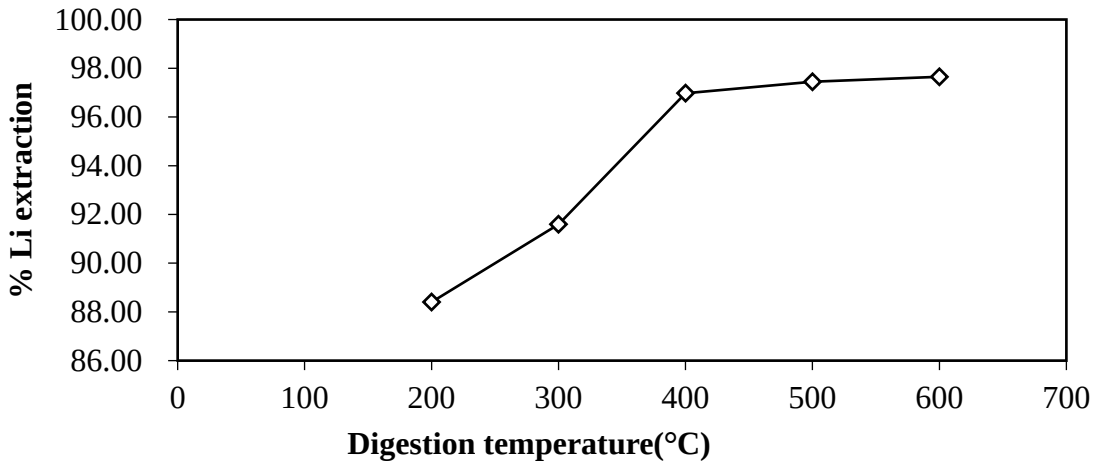

Figure 21: Effect of digestion temperature on the lithium extraction with the following conditions: 25% excess acid; sulfuric acid roasting temperature 300 °C; roasting time 30 min; water leaching temperature 90 °C; leaching time 60 minutes; stirring speed 400 rpm; and solid-liquid ratio (0.05 g mL^{-1}).

The lithium was extracted using an excess acid and high leaching temperatures to ensure complete dissolutions. These conditions were investigated in more details later in the study results are given below.

4.5 Sulfuric acid roasting studies

4.5.1 Effect of excess sulfuric acid after digesting of petalite with ABF

A number of experiments were done by varying the excess sulfuric acid between 0 and 20 % to determine the optimum condition of lithium extraction. According to the results presented

in Figure 22, it was established that 5 % excess of sulfuric acid, yield a constant extraction yield.

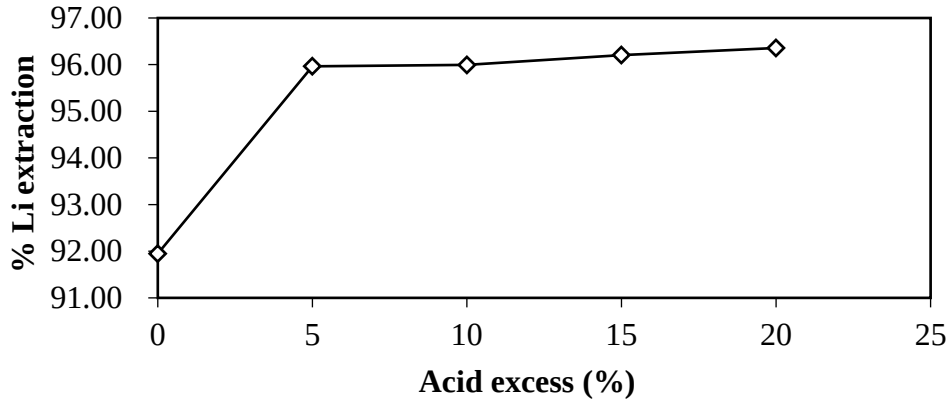

Figure 22: Effect of excess sulphuric acid on the lithium extraction with the following conditions: 500 °C digesting temperature; roasting temperature 300 °C; water leaching temperature 90 °C; leaching time 60 minutes; stirring speed 400 rpm; and solid-liquid ratio (0.05 g mL^{-1})

4.5.2 Effect of sulfuric acid roasting temperature after digesting of petalite

In order to determine the effect of acid roasting temperature on lithium extraction, a number of experiments were performed between 100 and 200 ^{o}C. According to the results presented in Figure 23, an increase in temperature brings about an increase in lithium dissolution. In order to minimize the industrial cost, the optimal extraction was fixed at 100 $^{\circ}$C, which corresponds to a 96.5 % yield.

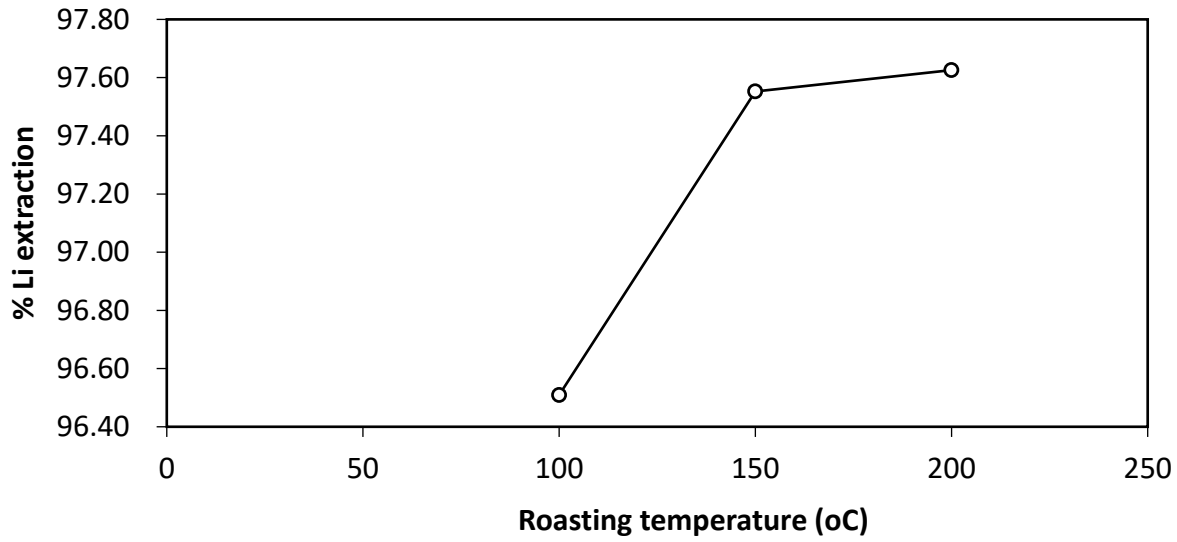

Figure 23: Effect of acid roasting on the lithium extraction with the following conditions: 500 °C digesting temperature; excess acid 5 %; roasting time 30 minutes; water leaching temperature 90 °C; leaching time 60 minutes; stirring speed 400 rpm and solid-liquid ratio (0.05 g mL^{-1})

4.5.3 Effect of acid roasting time after digesting of petalite

From Figure 24, roasting time of 15 minutes was noted to be the optimal for lithium extraction. A lithium extraction of 96.4 % was achieved after 15 minutes at 100 ºC roasting temperature.

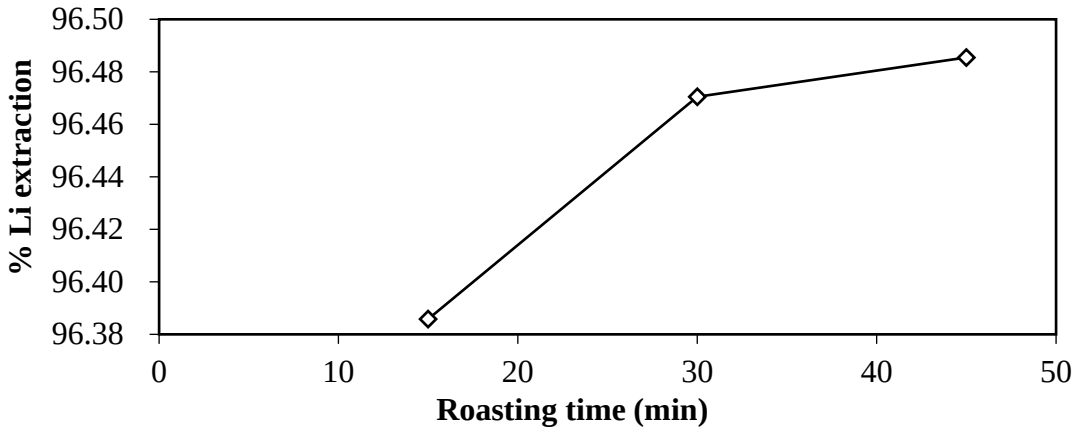

Figure 24: Effect of roasting time on the lithium extraction with the following conditions: 500°C digesting temperature; excess acid 5 %; roasting temperature 100 °C; water leaching temperature 90 °C; leaching time 60 minutes; stirring speed 400 rpm; and solid-liquid ratio (0.05 g mL^{-1}).

4.6 Leaching studies

The solvent used for leaching after the sulfuric acid roasting was distilled water. Parameters tested include stirring speed, solid/liquid mass ratio, leaching in different temperatures and times to optimize the leaching conditions.

4.6.1 Effect of stirring speed

Agitation was investigated in water leaching at 90 °C, varying the stirring speed from 100 to 400 rpm maintaining the solid-liquid ratio of (1/20 g/mL or 0.05). The role of agitation is to keep the solids in suspension, to homogenize the system and favor the diffusion through the solid-liquid boundary (mass transfer) to influence the reaction rate.

From the Figure 25, stirring has a significant influence on lithium extraction. By increasing the stirring speed, the extraction yield is increased. Above 300 rpm, the extraction yield stays constant. Based on the data given in Figure 25, the optimal extraction is fixed at 300 rpm where 96 % of lithium extraction was obtained. Sitando and Crouse (2012) reported similar results with efficiency of lithium extraction of 97.3 % with a stirring rate of 320 rpm using the same mineral.

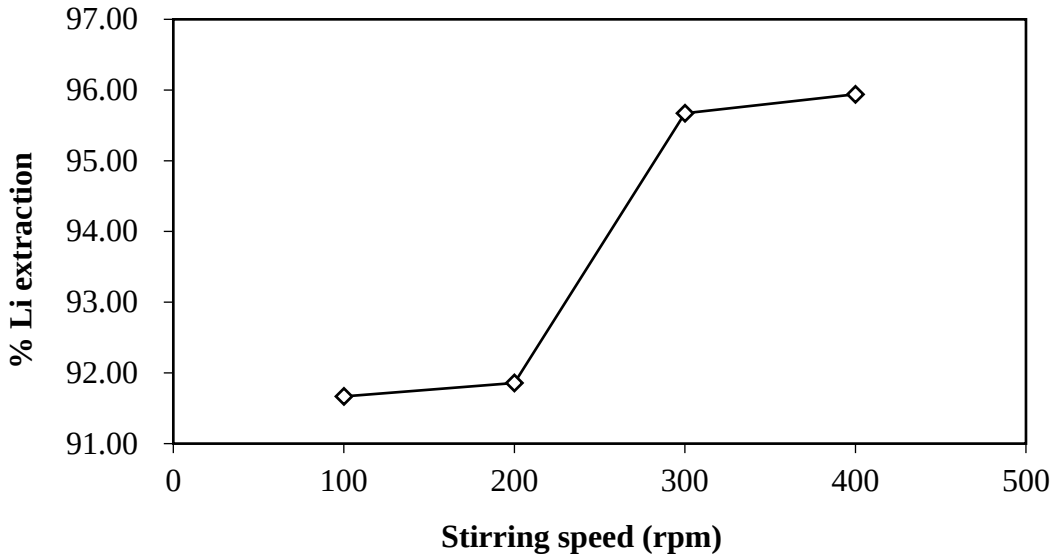

Figure 25: Effect of stirring speed on the lithium extraction rate with the following conditions: 500 ˚C digestion temperature, acid excess 5 %, roasting temperature 100 ˚C, leaching temperature 90 ˚C, leaching time 60 minutes, stirring speed 300 rpm and solid-liquid ratio (0.05).

4.6.2 Effect of solid-liquid (S/L) ratio

In this project, a comparative study on solid/liquid ratio (0.10, 0.07, 0.05, 0.04, and 0.03) was done working with temperatures at 40 °C and 80 °C to determine its influence on lithium extraction.

It can be seen from the Figure 26 that at 40 ºC, the solubility of lithium sulfate increases with increasing solid–liquid ratio. The extraction yields achieved from 0.05, 0.04 and 0.03 solid–liquid ratio corresponded respectively to 95, 4 %, 96, 7% and 96, 8 %.

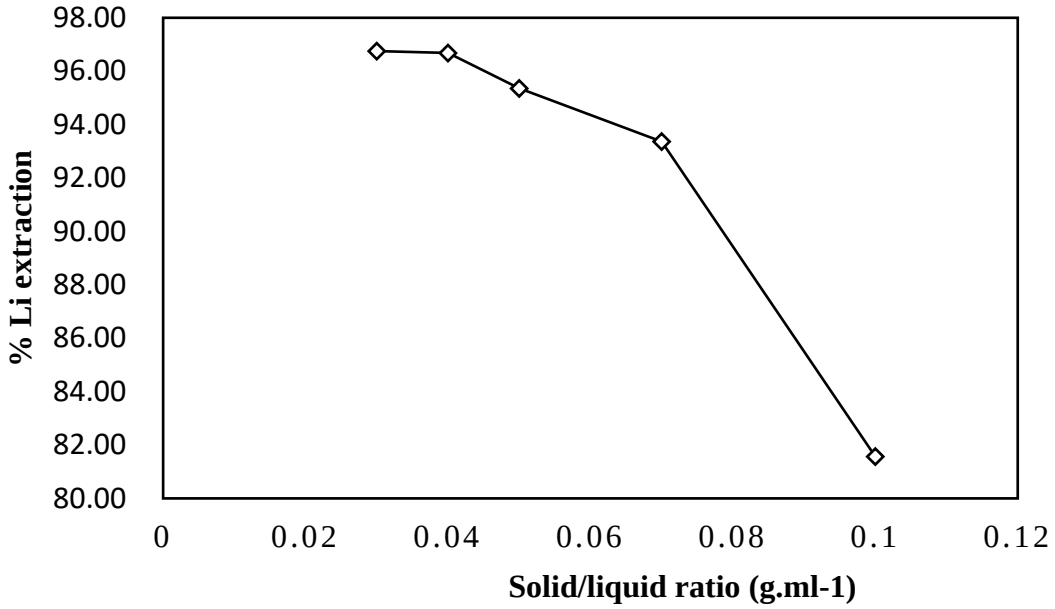

Figure 26: Effect of solid-liquid ratio on the lithium extraction rate with the following conditions: 500°C digestion temperature, acid excess 5 %, roasting temperature 100 °C, roasting time 15 minutes leaching temperature 40 °C, leaching time 60 minutes, stirring speed 300 rpm

A second investigation, working at even lower ratios (0.13, 0.10, 0.07 and 0.05) at 80 °C was done to minimize the use of water. By decreasing the solid-liquid ratio, the viscosity of the system decreased, which resulted in an increase of the mass transfer on the solid–liquid interface. From Figure 27, at the highest solid–liquid ratio (0.13), lithium was not completely dissolved and showed an extraction yield of 85.92 %. From each of the solid-liquid ratios (0.10, 0.07 and 0.05), the dissolution was almost constant with corresponding extraction yields of 96.99, 96.74 and 95.62 %, respectively.

For better extraction yields and to save water, the solid-liquid ratio of 0.10 was considered as the optimum and kept for further experiments in this project.

Moreover, the extraction at 80 °C consumed less water and showed a better extraction yield. Therefore, it was considered as the optimum extraction temperature for further use in this study. Jandová et al. (2010) reported an optimum solid-liquid ratio of 0.10 during the leaching in distilled water at 90 – 95 °C for 30 minutes with an extraction of lithium almost of 90 %.

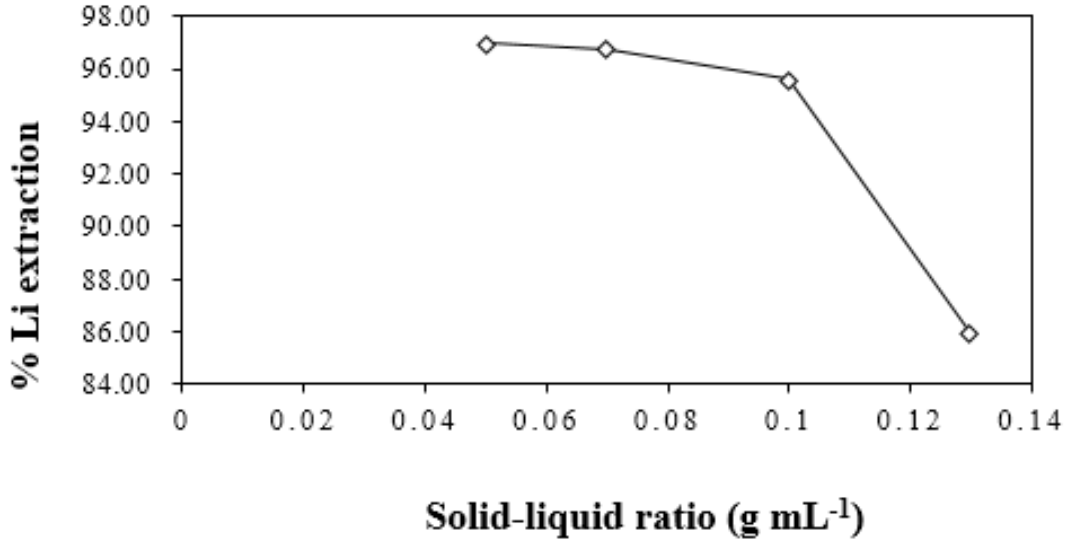

Figure 27: Effect of solid-liquid ratio on the lithium extraction rate with the following conditions: 500 ^{o}C digestion temperature; acid excess 5 %; roasting temperature 100 ^{o}C; roasting time 30 minutes; leaching temperature 80 ^{o}C; leaching time 60 minutes; stirring speed 300 rpm.

4.6.3 Effect of leaching temperature and time

Leaching temperature and time were varying between 40 ^{o}C and 80 ^{o}C using the solid–liquid ratio (0.10) and a stirring speed of 300 rpm. From Figure 28, it can be seen that temperature has a big effect on lithium extraction. An extraction of 98 % has been achieved at a leaching temperature of 80 ^{o}C after 30 minutes. Due to the small difference in leaching time between 20 and 30 minutes, the extractions of lithium were achieved at 97 and 98 %, respectively. The optimum leaching time was fixed at 20 minutes for water leaching. The optimum was fixed at 20 minutes of water leaching at 80 °C. Working at 40 ^{o}C at 0.10 dilution ratio, show little effect on lithium extraction. Jandová et al. (2009) also reported leaching temperature of 90 ^{o}C for 30 minutes on the extraction of lithium carbonate from zinnwaldite wastes.

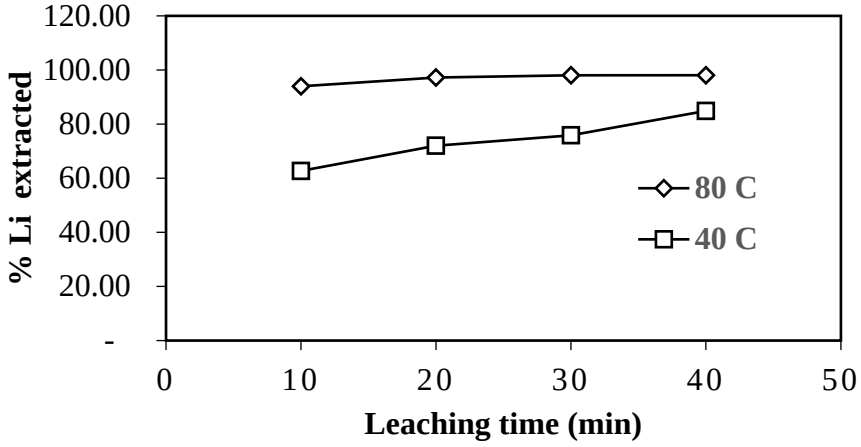

Figure 28: Effect of leaching temperature on the lithium extraction rate with the following conditions: 500 °C digestion temperature, acid excess 5 %, roasting temperature 100 °C, solid/liquid ratio (0.10), stirring speed 300 rpm

4.7 Comparison between sulfuric acid and ammonium bifluoride beneficiation processes

The extraction of lithium from Zimbabwean petalite has been reported earlier using the traditional sulfuric acid process (Sitando and Crouse, 2012).

The ABF method at 100 ^{o}C or at 500 °C seems to yield slightly lower lithium recovery than the sulfuric acid process. Less energy is used since it is not necessary to convert the crystal structure at 1 100 °C (Sitando and Crouse, 2012).

Sulfuric acid roasting of Zimbabwean petalite was done at 300 ^{o}C for 60 minutes to extract the lithium as lithium sulfate. For the ABF process acid roasting was done at 100 ^{o}C and 200 °C for 30 minutes respectively when the digestion of petalite is done at 500 °C and 100 °C.

Sitando and Crouse (2012) used 15 % excess acid during acid roasting while a 5 % acid excess was enough to achieve 97 % recovery in the ABF process.

The sulfuric acid process fixed the optimum solid–liquid ratio at 0.13 at 50 ^{o}C whilst the ABF process was fixed at 0.10 at 80 ^{o}C. Sitando and Crouse (2012) achieved an extraction yield of

97.3 % with 60 minutes leaching time. The ABF process extraction yield was 97 % in 20 minutes leaching time as shown in Table 13.

The use of ammonium bifluoride as a digesting agent, produces LiF, $Na_3Li_3[AlF_6]_2$ and AlF_3 as products to be dissolved in sulfuric acid.

Table 13: Experimental profiles and results of the two methods on processing Zimbabwean petalite

	Sulfuric acid roasting (Sitando and Crouse, 2012)	ABF fluxing
Li mineral	Zimbabwean petalite	Zimbabwean petalite
Li	1.91 %	2.0 %
Crystal structure conversion	1100 °C	None
ABF excess (%)	None	Three-time excess or stoichiometric amount
ABF digestion temperature	None	100 °C for three-time excess or 500°C for stoichiometric amount
Sulfuric acid roasting temperature using stoichiometric ABF amount	300 °C	100 °C
Sulfuric acid roasting temperature using 3×ABF excess	300 °C	200 °C
Roasting time	60 min	15 min and 30 min respectively at higher and lower temperature
Acid excess	15 %	5 % and 10 % respectively at petalite digestion of 100 °C and 500°C
Solid–liquid ratio	1:7.5	1:10
Stirring speed (rpm)	320	300
Water leaching time (min)	60	20
Leaching temperature (°C)	50	80
Maximum Li extracted (%)	97.3	97

4.8 Removal of cations

Table 12 shows the possible cations in the leach liquor, which include the alkaline metals such as (K^+, Na^+, Rb^+, Li^+) and other metals such as (Ca^{2+}, Fe^{3+}, Mg^{2+}, Al^{3+}). Calcium carbonate ($CaCO_3$) is used to precipitate aluminum and iron. Calcium hydroxide, $Ca(OH)_2$, is used to precipitate magnesium. Sodium carbonate (Na_2CO_3) was used to remove the excess of Ca. The relevant equations are shown below.

$$Al_2(SO_4)_3(aq) + 3CaCO_3(aq) \rightarrow Al_2(CO_3)_3(s) + 3CaSO_4\,(aq) \quad (23)$$

$$Fe_2SO_4(aq) + CaCO_3(aq) \rightarrow FeCO_3(s) + CaSO_4(aq) \quad (24)$$

$$MgSO_4(aq) + Ca(OH)_2(aq) \rightarrow Mg(OH)_2(s) + CaSO_4(aq) \quad (25)$$

$$CaSO_4(aq) + Na_2CO_3(aq) \rightarrow CaCO_3(s) + Na_2SO_4(aq) \quad (26)$$

$CaCO_3$ precipitate the Fe^{3+} and Al^{3+} to <1 ppm in solution. A minor yield loss of lithium during the purification process may be due to the fact that Li is co-precipitated onto the $CaSO_4$ and $Al(CO_3)$ at pH ~10. The overall recovery of lithium decreases from 97 % to 85 % after Li_2CO_3 precipitation (Hamzaoui et al., 2007).

As also shown in Table 14, the sodium concentration has increased due to the fact that sodium carbonate was used at two different stages; first when to remove excess of calcium carbonate and hydroxide used to precipitate Fe^{3+} and Al^{3+} ions and later for the precipitation of Li^{2+} ions.

Table 14: Concentration of elements in solution during the purification process

Solution	pH	Elemental concentration (mg L^{-1})						
		Li	Ca	K	Na	Al	Fe	Mg
Original leach liquor	1.47	4864.6	161.2	252.2	752.6	11887.9	50.1	13.93
Addition of $CaCO_3$ and $Ca(OH)_2$	10.7	3866.5	2241.5	202.1	616.7	566.2	1.95	1.5
Addition of Na_2CO_3	11.20	3453.5	<0.1	216.0	1601.9	<0.1	<0.1	<0.1
Concentrated leach liquor	8.00	6022.2	50.2	513.4	6580	12.5	<0.1	2.1
Mother liquor		2486.1						

4.9 Recovery and characterization of lithium carbonate

4.9.1 X–ray diffraction (XRD) results of the precipitate Li_2CO_3

The purified leach liquor was subjected to evaporation at 95 to 100 ^oC in order to precipitate Li_2CO_3.

Precipitation was done at high temperature, because the solubility of lithium carbonate is decreasing with increased temperature (Wietelmann and Bauer, 2003). Na_2CO_3 is used to precipitate Li_2CO_3. The soluble contaminants are washed from the precipitate with hot water during filtration (Lagos and Becerra, 2005).

The chemical reaction below was used to precipitate lithium carbonate using Na_2CO_3 (27):

$$Li_2SO_4(aq) + Na_2CO_3\,(aq) \rightarrow Li_2CO_3(s) + Na_2SO_4(aq) \quad (27)$$

An overall lithium recovery of 86 % was achieved and corresponds to the recovery achieved by Sitando and Crouse (2012) of 86%. Jandová et al. (2009) reported a total efficiency of

73 % Li_2CO_3 as a precipitate from concentrated leach liquors with a purity of 99 % using K_2CO_3 as a precipitating agent. Extracting lithium from lithium titanate, Lagos and Becerra (2005) reported an average yield of 83 % in a leaching solution of lithium chloride using Na_2CO_3 as a precipitating agent.

Lithium carbonate was precipitated with 15 % excess sodium carbonate from the concentrated leach liquor solution between 95 and 100 ^oC. The resulting lithium carbonate was filtrated and washed with hot water and dried.

The product obtained was characterised and compared with commercial Li_2CO_3 using X-ray diffraction shown below. As can be seen in Figure 29, the XRD patterns for the two Li_2CO_3 powders are identical.

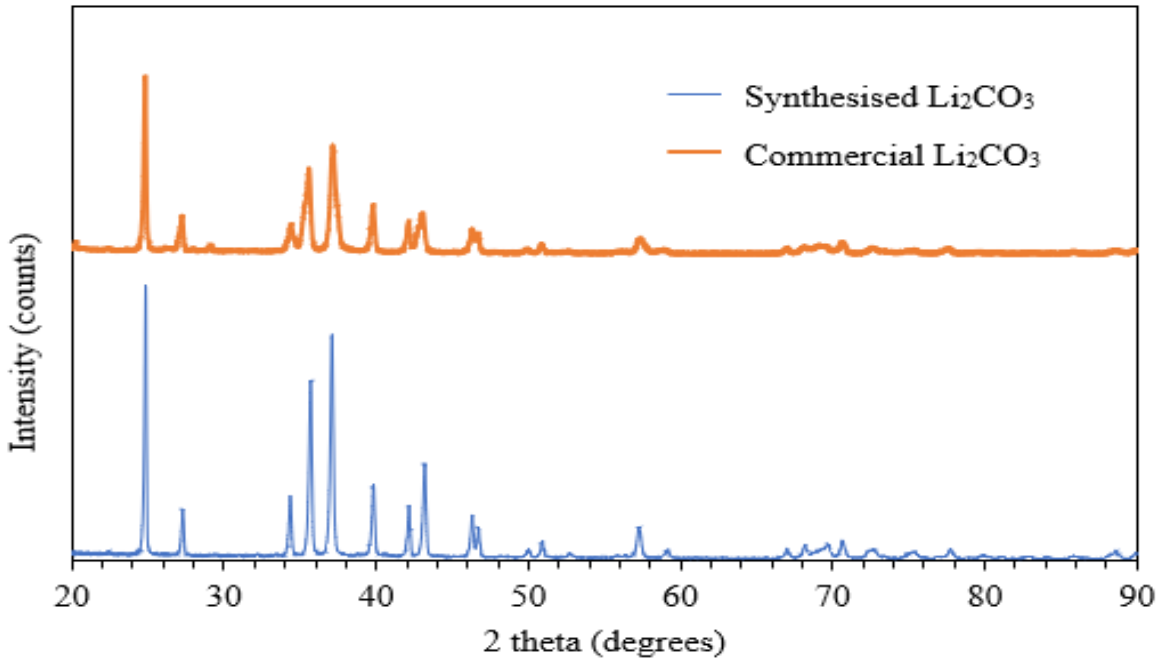

Figure 29: X–ray patterns of synthesised and commercial Li_2CO_3

Table 15 below reports the purity of the synthesized product. It can be seen from the results that the purity of the resulting product after precipitation is 99 %. After analysis of the precipitate, Na and Ca were recorded to be the major impurities that can be attributed to the residual Na_2SO_4 due to the excess of Na_2CO_3 which could not be washed properly.

Table 15: Impurities in Li_2CO_3

Li_2CO_3 purity (%)	Content of major impurities (wt %)					
	Ca	Al	Fe	K	Mg	Na
99	0.53	<0.05	<0.01	<0.02	<0.01	0.56

4.9.2 Scanning electron microscope (SEM) results of the precipitate Li_2CO_3

The morphology of the Li_2CO_3 particles synthetized (Figure 31) was examined and compared to the commercial Li_2CO_3 powder (Figure 30) using SEM. The morphology of the Li_2CO_3 synthesized and the commercial product are monodispersed truncated octahedron and the surfaces of the particles are smooth.

The produced particles are small and highly agglomerated as indicated in Figure 31 and Figure 30 compared to the commercial powder.

The finer size distribution results at higher concentration of lithium in the starting solution. Increasing concentration results in increasing of the nucleation rate by increasing the number of nucleation sites.

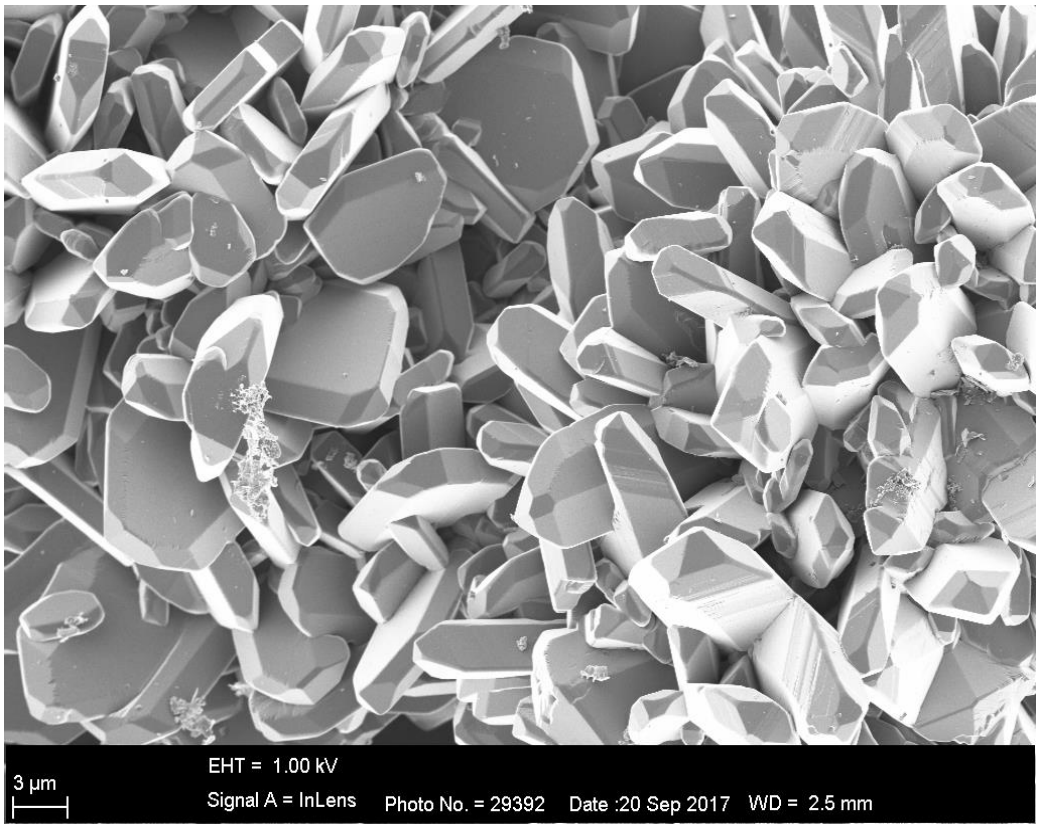

Figure 30: SEM images of commercial Li_2CO_3

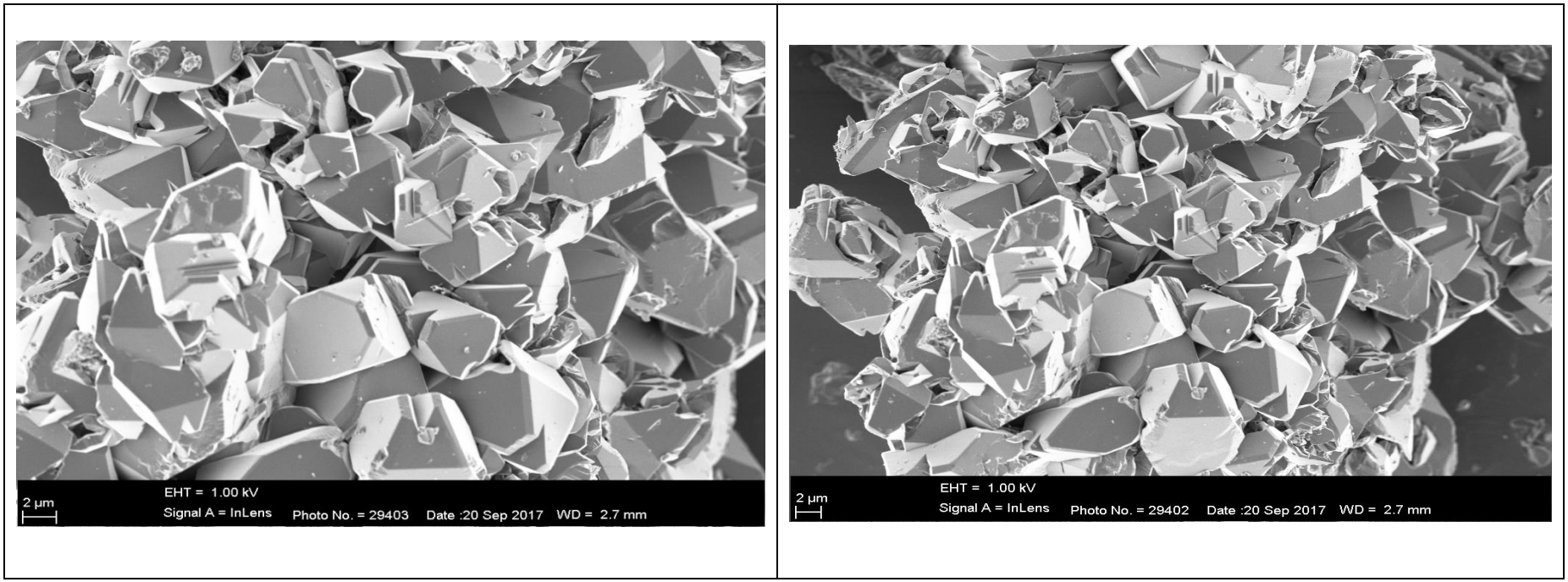

Figure 31: SEM images of synthesised Li_2CO_3

4.10 Summary on the recovery of lithium from Zimbabwean petalite using ammonium bifluoride

In previous studies, the production of lithium carbonate via the processing of petalite (spodumene) and sulfuric acid had the flow sheet shown in Wietelmann and Bauer (2003). These studies adopted high temperature calcination for phase transformation from α-spodumene into β-spodumene and are energy consuming and costly for lithium extraction (Sitando, 2012, Kuang et al., 2012).

With several experimental tests, the flow sheet for lithium extraction from the Zimbabwean concentrate with ammonium bifluoride is shown in Figure 12. With the new method, the proposed flow sheet for lithium extraction uses the same concentrate with qualitatively less energy consumed because a lower temperature was used (less than 600 °C Instead of 1100 °C), and thus may be an economic improvement over the previous method. At 100 °C (low temperature option) only a preliminary optimization process was done whilst at 500 °C (high temperature option) the comparative optimization study was done for the petalite digestion. The suggested conditions for each steps are given in Table 16.

Table 16: Suggested conditions for each process step

Lithium mineral	Zimbabwean petalite
ABF (excess)	3
Digestion temperature (°C)	100
Digestion time (min)	30
H_2SO_4 (excess)	10
Roasting temperature (°C)	200
Roasting time (min)	30
Solid-liquid	1:10
Leaching temperature (°C)	80
Leaching time (min)	20
Lithium mineral	Zimbabwean petalite
ABF (excess)	0
Digestion temperature (°C)	500
Digestion time (min)	120
H_2SO_4 (% excess)	5
Roasting temperature (°C)	100
Roasting time (min)	15
Solid-liquid	1:10
Leaching temperature (°C)	80
Leaching time (min)	20

5 Conclusions and recommendations

5.1 Conclusions

Ammonium bifluoride digestion has been demonstrated to be successful for the lithium extraction from Zimbabwean petalite.

The ICP-OES and XRF data showed that the petalite sample contained 4.3 % Li_2O on average. The XRD results on the other hand showed that the major mineral phase in the Zimbabwean concentrate was petalite but contains also other mineral phases like quartz, spodumene, and bikitaite.

The lithium extraction rate is influenced by parameters such as ammonium bifluoride concentration, digesting temperature, water leaching temperature of the lithium fluoride and cryolithionite, stirring speed and the solid-liquid water ratio. A maximum lithium extraction yield of 97 % was achieved under the following conditions: a three molar ammonium biofluoride excess, acid roasting temperature of 200 ºC in 15 minutes after digesting the concentrate at 100 ºC with a solid-liquid ratio of 0.1 $g.mL^{-1}$, water leaching temperature at 80 ºC in 30 minutes and stirring rate of 300 rpm.

When the digestion is raised above 200 °C, a maximum of lithium extraction yield of 97 % was achieved again under the following conditions: a stoichiometric molar mass; acid roasting temperature of 100 ºC in 15 minutes after digesting the concentrate at 500 ºC with a solid-liquid ratio of 0.1 $g.mL^{-1}$; water leaching temperature at 80 ºC in 20 minutes; and stirring rate of 300 rpm

The fluoride digestion method offers a good alternative with possible economic benefits for extracting lithium from the Zimbabwean petalite.

The purification process was focused on the removal of the impurities which was dissolved during the acid roasting and water leaching stages. The overall impurity concentration was reduced to less than 1.2 %.

The precipitation of Li_2CO_3 was carried out between 90 and 100 ºC and the results showed that the purity of Li_2CO_3 produced was 99 %.

5.2 Recommendations

Optimum conditions using ammonium bifluoride for digestion of petalite were determined in order to extract lithium from Zimbabwean petalite. However, several factors influence the process and need to be further studied in order to produce high purity Li_2CO_3 from the Zimbabwean petalite.

The following recommendations are made in order to improve the process for Li_2CO_3 production:

- Li_2CO_3 produced after precipitation needs to be further processed since its purity is about 99 %. Technical grade lithium carbonate is only suitable for application in the glass and ceramics as well as the aluminum industry. However, this grade is not suitable for the batteries in hybrid vehicles, electronic grade crystals and lithium metal anodes for these applications, the required purity of lithium carbonate should be 99.9 %. According to Amouzegar et al. (2000), the impurities that co-precipitate with Li_2CO_3 can be dissolved with carbon dioxide under pressure and physically separated from lithium bicarbonate by ion exchange or solvent extraction and then evaporate the solution to precipitate lithium carbonate;
- Lithium losses during the process of purification (11.5%) need to be reduced by improving the washing process;
- Further treatment of the aqueous Li_2SO_4 when petalite is digested at 100 °C should be continued up to the precipitation of Li_2CO_3 to determine if digestion of petalite at 500 °C is necessary, NH_4HF_2 molar ratio and H_2SO_4 excess used here should also be studied to determine if the amount can be reduced.;
- A study can be done to determine whether the acid roasting step can be eliminated;
- As byproducts, aluminum and sodium sulfate can be valorized since, during water leaching, a lot of aluminum was leached and this can lead to a new project. Sodium sulfate, after precipitation of lithium carbonate, can also lead to a new project for its valorization, since both are impurities in the lithium production process.

The full economic aspects of lithium carbonate production should obviously be evaluated. The work presented here provides the technical detail required.

6 References

Alvani, C, Casadio, S, Contini, V, Bartolomeo, AD, Lulewicz, J and Roux, N (2002) "Li_2TiO_3 pebbles reprocessing, recovery of ^6Li as Li_2CO_3" *Journal of Nuclear Materials,* 307-311**,** 837-841.

Amouzegar, K, Amant, GS and Harrison, S (2000) "Process for the purification of lithium carbonate" *U.S Patent,* 6 048 507, assigned to Limtech, Cape Rouge, Canada.

Andreev, VA, Buynovskiy, AS, Andreev, AA and Dyachenko, AN (2007a) "Topaz concentrate desiliconization with ammonium bifluoride" *Russian Journal of Bulletin of the Tomsk Polytechnic University,* 311**,** 27-31.

Andreev, VA, Buynovskiy, AS, Dyachenko, AN and Kraidenko, RI (2007b) "Studying the utilization techniques of ammonium hexafluorosilicate" *Russian Journal of Bulletin of the Tomsk Polytechnic University,* 311**,** 31-34.

Azaroff, LV (1968) *Elements of X-ray Crystallography,* McCraw-Hill Book Company, New York.

Bale, M and May, A (1989) "Processing of ores to produce tantalum and lithium" *Minerals Engineering* 2(3)**,** 299-320.

Biswas, G, Kumari, M, Adhikari, K and Dutta, S (2017) "A critical review on occurrence of fluoride and its removal through adsorption with an emphasis on natural minerals" *Current Pollution Reports* 3**,** 104-119.

Bradley, DC and Jaskula, B (2014) "US Geological Survey, Lithium-for Harnessing Renewable Energy: US Department of the Interior", US Geological Survey 2014. Available at <https://pubs.usgs.gov/fs/2014/3035/pdf/fs2014-3035.pdf> (accessed on 14.12.2017).

Brandt, F and Haus, R (2010) "New concepts for lithium minerals processing" *Minerals Engineering* 23**,** 659-661.

Brown, ME (2001) *Introduction to Thermal Analysis,* Kluwer Academic Publisher, London.

Brown, PM and Beckerman, SJ (1990) ‘'Production of lithium metal grade lithium chloride from lithium-containing brine", *US Patent 4980136*, assigned to Cyprus Foote mineral company, Malvern, Pa, USA.

Brown, TJ, Walters, A, Idoine, NE, Gunn, G, Shaw, RA and Rayner, D (2016) "British geological survey, Mineral profile: Lithium", British geological survey 2016. Available <http://minerals.usgs.gv/minerals/pubs/MSc/2011/msc2011 > (accessed on 19.06 2017).

Bruno, J and Sandino, A (1987) *Radionuclide co-precipitation*, Swedish Nuclear Fuel and Waste Management Co.

Burkert, GM and Ellestad, RB (1970) ‘'Precipitation of lithium carbonate from lithium chloride solution", *US Patent* 3523751, assigned to Lithium Corporation of America.

Choubey, PK, Kim, MS, Srivastava, RR, Lee, JC and Lee, JY (2016) "Advance review on the exploitation of the prominent energy-storage element: Lithium. Part I: From mineral and brine resources" *Minerals Engineering* 89**,** 119-137.

Cooper, DG (1964) *Some ore deposits in Southern Africa, the geology of the Bikita pegmatite,* Geology Society of South Africa, Vol.2.

Coulson, JM and Richardson, JF (1996) *Chemical Engineering-Particle Technology and Separation Process,* Butterworth-Heinemann, Oxford.

Daitch, PJ (2018) *Lithium Extraction from Oilfield Brine*, MSc Thesis, University of Texas, Texas, USA.

Du plessis, W, Pienaar, AD, Postma, CJ and Crouse, PL (2016) "Effect of the value of x in NH_4FxHF on the digestion of plasma-dissociated zircon" *International Journal of Mineral Processing*, 147**,** 43-47.

Duke, CV, Miller, JM, Clark, JH.and Kybett, AP (1990) "^{19}F mas NMR and FTIR analysis of the adsorption of alkali metal fluorides onto alumina" *Journal Molecular Catalysis,* 62**,** 233-242.

Ebensperger, A, Maxwell, P and Moscoso, C (2005) "The lithium industry: its recent evolution and future prospects" *Resources Policy,* 30**,** 218-231.

El Guendouzi, M, Skafi, M and Rifai, A (2016) "Hexafluorosilicate Salts in Wet Phosphoric Acid Processes: Properties of X_2SiF_6–H_2O with X= Na^+, K^+, or NH_4^+ in Aqueous Solutions at 353.15 K" *Journal of Chemical & Engineering Data,* 61**,** 1728-1734.

Evans, RK (2014) *Lithium*. In Gunn, A.G (Ed). 2014. Critical Metals Handbook Chapter 10 John Wiley & Sons Ltd, Chichester.

Gama, JS, Wagener, JB and crouse, PL (2013) "A thermogravimetric study of the reactions of molybdenum disilicide with anhydrous hydrogen fluoride and fluorine" *Journal of Fluorine Chemistry,* 145**,** 66-69.

Garrett, DE (2004) *Handbook of Lithium and Natural Calcium Chloride,* Elsevier,Oxford.

Grady, H (1980) "Lithium metal for the battery industry" *Journal of Power Sources,* 5**,** 127-135.

Guo, H, Kuang, G, Wan, H, Yang, Y, Yu, HZ and Wang, HD (2019) "Enhanced acid treatment to extract lithium from lepidolite with a fluorine-based chemical method" *Hydrometallurgy,* 183**,** 9-19.

Hamzaoui, AH, Hammi, H and M'nif, A (2007) "Operating conditions for lithium recovery from natural brines" *Russian Journal of Inorganic Chemistry,* 52**,** 1859-1863.

Heinrich, EW, Salotti, C and Giardini, A (1978) "Hydrogen-mineral reactions and their application to the removal of iron from spodumene. *Energy,* 3,273-279.

Hien-dinh, T (2015) *Processing of Vietnamese lithium ores to produce LiCl*, PhD Thesis**,** Freiburg im Breisgau university, Freiburg im Breisgau, Germany.

Hien-dinh, TT, Luong, VT, Gieré, R and Tran, T (2015) "Extraction of lithium from lepidolite via iron sulphide roasting and water leaching" *Hydrometallurgy*, 153**,** 154-159.

Hoshino, D and Adachi, S (2007) "Stain Etching Characteristics of Silicon (001) Surfaces in Aqueous HF/ $K_2Cr_2O_7$ Solutions" *Journal of The Electrochemical Society,* 154 (10)**,** E139-E144.

House , JE and Engel, DA (1993) "Decomposition of ammonium bifluoride and the proton affinity of the bifluoride ion" *Thermochimica Acta,* 66**,** 343-345.

Jackson, E (1986) *Hydrometallurgical Extraction and Reclamation*, Ellis Horwood Ltd, Chichester.

Jandova, J, Dvořák, P, Formánek, J and Vu, HN (2012) "Recovery of rubidium and potassium alums from lithium-bearing minerals" *Hydrometallurgy,* 119**,** 73-76.

Jandová, J, DVořák, P and Vu, HN (2010) "Processing of zinnwaldite waste to obtain Li_2CO_3" *Hydrometallurgy,* 103**,** 12-18.

Jandová, J, Vu, HN, Belkova, T, Dvorák, P and Kondás, J (2009) "Obtaining Li_2CO_3 from zinnwaldite wastes" *Ceramics-Silikáty,* 53**,** 108-112.

Jaskula, BW (2011) "U.S. Geological Survey", Mineral commodity summaries lithium: U.S. Geological Survey 2011, 94-95.Available at <https://minerals.usgs.gov/minerals/pubs/mcs/2011/mcs2011.pdf> (accessed on 28.01.2017).

Jaskula, BW (2015) " U.S. Geological Survey", Lithium [Advance Release] :U.S. Geological Survey Minerals Yearbook- 2015. Available at <http://minerals.usgs.gov/minerals/pubs/commodity/lithium/myb1-2013-lithi.pdf>(accessed 11 October 2018).

Kabacelik, I and Ulug, B (2008) "Further investigation on the formation mechanisms of $(NH_4)_2SiF_6$ synthesized by dry etching technique" *Applied Surface Science,* 254**,** 1870-1873.

Kondás, J, Jandová, J and Nemeckova, M (2006) "Processing of spent Li/MnO_2 batteries to obtain Li_2CO_3" *Hydrometallurgy,* 84**,** 247-249.

Kuang, G, Chen, ZB, Guo, H and Li, MH (2012) "Lithium Extraction Mechanism from α-Spodumene by Fluorine Chemical Method" *Advanced Materials Research,* 2011-2016.

Lagos, S and Becerra, R (2005) "Methodology for the recovery of lithium from lithium titanate" *Journal of Nuclear Materials,* 347**,** 134-139.

Lee, J (2015) "Extraction of lithium from lepidolite using mixed grinding with sodium sulfide followed by water leaching" *Minerals,* 5**,** 737-743.

Linnen, R.L., Van Lichtervelde, M and Černý, P (2012) "Granitic pegmatites as sources of strategic metals" *Elements,* 8**,** 275-280.

Löf, GO and Lewis, WK (1942) "Lithium chloride from lepidolite" *Industrial & Engineering Chemistry,* 34**,** 209-216.

Loubser, M and Verryn, S (2008) "Combining XRF and XRD analyses and sample preparation to solve mineralogical problems" *South African Journal of Geology,* 111**,** 229-238.

Margarido, F, Vieceli, N, Durão, F, Guimarães, C and Nogueira, C (2014) "Minero-metallurgical processes for lithium recovery from pegmatitic ores" *Comunicações Geológicas,* 101**,** 795-798.

Martin, G, Rentsch, L, Höck, M and Bertau, M (2017) "Lithium market research–global supply, future demand and price development" *Energy Storage Materials,* 6**,** 171-179.

Marya, M and Edwards, G (2002) "Chloride contributions in flux-assisted GTA welding of magnesium alloys" *Welding Journal-New York,* 81**,** 291-S-298-S.

Meshram, P, Pandey, B and Mankhand, T (2014) "Extraction of lithium from primary and secondary sources by pre-treatment, leaching and separation: A comprehensive review" *Hydrometallurgy,* 150**,** 192-208.

Mohandas, E and Rajmohan, V (2007) "Lithium use in special populations" *Indian journal of psychiatry,* 49**,** 211.

Muzenda, E, Ramatsa, I, Ntuli, F, Belaid, M and Tshwabi, P (2011) "An investigation into the effect of temperature on the leaching of copper-matte" *World Academy of Science, Engineering and Technology 52*.

Nel, JT, Du plessis, W, Nhlabathi, TN, Pretorius, CJ, Jansen, AA and Crouse, PL (2011) "Reaction kinetics of the microwave enhanced digestion of zircon with ammonium acid fluoride" *Journal of Fluorine Chemistry,* 132**,** 258-262.

Nhlabathi, TN, Nel, JT, Puts, GJ and Crouse, PL (2012) "Microwave digestion of zircon with ammonium acid fluoride: Derivation of kinetic parameters from non-isothermal reaction data" *International Journal of Mineral Processing,* 114**,** 35-39.

Ober, JA (2007) "Lithium, Minerals Yearbook-2005", U.S. Geological Survey, 2007, 44.1-44.7.
Availableat<https://minerals.usgs.gov/minerals/pubs/commodity/lithium/lithimyb06.pdf> (accessed on 27.6.2017).

Peiró, LT, Méndez, GV and Ayres, RU (2013) "Lithium: sources, production, uses, and recovery outlook" *Jom,* 65**,** 986-996.

Retief, WL, Nel, JT, Du plessis, W and Crouse, PL (2014) "Treatment of zirconia-based material with ammonium bi-fluoride", *US Patents* 0011329 A1, assigned to South African Nuclear Energy Corporation Limited.

Rosales, GD, Del Carmen ruiz, M and Rodriguez, MH (2013) "Alkaline metal fluoride synthesis as a subproduct of β-spodumene leaching" *Hydrometallurgy,* 139**,** 73-78.

Rosales, GD, Del Carmen ruiz, M and Rodriguez, MH (2014) "Novel process for the extraction of lithium from β-spodumene by leaching with HF" *Hydrometallurgy,* 147**,** 1-6.

Segal, E.B (2000) "First aid for a unique acid, HF: A sequel" *Chemical Health and Safety,* 7**,** 18-23.

Sitando, O (2012) *Beneficiation of Zimbabwean petalite: extraction, purification and compound synthesis* , MSc Thesis, University of Pretoria, Pretoria, South Africa.

Sitando, O and Crouse, PL (2012) "Processing of a Zimbabwean petalite to obtain lithium carbonate" *International Journal of Mineral Processing,* 102**,** 45-50.

Smit, DS (2001) *The leaching behaviour of a Ni-Cu-Co sulphide ore in an oxidative pressure-acid medium*, MSc Thesis, North West University, Potchefstroom, South Africa.

Solvay (2013) "Solvay America. Product safety summary statement: Ammonium Bifluoride". Available at <https://www.solvay.us/en/binaries/PSS-Ammonium-Bifluoride-164339.pdf> (accessed on 24.07.2017)".

Srivatsan, T and Sudarshan, T (1991) "Welding of lightweight aluminumlithium alloys" *Welding journal*, 70**,** 173-185.

Staiger, J and Rödel, T (2016) "Lithium Report 2016". Available at <https://www.resource-capital.ch/fileadmin/reports/2016/kw38/en_Lithium_ES.pdf> (accessed on 4.6.2017).

Stubblefield, CB and Bach, RO (1972) "Solubility of lithium fluoride in water" *Journal of Chemical and Engineering Data*, 17**,** 491-492.

Vikström, H, Davidsson, S and Höök, M (2013) "Lithium availability and future production outlooks" *Applied Energy*, 110**,** 252-266.

Virolainen, S, Fini, MF, Miettinen, V, Laitinen, A, Haapalainen, M and Sainio, T (2016) "Removal of calcium and magnesium from lithium brine concentrate via continuous counter-current solvent extraction" *Hydrometallurgy*, 162**,** 9-15.

Vu, H, BernardI, J, Jandová, J, Vaculíková, L and Goliáš, V (2013) "Lithium and rubidium extraction from zinnwaldite by alkali digestion process: Sintering mechanism and leaching kinetics" *International Journal of Mineral Processing*, 123**,** 9-17.

Wietelmann, U and Bauer, RJ (2003) "Lithium and Lithium Compounds", in *Ullmann's Encyclopedia of Industrial Chemistry*, vol. 20. Wiley-VCH Verlag GmbH & Co. Weinheim, Germany.

Yan, Q, Li, X, Yin, Z, Wang, Z, Guo, H, Peng, W and Hu, Q (2012) "A novel process for extracting lithium from lepidolite" *Hydrometallurgy*, 121**,** 54-59.

7 Appendix

The analytical techniques discussed were used during this research project.

7.1 Inductively coupled plasma optical emission spectrometry (ICP-OES)

For the analysis of lithium and other elements in solution, ICP-OES was used as the analytical technique. The advantages of ICP-OES compared to atomic absorption spectrophotometers with excitation temperature of the air-acetylene flame, is between 2000 to 3000 K, excitation temperature of argon ICP varying between 5000 K and 7000 K, multiple measurements in the same run, high sample throughput, low detection concentrations, accuracy, and less susceptible to interferences than comparable spectrometric techniques (Sitando, 2012).

The sample to be analysed is introduced through the nebulizer into a spray chamber via the peristaltic pump in the form of an aerosol straight to the argon plasma. Plasma is known to be the fourth state of the matter after the solid, liquid and gaseous state. Argon gas is supplied to the torch and then the high frequency electric current is applied to the work coil at the tip of the torch creating an electromagnetic field in the torch tube. The electromagnetic field is accelerating electrons in a circular trajectory. A collusion between argon atom and electrons lead to ionisation and creating a stable plasma. With sample introduction, desolvation, atomisation and ionisation takes place in the torch. The energy taken up by the electrons leads to a higher excited state by releasing light when they return to low energy state. The colours of the emitted light and the light intensity in various frequencies are used to identify the element and quantify its concentration using a charged coupled detector (CCD).

A typical ICP-OES instrument consists of the following components:

- Sample introduction system;
- ICP torch;
- Computer;
- Radio frequency generator;
- Spectrometry;
- Detector .

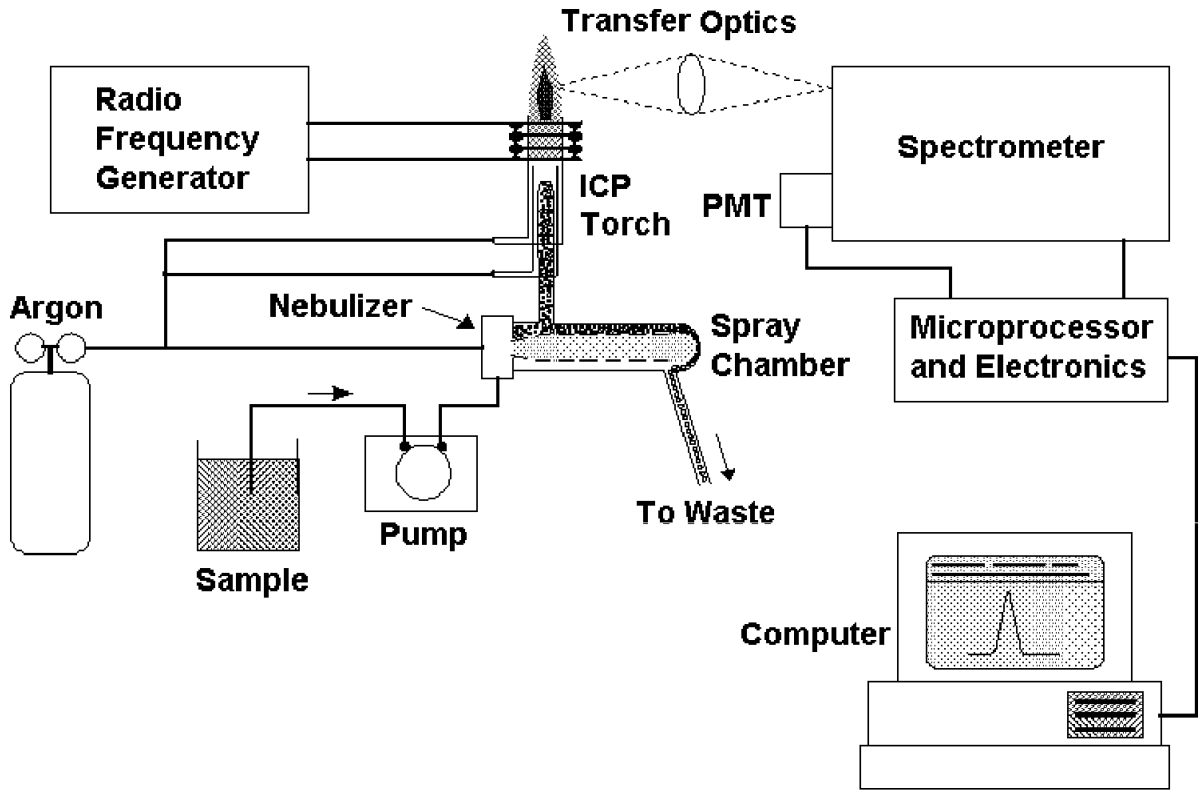

Figure 32: Schematic diagram of an ICP-OES instrument

7.2 X-ray diffraction spectrometry (XRD)

X-ray diffraction is a method used in determination of crystallinity, composition and physical properties of a compound.

Sample analysis using XRD is based on the interference of monochromatic x-rays and its crystalline structure. A cathode tube is used to generate x-rays, which are filtered to produce a monochromatic radiation, parallel to one of the pinacoid faces of the crystal and directed toward to the sample.

The interaction between X-rays and the sample results in the constructive interference when Bragg's law is satisfied ($n\lambda=2d \sin \theta$). θ (theta) is known as the angle of incidence, variable d is the distance between atomic layers in a crystal and λ (lambda) is the wavelength of the incident X-ray beam and n is an integer. Bragg's law is related to the wavelength of electromagnetic radiation to the diffraction angle and the presence of the lattice spacing in a crystalline sample.

The analysis is based on the fact that, for any distance between the atomic layers, there are some specific angles at which the X-rays with a specific wavelength existing the layers, will be picked up by the detector and will be producing peaks on the diffractometer (Azaroff, 1968). During the analysis, the detector through the X-rays will be moving around the sample, measuring the intensity and the diffraction angles (2θ) of the peaks, because every mineral compound has its own diffraction peak for identification. The highest peak is defined as the 100 % peak and the intensity of other peaks are measured as a percentage of the 100 % peak (Sitando, 2012, Burkert and Ellestad, 1970).

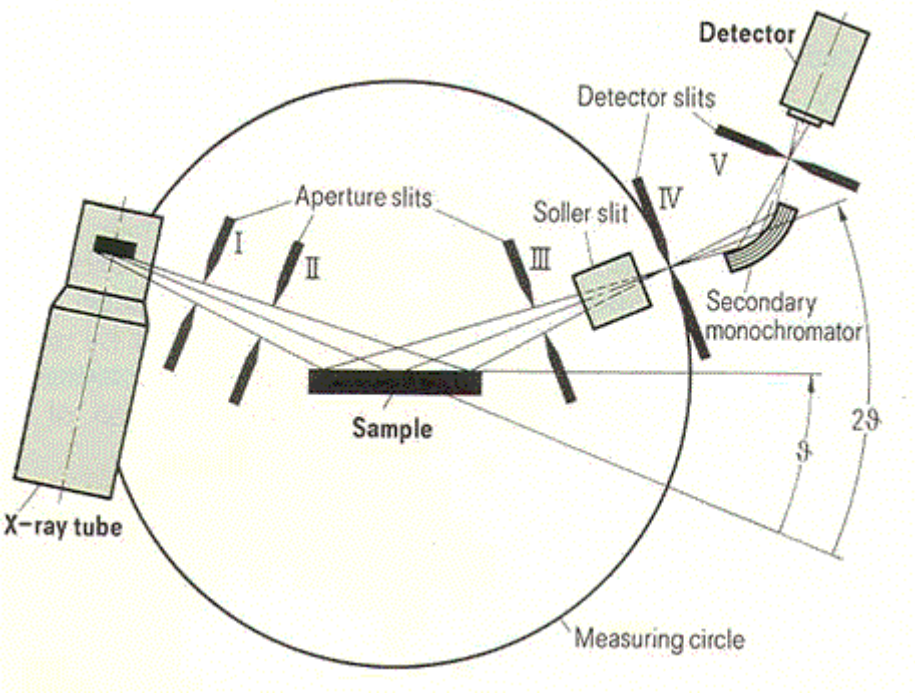

Figure 33: Schematic diagram of an X-ray diffraction instrument

7.3 X-ray fluorescence spectroscopy (XRF)

X-ray fluorescence (XRF) spectrometry is one of the elemental analysis techniques which find many applications in research sciences and mining industries (Loubser and Verryn, 2008) and is used to determine a bulk composition of a sample. The range of elements from fluorine to uranium in the periodic table can be analysed using XRF with a detection limit varying from heavier elements like molybdenum (0.5 ppm) to lightest element like fluorine (100 ppm). The advantage of this technical analysis is such as it is non-destructive, multi-elemental, fast and cost effective (Loubser and Verryn, 2008).

The analysis principle using XRF is based on the fact that, when individual atoms are excited in a sample by an external source of energy, X-rays photons are emitted from the sample of a characteristic wavelength or energy. The identification or quantification of the element present in the sample is done by counting the number of photons of each energy emitted from that sample. The figure below summarised the XRF principle.

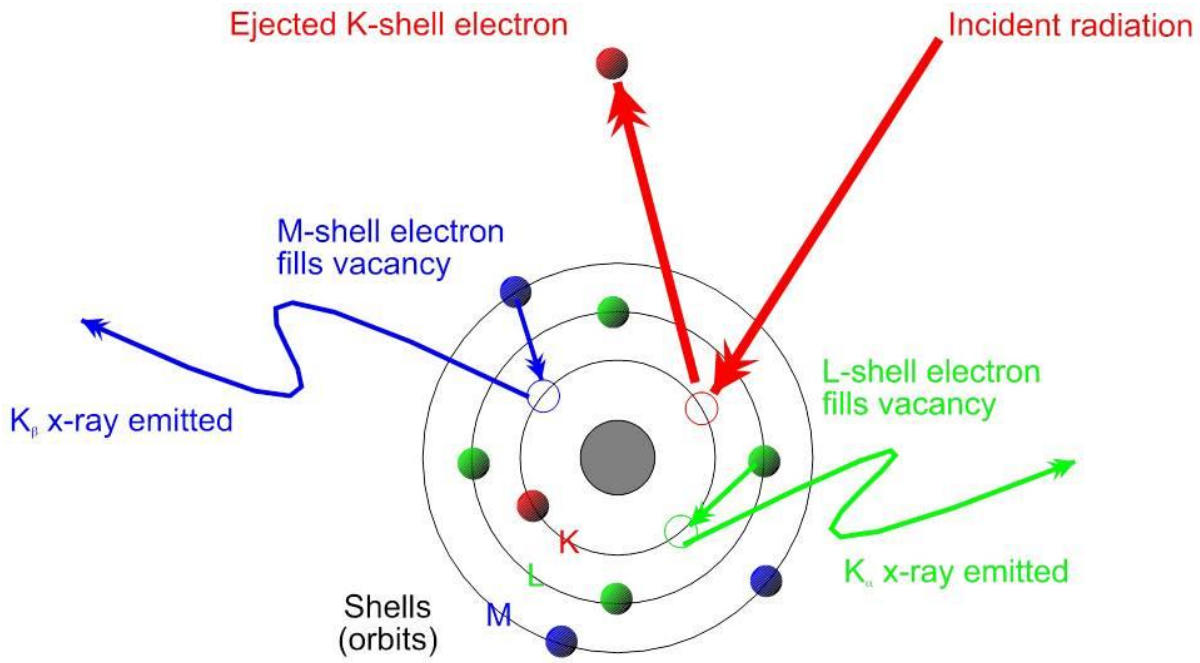

Figure 34: X-ray fluorescence principle

When the inner shell electron is excited by an incident photon in the X-ray region, during the process of its de-excitation (from higher energy state to the lower energy state), the electron moves from the higher energy region to the lower energy region to fill the vacancy. The photon emitted by the atom during the de-excitation has an energy equal to the difference in the energy of the two regions. The X-ray photons emitted from the sample according to the process mentioned above are used to determine the characteristic energy or wavelength; the energy and intensity peaks lead to the determination of the element and the concentration in the sample.

According to Loubser and Verryn (2008), sample preparation consists of drying, crushing to 10 mm, riffle splitting and milling in a tungsten carbide milling pot to a particle size 80 % below 75 µm. Samples should be dried and weighed at 110 ºC, then roasted and weighted again at 1000 ºC to determine the percentage loss on ignition (LOI) using the following equation:

$$\%\text{LOI} = \frac{\text{Weighty1} - \text{Weight2}}{\text{Weight1} - \text{Weight crucible}}$$

7.4 Scanning electron microscope (SEM)

A scanning electron microscope (SEM) is an analysis method giving high resolution images, topography and composition of a sample by scanning the surface with a focused beam of electrons. The interaction between the beam electrons and atoms in a sample produce various signals that contain sample's information to be used for analysis of the topography and composition of a sample. This interaction also produces an image at various depths within the sample. During the process, different types of signals are also produced including secondary electrons (SE) which emitted from the sample's surface. Note that, secondary electrons are emitted when electron beams are scanned across the sample and then detector attracted by the detector by a positive charge. During this process, the electrons and the signals are counted sent to an amplifier by the detector. A number of electrons emitted from each spot on the specimen are used to build up a final image inside of the machine (Sitando, 2012). The figure below shows a schematic diagram of a SEM.

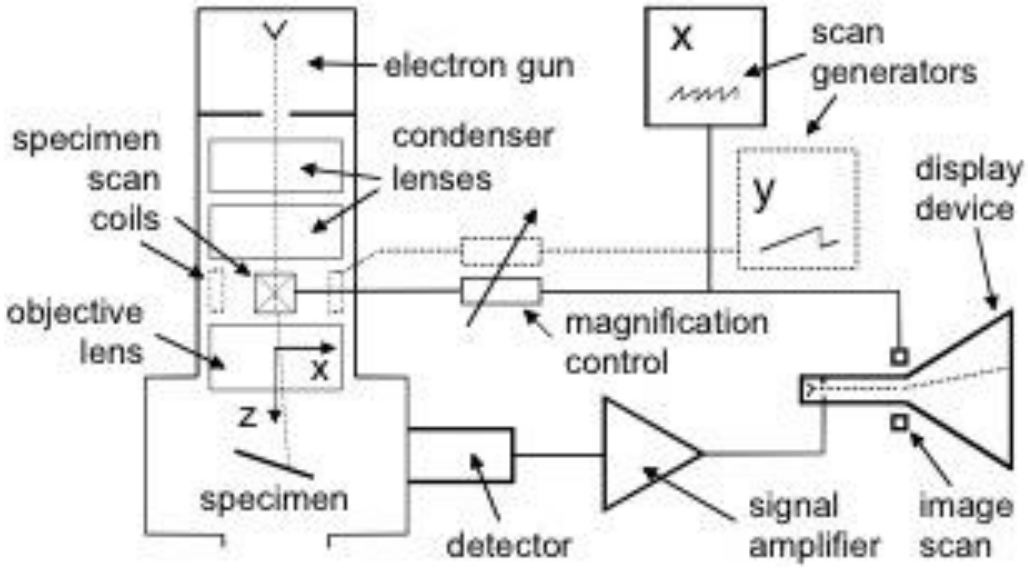

Figure 35: Schematic diagram of a scanning electron microscope

7.5 Thermogravimetric analysis (TGA)

TGA is defined as a technique in which of changes in sample mass are measured in function of the temperature and time using a thermobalance (Brown, 2001). A TGA instruments consists of a precision balance on which is placed a sample pan. This pan placed in a furnace and is heated or cooled during the experimental test. The mass of the sample is controlled during the experiment (Brown, 2001) as shown in the figure below.

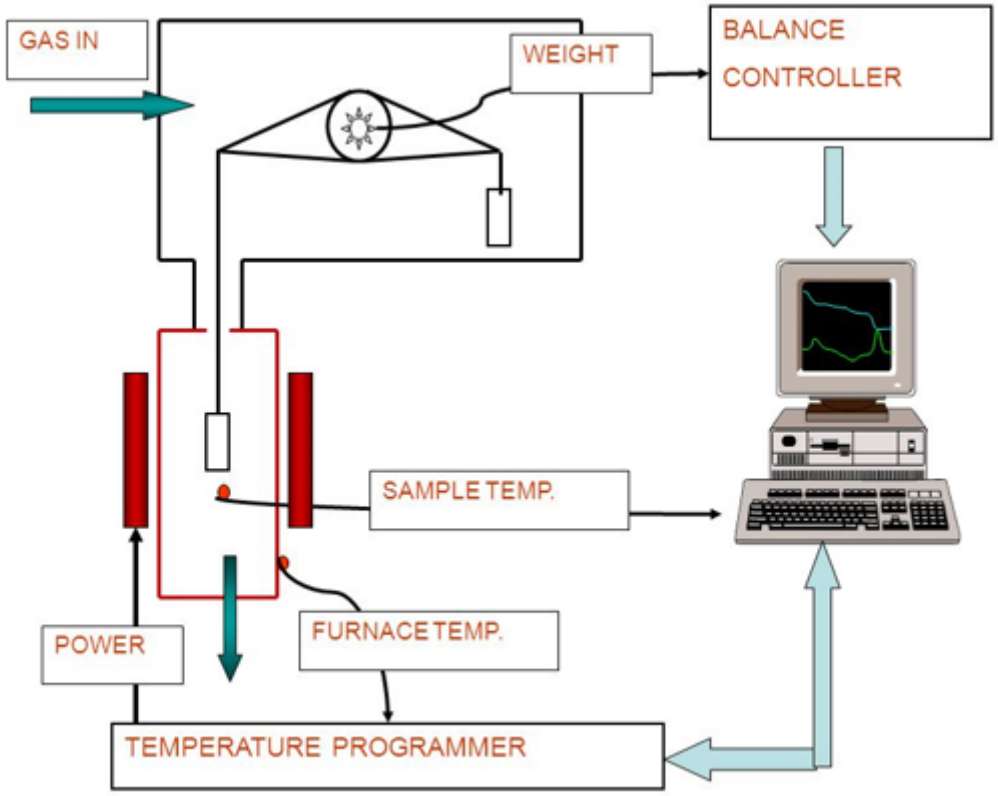

Figure 36: A schematic diagram of a thermobalance

A thermobalance is an instrument that allows sample to be simultaneously weighed, heated and cooled down in a controlled way and the mass, time, temperature to be captured. For this to be done, the thermobalance is made up in combination of electronic microbalance with a furnace, a temperature programmer and computer controller. The balance should be kept in an enclosed system so that the atmospheric pressure surrounding the sample can be controlled as shown in the Figure 36.